NOVEL APPROACHES TO HIGH SENSITIVITY CAPILLARY LIQUID CHROMATOGRAPHY – MASS SPECTROMETRY AND APPLICATION TO IN VIVO NEUROPEPTIDE MONITORING

by

Qiang Li

A dissertation submitted in partial fulfillment
of the requirements for the degree of
Doctor of Philosophy
(Chemistry)
in The University of Michigan
2010

Doctoral Committee:

Professor Robert T. Kennedy, Chair
Professor Nils G. Walter
Professor Jon-Kar Zubieta
Associate Professor Kristina I. Hakansson

To my family

ACKNOWLEDGMENTS

I would like to express my earnest gratitude to my advisor, Professor Robert T. Kennedy. His guidance, assistance, patience, and encouragement have been of enormous importance to my research and the completion of the dissertation. I would also like to thank my other committee members, Professor Jon-Kar Zubieta, Professor Nils Walter, and Professor Kristina Hakansson, for their helpful advice and comments. I have learned from them not only how to do research in graduate school but also how to be a life-long successful scientist.

I want to thank Dr. Gary Valaskovic from New Objective and Dr. Mike Lee from Milestone Development Services for the fruitful collaboration for part of my dissertation work and their kind support of our instrumental improvement. I am also indebted to the Department of Chemistry at the University of Michigan for the excellent graduate education and financial support for the last semester of my graduate study. I have enjoyed the five years here in Ann Arbor, in the artistic and peaceful atmosphere of such a nice town.

It has been a great pleasure working in the Kennedy lab as a doctoral student. Many thanks to my fellow graduate students for their help, discussion, and all the good times we have had in the office. I will not forget all the names of our current lab members: Claire Chisolm, Anna Clark, Amy Payeur, Maura Perry, Meng Wang, Jing Nie, Gwendolyn Anderson, Peng Song, Thomas Slaney, Neil Hershey, Colin Jennings, Matthew Lorenz, David Cepeda, Dr. Chunhai Ruan, Dr. Omar Mabrouk, Dr. Maojun

Gong and Dr. Ting Zhang. And I also appreciate the kind help of many previous lab-mates, Dr. Peilin Yang, Dr. Hui Wei, Dr. Minshan Shou, Dr. Jian Pei, Dr. Kristin Schultz, Dr. Kendra Evans and Dr. Charles Evans. I believe everyone going out from Kennedy lab will own a successful career and life.

Finally, I want to express my deepest thanks to my dearest mom Qian Chen and my dad Baomin Li, for the boundless love and support they have given to me. I would also like to thank all my family members and friends from the other end of the earth for their help and attention over long distance through the years. And I do not even need to say thanks to my husband, Jinming Liu, because of our persistent faith in sharing our life and our commitment to face difficulties and embrace happiness together forever.

TABLE OF CONTENTS

LIST OF FIGURES

LIST OF TABLES

LIST OF ABBREVIATION

μL	microliter
α-MSH	α-Melanocyte-stimulating-hormone
ACC	anterior cingulated cortex
aCSF	artificial cerebrospinal fluid
AGC	Automatic gain control
ALiPHAT	augmented limits of detection for peptides with hydrophobic alkyl tags
AMPH	amphetamine
Ang	angiotensin
BDNF	brain-derived neurotrophic factor
BE	β-endorphin
CCK	chrolecystokinin
CE	capillary electrophoresis
CEC	capillary electrochromatography
CGRP	calcitonin gene-related peptide
CID	collision-induced dissociation
CNS	central nervous system
CPu	caudate-putamen
CRH	corticotropin releasing hormone
CZE	capillary zone electrophoresis
DAD	diode array detector
Dyn	dynorphin
EIA	enzyme immunoassay
ELISA	enzyme-linked immunosorbent assay
EM1 & EM2	endomorphin 1 and 2
ESI	electrospray ionization
GABA	γ-aminobutyric acid
GAL	galanin
GHRH	growth hormone releasing hormone
GP	globus pallidus
Hcrt	hypocretin
HPLC	high performance liquid chromatography
HTS	high-throughput screening
i.d.	inner diameter

i.p.	intraperitoneal
IS	internal standard
LC	liquid chromatography
LE	leucine-enkephalin
LIF	laser-induced fluorescence
LIT	linear ion trap
LOD	limit of detection
MALDI	matrix assisted laser desorption ionization
ME	methionine-enkephalin
MS	mass spectrometry/mass spectrometer
MWCO	molecular weight cut-off
N/OFQ	nociceptin/orphanin FQ
NAc	nucleus accumbens
NAc	nucleus accumbens
NDA	naphthalene-2,3-dicarboxaldehyde
NKA & NKB	neurokinin α and β
nL	nanoliter
NMR	nuclear magnetic resonance
NPY	neuropeptide tyrosin
NT	neurotensin
ODS	octadecylsilane
OXT	oxytocin
PET	positron emission tomography
PFC	prefrontal cortex
pM	picomolar
PPE	preproenkephalin
PVN	paraventricular nucleus
QIT	quadrupole ion trap
RIA	radio immunoassay
RSD	relative standard deviation
S/N	signal-to-noise ratio
SN	substantia nigra
SOM	somatostatin
SP	substance P
SPE	solid phase extraction
STN	subthalamic nucleus
TOF	time of flight
TRH	thyrotropin releasing hormone
VIP	vasoactive intestinal peptide
VP	ventral pallidum

CHAPTER 1

INTRODUCTION

1.1. Neuropeptides

Neurotransmitters are endogenous chemicals that relay, amplify, and modulate signals between neurons in central nervous system (CNS). Neurons chemically communicate by releasing neurotransmitters into the synaptic gap as depicted in Figure 1.1. Once released, neurotransmitters may be subjected to a variety of processes: binding to receptors on postsynaptic neurons for excitation or inhibition,[1] diffusion into the extracellular space to exert actions farther from the synapse, inactivation by enzymes[2, 3] or recycling back to the releasing neuron by transporters[4]. Studying neurotransmitters is important for understanding normal brain functions, pathophysiology and pharmacology.

Among a variety of molecule types, neuropeptides constitute the biggest family functioning as neurotransmitters to facilitate chemical communications in the CNS. Neuropeptide signaling has been implicated in many physiological functions, including learning, memory, sensory perception and appetite regulation.[5] Neuropeptides are synthesized as large precursor proteins, generally named prepropeptides, at ribosomes in the peptidergic neurons, where the mRNA of them translated into the protein amino acid sequence.[6] Neuropeptides are produced via proteolytic cleavage of these precursor proteins by proteases and peptidases within dense-core vesicles in the releasing neurons.

The dense-core vesicles are generated in the Golgi apparatus in the neuron cell body and then transported down the axon. Neuropeptides are released into the synaptic gap when the dense core vesicles are exocytocically released, and then bind to and activate specific receptors located on their target cells. Neuropeptides are usually inactivated by exopeptidases so that for drug development specific inhibitors can be directed at those enzymes.

Opioid neuropeptides are known to play important roles in a wide variety of physiological processes including the perception of reward, learning and memory, drug abuse, and have critical effects in modulating endocrine, cardiovascular, gastrointestinal, autonomic and immune functions.[7-11] Opioid peptides have been shown to have a beneficial effect in various pathological conditions such as pain or depression. Study of these endogenous peptides provides a rational and powerful approach in the design of peptide therapeutics. There are three families of endogeneous opioid peptides based on their precursors: methionine-enkephalin (ME) and leucine-enkephalin (LE) derived from proenkephalin; dynorphin A and B (Dyn A and B) from pro-dynorphin; and β-endorphin (BE) from pro-opiomelanocortin. They have different affinities toward the three opioid receptor families (μ, δ and κ). In 1997,[12] another two endogeneous peptides, endomorphin 1 and 2 (EM1 and EM2), were discovered, showing high and selective affinity for μ-opioid receptor. However, they are not derived from the above precursors, but via a yet unclear pathway.

In this dissertation, we investigated opioid peptide activities in basal ganglia (BG). BG is a group of nuclei in the mammalian brain involved in the control of normal movement programming and motivational processes. The principal structures of the BG

are the striatum, pallidum, substantia nigra (SN), and subthalamic nucleus (STN). The striatum and pallidum can be further compartmentalized into dorsal and ventral tiers. The dorsal striatum, or caudate-putamen (CPu), is mainly involved in locomotor processes, while the ventral striatum, or nucleus accumbens (NAc) is associated with motivational processes and is a major component of the brain's reward circuitry. As in the striatum, the pallidum displays structural heterogeniety. The dorsal pallidum, or globus pallidus (GP) and the ventral pallidum (VP) also serve diverse functions; the dorsal section is related to movement and the ventral one to reward and motivation. In humans and other primates the external section of the GP (GPe; corresponds to rodent GP) and its internal segment (GPi; corresponds to rodent entopeduncular nucleus) are further divided by the medial medullary lamina.

Under normal BG conditions, midbrain dopamine (DA) synthesized in the SN and ventral tegmental area (VTA) is released via long projecting neurons into the CPu and NAc, respectively (for full schematic represenation of BG see Figure 1.2). As DA is released into these striatal areas, downstream events take place that relay these signals to cortical areas of the brain (the cortex being responsible for higher cognitive processes and motor control informational processing). Under pathological conditions, however, an imbalance in signaling between these structures exists, resulting in diseases such as Parkinson's disease, Huntington's chorea, Tourette's syndrome, and addiction.[13-16] In particular, DA dysregulation in SN-CPu (nigrostriatal pathway) projections is related to movement disorders while DA dysregulation of VTA-NAc (the mesolimbic pathway) projections is related to addictive disorders and abnormal reward processing. The DA that is released in these striatal areas plays an important role in differentially modulating

downstream events in the BG. To this end, there are two types of medium spiny neurons that DA acts on in CPu and NAc. One group expresses DA D2 receptors, which are inhibitory while another expresses DA D1 receptors which are excitatory.[17] The half that expresses DA D2 receptors contain γ-aminobutyric acid (GABA) as well as the opioid neuropeptide enkepahlins (ENK) and project to the GP/VP. The other half that expresses DA D1 receptors contain GABA and the neuropeptides dynorphin and substance P that project back to the SN.

Opioid peptides and their receptors are highly localized throughout the BG.[18-20] Since BG diseases cause pathological imbalances in neurotransmitter signaling, it is necessary to understand neuropeptide modulation of BG structures in the pursuit of novel therapeutic strategies. Of particular interest are enkephalins (ENK) which, through their actions at both μ- and δ-opioid receptors, are strongly associated with reward processes and movement disorders.[21-23] In fact, stimulation of the delta opioid receptor with analogues of ENK have been shown to improve locomotor activity in experimental Parkinson's disease and to reverse neurotoxicity caused by methamphetamine (METH; for review see Borlongan et al.[24]).

In view of the importance of opioid peptides in locomotor and, with respect to the VP, reward-related behaviors, it is essential to investigate the factors regulating the release or inhibition of opioid peptides in these brain regions.

Amphetamine (AMPH) is a potent monoamine (particularly DA) releaser with high abuse liability[25-27] that causes hyperactivity, euphoria, addiction, anxiety, depression and psychosis.[28-32] AMPH reverses DA transporters (reversing uptake) on the surface of DA containing/releasing cells and reverses vesicular monoamine transporters within DA

terminals. Both these actions work in concert to cause over-release of DA into synapses. AMPH has also been shown to modulate other neurotransmitter systems including serotonin,[33] diadenosine polyphosphates,[34] ascorbic acid,[35] aspartate,[36] taurine[37] and glutamate[36]. Therefore it is not surprising that AMPH and METH, a more potent analogue of AMPH, dramatically alter neuropeptides (neurotensin, dynorphin and substance P) and neuropeptide precursor mRNA.[38-42] However, to date, actual release of opioid peptides has not been accurately characterized due to technical challenges. This is also true for the measurement of ENK and groups have therefore used analyses of the precursor of ENK mRNA as a marker for ENK activity.[43, 44]

ENK are important for their role as neuromodulators in the BG and it has been speculated that the function of the main ENK products ME and LE is to dampen excessive neurotransmission in the BG system.[45-47] However, based on the localization of the μ- and δ-opioid receptors on which ENK act, they may also stimulate neurotransmitter release. For instance, Johnson and North (1992) showed that μ-opioid receptors in the VTA were positioned on GABAergic interneurons and when these receptors are stimulated a disinhibition occurrs resulting in an excessive release of DA in striatal areas.[48] Therefore it appears that ENK actions on DA may be indirect.

In chapter 4 of this dissertation, I will discuss in further detail the interaction between DA and ENK from a review of the literature and then discuss our most recent findings of AMPH induced DA release on ENK levels *in vivo*.

1.2. *In vivo* neurochemical monitoring methods

In vivo monitoring of neurotransmitters is invaluable because of its ability to

investigate the intact network of neurotransmission regulation, how pharmacological treatment affects specific brain regions and how behavior correlates to chemical changes in brain. Previous indirect studies of neurotransmitters have focused on measuring the chemical content extracted from brain tissue, or mRNA expression of precursor proteins for neuropeptides. Although these methods allow us to quantify total neurotransmitter content in the brain or a specific brain region, they do not provide the ability to determine the temporal pattern of neurotransmitter release nor do they allow for correlation of release to behavior. Furthermore, for peptides, changes in mRNA level also may be misleading because of numerous regulatory steps from mRNA to protein and finally to the peptides. Thus, a variety of techniques for *in vivo* monitoring has been developed to obtain dynamics of neurotransmitter levels in living brain. Prominent among these methods are microsensors, positron emission tomography (PET) and microdialysis sampling.

Microsensors have excellent spatial and temporal resolution, however, have weaknesses including an unproven ability to determine basal concentrations, long-term dynamic changes and multiple analytes. Due to the difficulties in developing the sensors, there is no sensor developed for peptides yet.

PET is a powerful noninvasive tool to achieve functional imaging of the brain. It provides quantitative measurement of neurotransmitter receptors with radiolabelled ligands in the CNS. Some review papers[49, 50] provided a list of recent studies with this method. However, limitations to the widespread use of PET arise from high cost, low spatial resolution, and the complication of interpreting the relationship between the release of the neurotransmitters and the activity of their receptors.

Microdialysis can provide complementary information to these two methods, and is generally used for most neurotransmitters including the peptides. It utilizes a probe with a semi-permeable membrane with certain molecular weight cut-off (MWCO) to serve as a barrier between the perfusion fluid, artificial cerebral spinal fluid (aCSF) in our experiments, and the surrounding tissue. Figure 1.3 depicts the microdiaylsis probe I have used in most of experiments described in this dissertation, with a concentric design and scales marked in the figure. As fluid is perfused through the internal lumen of the probe, a concentration gradient is generated that allows smaller molecule analytes to diffuse into the probe, while keeps larger molecules such as enzymes and other proteins outside. Local pharmacological manipulations can also be performed by adding the agent into the perfusion solution, such as the K^+ stimulation we carried out in Chapter 2 and 3.

In measuring the efficiency of microdialysis sampling, both absolute recovery and relative recovery are used. Absolute recovery is the value that measures the amount of analyte in one microdialysis fraction collected in a period of time, while the relative recovery is the ratio of the concentration of analyte in the dialysate to the concentration of the sample analyte in the tissue extracellular fluid. For a given microdialysis probe and analyte, the higher the perfusion flow rate is, the higher the absolute recovery and the lower the relative recovery.

As a sampling tool, microdialysis can be coupled to various analytical techniques such as enzyme assays, immunoassays, liquid chromatography (LC) and capillary electrophoresis (CE). In these methods, temporal resolution is a critical parameter for *in vivo* brain chemical measurements because the neurotransmitters are rapidly released by

exocytosis and quickly eliminated from the synapse by reuptake or enzymatic degradation. Dynamic fluctuations in neurotransmitter levels can occur on the millisecond scale, and last over longer time scales to reduce cellular responses at the minute timescale and pharmacological effects lasting from minutes to hours (for review, see the reference[51]). Achieving better temporal resolution in measuring neurochemicals is therefore commonly desired to obtain better accuracy in monitoring.

In most cases of microdialysis sampling, the temporal resolution is set by three factors: analysis time of the analytical technique, the mass sensitivity of the analytical method, and zone dispersion during sampling.

For on-line detection where the dialysate is directly interfaced to the analytical system, the temporal resolution is always determined by the running time of the detection method. For peptide studies, this can be limited by long liquid chromatography and mass spectrometry (LC-MS) running time at 40 min[52], which can be cut to 16.5 min by optimizing gradient and other parameters.[53] For other neurotransmitters with easier fluorescence labeling, on-line derivatization and detection with faster technique CE has been achieved. The temporal resolution can be improved to 3-30 s for amino acids and monoamine neurotransmitters in pilot studies of our group in the recent decade.[54-58]

Compared to on-line detection, off-line analysis has the advantage of higher overall throughput and the temporal resolution can be further improved. In off-line analysis, the mass LOD of analytical method is the limiting factor for temporal resolution. To increase the temporal resolution, shorter sample collection time is needed and smaller fractions are thus generated, resulting in decrease of the analyte amount per sample. Immunoassays coupled with microdialysis generally achieve temporal resolution of 30 min.[59, 60] When

using LC as separation method, neurotransmitters can be monitored at low min timescales. With traditional HPLC, samples are usually collected in 5-30 min fractions[61-64] and in some cases 1-2 min[64, 65] by combining high-sensitivity detection. The mass sensitivity generally depends on the detector coupled to the LC separation, for example , use of electrochemical detectors or mass spectrometers offered substantial improvement over UV detection. Capillary LC with micro-bore columns with inner diameter (i.d.) smaller than 300 μm has been developed to increase mass sensitivity over HPLC. With smaller column diameters, a given amount of sample is diluted less, and when it is coupled to MS with electrospray ionization (ESI), the inherent lower flow rate on the smaller column also results in better ESI efficiency. Therefore, some microbore LC assays have reported temporal resolution at 1-2 min for dopamine (DA) measurement.[66, 67] With superior detection sensitivity, CE is used more for high temporal resolution detection. By coupling CE with laser induced fluorescence (LIF), detection at yoctomole level can even be achieved,[68] suggesting potential for second level temporal resolution for some neurotransmitters. Thus, for CE analysis, the temporal resolution with off-line analysis has been improved by using various strategies for derivatizing and manipulating smaller samples from 20 s, 6 s to as low as 1 s.[69-71]

While some reports claimed temporal resolution at low second scale, however, the inherent Taylor dispersion in transfer tubing of microdialysis system was not counted in those cases. The inherent sample band broadening during sampling starts to limit temporal resolution at timescale of seconds. Especially when operating freely-moving animal experiment, the connection tubing length is difficult to be shortened, and the flow rate is also difficult to be increased for maintaining adequate recovery, such dispersion

can become dominant in determining the temporal resolution. For example, in one previous work of our lab, 3 s temporal resolution has been described for sampling from an anesthetized animal at high flow rate, however the temporal resolution was decreased to 90 s for low flow rates or work with freely-moving animals.[54] To overcome this effect, our group has adopted a segmented flow microfluidic device to conserve temporal resolution by reducing the dispersion of microdialysis samples in the transfer tubing.[72] That is approved emerging with great potential to solve many basic analytical chemistry problems, however, in the detection of neuropeptides with relatively low *in vivo* concentrations, the temporal resolution is still limited the the minute timescale. In the third chapter of this dissertation, we will further discuss the temporal resolution of our particular system used for neuropeptide studies.

1.3. Techniques for *in vivo* monitoring of neuropeptides

Monitoring the concentration dynamics of neuropeptides is a key tool in the effort to understand brain function, disease, and treatment. However, while microdialysis provides a way to continuously collect samples from the brain, detection of neuropeptides in dialysates has proven difficult for several reasons. The *in vivo* concentration of neuropeptides is at 1-100 pM level and the microdialysis sampling relative recovery ratio is usually about 10%-40% for different peptides. In microliters of microdialysis samples, the absolute amount of peptide to be quantified is thus only at the attomole level. In addition, because neuropeptides are produced by the action of numerous proteases and peptidases on precursor proteins, many similar sequences among different neuropeptides are present in the dialysate, which also require high selectivity of the detection methods.

Traditional approaches to analyze neuropeptides include immunoassays, particularly radio immunoassay (RIA) and enzyme-linked immunosorbent assay (ELISA). These methods achieve sensitivities with 100-500 amol LOD,[59] which limiting the temporal resolution at about 30 min as discussed above. Furthermore, cross-reactivity among similar sequences of neuropeptides can reduce the assay specificity, and they also limit the measurement to only a single peptide per fraction.

Due to the low concentration and small volumes supplied by microdialysis sampling, capillary LC coupled with MS system has become an attractive way to monitor *in vivo* neuropeptides due to the ultimate sensitivity and specificity offered by additional structure information from MS analysis. Choosing miniaturized capillary LC columns shows advantages mainly in terms of sensitivity compared to traditional HPLC. As mass spectrometry is a concentration dependent technique, capillary LC, in particular, has the effect of concentrate μL sample into nL level. With the miniaturized reverse phase column, microdialysis sample can be preconcentrated at the head of octadecylsilane (ODS) column bed in a fused silica capillary, and then rinsed with an aqueous solvent to desalt. The peptides, however, still retain on the reverse phase column by strong interaction with the stationary phase. They are then eluted out by decreasing the polarity of the mobile phase via a gradient elution. Separation efficiency, as well as the chromatographic resolution, can be enhanced by reducing the inner diameter (i.d.) of the capillary and the particle size.[73] We pack capillary columns with 25 μm i.d. (shown in Figure 1.4) in lab for all the experiments. Packing columns in-house is necessary because such miniaturized columns are not commercially available. In addition, in-house packing of columns allows the use of a variety of available stationary phase particles as in method

development step.

The capillary column is coupled on-line with mass spectrometer by electrospray ionization (ESI).[74, 75] ESI provides a sensitive interface between capillary LC and MS. An electrical voltage must be applied between the emitter tip of the capillary column and the entrance of the MS to generate a Taylor cone of charged droplets, which undergo fission and solvent evaporation when travel to the heated inlet of the MS. The ionization efficiency depends on the flow rate, mobile phase composition, distance between the emitter tip and the MS inlet, the voltage added, hydrophobicity of the analyte, the tip shape and so on.[75, 76] ESI can accept flow rate ranging from 10 nL/min to 0.2 mL/min. Because its sensitivity is more dependent on concentration than on the total quantity injected, there are advantages of using it at low flow rate.[77] Low flow rate, resulting in nano-ESI, enable either significant reduction in analysis volume and/or extension of analysis time, while maintaining, or even improving, signal-to-noise (S/N) ratio. Furthermore, nanospray is more than simply a reduction of ESI flow rate.[78, 79] It typically generates a smaller initial droplet size at the emitter orifice, which can impact the quality of ESI spectra and minimize ion suppression. Indeed, Vouros and coworkers observed significant reduction of signal suppression effects when the flow rate was decreased from 200 mL/min to 100 nL/min for LC/MS.[80]

Ion trap as a mass analyzer also provides the ability to conduct multiple levels of fragmentation tandem-in-time to identify various molecules. To achieve MS^3 fragmentation, a specific parent ion is isolated and fragmented through collision-induced dissociation (CID) into daughter ions, and one specific daughter ion is fragmented to form granddaughter ions by repeating the collision. An ion trap is well-suited for

fragmentation because it generates predictable ion patterns of peptide molecules[81, 82] allowing for structure elucidation and thus increase specificity for certain neuropeptides. Both quadrupole ion trap QIT (LCQ, Thermo) and linear ion trap LIT (LTQ, Thermo) have been used in this work and comparison of sensitivities of them for selected neuropeptide samples will be shown in chapter 2. Generally, LIT can reach higher sensitivity for most analytes due to its larger ion capacity in the analyzer.

The greatest advantage of this capillary LC-MS^3 system is that it could reach LOD at low (0.5-5) amol level. Also, capillary LC coupled with MS detection make it possible to both monitoring known peptides and discovering novel peptides in the CNS. The overall performance (separation efficiency, sample recovery, ionization efficiency, detection limits, etc.) continues to improve as the mechanical scale of separation and electrospray devices reaches the micrometer and submicrometer regime. Mass spectrometry allows for sensitive and specific quantification of multiple peptides simultaneously, with the additional ability to provide structural information through ion fragmentation.

1.4. Review of recent detection methods for a variety of neuropeptides

In the following, a review of these recent techniques including RIA, LC, CE and MS detection used for monitoring different types of neuropeptides will be discussed. One technique or a combination of different methods for detection and quantification of them are listed in the order of neuropeptide groups defined by Hokfelt's paper[83] and summarized in Table 1.1. Table 1.2 listed a summary of reported *in vivo* dialysate concentrations of some neuropeptides measured in certain brain regions.

(1) Opioid peptides:

Enkephalins are frequently used as model compounds for new analytical chemistry methods. Microdialysis coupled with LC-electochemical detection method was developed for high temporal resolution detection of enkephalins.[84] In that study, capillary LC column with 25 μm i.d. was used to obtain over 100 fold on-column concentration to reach detection limits as of 20 pM for ME. This sensitivity allows it to be combined with microdialysis for monitoring ME *in vivo* with 5 min temporal resolution. Another group also coupled HPLC with electrochemical detection, and monitored ME, LE, EM 1 and 2 simultaneously.[85]

Our group continued to develop the capillary LC methods coupling with MS^2 and MS^3 later on for even better sensitivities for ME and LE.[53, 86, 87] In this dissertation, we will discuss the ability of our system on off-line detection of the dialysate fractions. This method has been proven to be effective to several neuropeptides including enkephalins, neurotensin and dynorphin. To prevent sample degradation, adding protease inhibitors has been a choice.[88, 89] Faster methods such as CE were under development[90-93] showing potential for the analysis of biological samples. Limit of its application for *in vivo* study is still the lack of sensitivity, so developing effective preconcentration method such as adding a prior solid phase extraction (SPE) column[94] may be helpful.

Dynorphins are another class of opioid peptides including different sub-family peptides. When the precursor prodynorphin is cleaved, multiple active peptides are released: dynorphin A, dynorphin B, and α/β-neo-endorphin. Among these forms, dynorphin A1-8 (Dyn A1-8) was studied the most. Micordialysis coupled with RIA was first used to measure Dyn A1-8 release in the nucleus accumbens.[95] In this dissertation,

we have also detected it together with ME and LE in rat brain by LC-MS[3].

BE is a relative larger opioid peptide with 34 amino acids. Microdialysis coupled with RIA was used successfully for measurement of it together with ME and Dyn A1-8.[96] For methods involving MS, the LOD for intact BE was too high to achieve enough sensitivity for *in vivo* measurement. But with trypsin digestion and measuring a characteristic fragment peptide of BE, BE level could thus be estimated indirectly.[97] We adopted this idea to achieve a quantitative measurement of BE in dialysates from rat brain.

Although the origin of endomorphins is still not completely clarified, we discuss them together with the other opioid peptides. Researchers also tried to measure them together with enkephalins, and successfully determined the concentrations in rat spinal cord with HPLC coupled to electrochemical detection.[85] Separation of endomorphins and other opioid peptides have also been developed with CE and coupled to UV detection and ESI-MS[98] or by on-line SPE-CE-ESI-MS.[99] But these data were obtained from human plasma samples but not brain samples.

In the work of this dissertation, opioid peptides have been chosen as the most important analytes for both analytical method development and pharmacological studies. Other neuropeptides, studied less in our work, but are equally important in CNS are also discussed in the following and related analysis methods will be given as a summary of the research system for most types of neuropeptides.

(2) Hypothalamic hormones:

It is an exciting time of research in the field of hypothalamic hormones oxytocin (OXT) and vasopressin (VP). OXT is well-known as a "love" hormone that plays

important roles in female reproduction,[100] social recognition,[101, 102] trust,[103] sexual behaviors,[104] and maternal behaviors.[105] VP is also shown to have a role in various systems, such as re-absorption of molecules in the tubules of the kidneys and regulation of water, glucose, and salts in the blood.[106] Both of the peptides have similar structures with a sulfur bridge in their molecules, which lead to more complexity for detection.

Release of OXT in the hypothalamic paraventricular nucleus (PVN) was measured via microdialysis-RIA.[107] In this study, effect of maternal defense on relative OXT level changes was shown without giving a basal concentration. VP level could also be measured with RIA.[108] LC-MS methods for detection of OXT and VP are still under development that no *in vivo* data was shown due to lack of sensitivity. Therefore, to effectively determine low level peptides *in vivo* by ESI-MS, the LOD must be improved upon. Muddiman group has looked into modification of peptides containing disulfide bond with hydrophobic tagging,[109, 110] taking advantage of higher ESI efficiency for more hydrophobic molecules. With the ALiPHAT strategy (augmented limits of detection for peptides with hydrophobic alkyl tags), 2-3 folds higher sensitivity was achieved for such peptides. Meanwhile, improvement of the nano-ESI emmiter tip was also developed to increase detection sensitivity toward OXT and other peptides like NPY by hydrophobic polymer coating on the tip.[111] With further improvement of the LC-MS system, detecting of OXT and VP *in vivo* might be feasible in future.

(3) Hypothalamic releasing and inhibiting hormones:

Corticotropin releasing hormone (CRH or CRF) acts on cells in the anterior lobe of the pituitary to release adrenocorticotropic hormone. Growth hormone releasing hormone (GHRH) stimulates cells in the anterior lobe of the pituitary to secrete growth

hormone. Thyrotropin releasing hormone (TRH) regulates secretion of thyrotropin.[112] Somatostatin (SOM) acts on the anterior lobe of the pituitary to inhibit the release of growth hormone and thyroid-stimulating hormone.[113, 114]

Because these peptides are relatively big and thus lead to lower ESI efficiency and beyond the most sensitive detection range of MS, there is no LC-MS or CE methods have been developed yet. RIA was the main solution for detection of them. CRH level was measured together with VP with push-pull sampling and RIA in rat brain.[108] GHRH was measured in cattle plasma together with SOM.[115, 116] For TRH, Pekary and colleagues did a series of studies on relative TRH and TRH-like peptides level changes in various rat brain region tissue with HPLC-RIA under different drug treatment.[117-119] And SOM levels in the rat nucleus accumbens (NAc) was investigated, showing releasing caused by chronic administration of antidepressants.[120]

(4) Tachykinins:

The most well studied tachykinin peptide is Substance P (SP). SP plays a variety of roles, as in a previous review of this important peptide.[121, 122] Earlier reports using RIA combined with a high-recovery liquid-liquid extraction has measured SP in human CSF, which compared the SP level between control group and patients with chronic pain.[123] Research is ongoing to find a better method that overcomes the disadvantages of RIA. Combination of CE with matrix assisted laser desorption ionization –time of flight–mass spectrometry (MALDI-TOF-MS) was used to determine SP in rat brain tissue.[124] The method was suitable for analyzing SP in the μM range. The detectability of SP can be extended to 100 pM level by using CE-LIF with NDA derivatization and quantification of SP in saliva samples.[125] Later on, an HPLC-ESI-MS/MS method was developed on

measuring tissue level of SP in spinal cord,[126] giving LOD at 10 fmol injected on column (~667 pM). With LC-MS/MS, SP metabolisms were also measured with bovine brain microvessel endothelial cell (BBMEC) system.[127]

Another group of tachykinin peptides is neurokinin α and β (NKA and NKB). Pharmacological effects of NKA and NKB mainly include algogenic actions, which is associated with increased capillary permeability, production of edema, and the initiation of pain and associated reflexes.[128, 129] Reports from one group with CE-LIF method showed results separating and measuring NKA[130] and NKB[131] in human body fluids.

(5) Neuropeptide tyrosin (NPY):

NPY has been associated with a number of physiologic processes in the brain, including the regulation of energy balance, memory and learning, and epilepsy.[132, 133] The main effect is increased food intake and decreased physical activity.[134, 135] For measurement of NPY in plasma, HPLC-ESI-MS with a cation exchange sample clean-up procedure was utilized.[136] For measurement in rat brain, microdialysis coupled with RIA was carried out for monitoring dynamic changes of NPY and neurotensin (NT) with amphetamine treatment.[137]

(6) VIP-glucagon family:

VIP induces smooth muscle relaxation,[138] causes inhibition of gastric acid secretion and absorption from the intestinal lumen.[139] It also helps to regulate prolactin secretion.[140] Studies have mainly focused on the function of VIP, and there were few papers about the measurement of its *in vivo* level. Early in 1992, capillary zone electrophoresis (CZE) and micellar electrokinetic chromatography using a commercial HPCE instrument with UV detection was used to analyze VIP-rich fractions from

cerebral cortex of rat brain.[141] No recent improvement of the method was found.

(7) Other peptides:

Neurotensin:

There are many other neuropeptides not included in the above families but also play essentials roles in CNS. Neurotensin (NT) has been studied intensively and has been shown to have significant interaction with the dopaminergic system[142] and is indicated to play a role in the regulation of luteinizing hormone and prolactin release.[143, 144] For *in vivo* monitoring of NT, microdialysis coupled with RIA was used too.[137] For more efficient and faster separation, CZE has been developed and conditions were optimized for quantitative analysis of neuropeptides in human plasma.[145] Separation of trace neuropeptides NT together with SOM, VP and TRH in plasma by CZE was achieved with LOD at the 4.5 nM for NT. However, coupling CE to MS led to lower sensitivity. A method based on CE coupling with a DAD and ESI-MS was established obtaining LOD in the range of 0.10-0.60 μM.[146] Another LC-MS method with the help of an on-capillary UV detection resulted in LOD of NT at about 600 pM.[147] Both reports did not reach the sensitivity for *in vivo* measurement. However, one report was successful on measuring NT from human CSF samples.[131] This method utilized CE-LIF to determine some peptide hormones and their fragments and established a transient pseudo-isotachophoresis (pseudo-tITP) preconcentration in this study. LODs were found to be 0.04, 0.1, 0.2, and 0.08 nM for NT8-13, NT, NKB, and CCK-4, respectively. This method was validated and applied to quantitative analysis of NT and NT8-13 in human cerebrospinal fluid sample.

Nociceptin/orphanin FQ:

Nociceptin/orphanin FQ (N/OFQ) exerts a variety of biological functions, including modulation of nociception,[148] of stress responses and anxiety,[149] and of learning and memory.[150, 151] Microdialysis coupled with RIA has been developed allowing measurement of N/OFQ release from the hippocampus and thalamus of freely moving animals.[152] This study indicated that kainite seizures caused a twofold increase in N/OFQ release followed.

CCK:

Chrolecystokinin (CCK) is well known as involving in pain modulation especially regarding anti-opioid mechanisms.[153] Microdialysis coupled with RIA was chosen for monitoring CCK levels in rat brain regions like anterior cingulated cortex (ACC).[154, 155] It was found that at the time when the animals are known to show pain-related behavior, CCK release is elevated in ACC in awake rats.

Galanin:

Galanin is involved in a number of physiological processes such as regulation of food intake, and regulation of other neurotransmitter and hormone release.[156, 157] Quantification of galanin was conducted using protein precipitation and LC-MS with LOD at nM level.[158] *In vivo* study on microdialysis samples from rat brain could be achieved with RIA[159] or coupling LC with RIA with LOD at pM level.[160]

Calcitonin gene-related peptide (CGRP):

CGRP is thought to play a role in cardiovascular homeostasis, nociception, glucose uptake and the stimulation of glycolysis in skeletal muscles.[161] For measurement of CGRP, a novel microdialysis probe was constructed and coupled to capillary electrochromatography (CEC) to detect it from human skeletal muscle.[162]

α-Melanocyte-stimulating-hormone:

α-Melanocyte-stimulating-hormone (α-MSH) is produced in the anterior pituitary and released into the brain that has effect on appetite.[163] It also stimulates the production and release of melanin by melanocytes in skin and hair.[164, 165] To analyze the effects of α-MSH at skin, dermal microdialysis probe was planted in dorsal skin of rat for recovering of peptides like α-MSH and SP. EIA was used for measurement.[166]

Hypocretins/orexins:

Hypocretin (Hcrt) including a pair of peptides (Hcrt-1 and -2) are synthesized in the perifornical and lateral hypothalamus and stimulate food intake, wakefulness and energy expenditure.[167] Microdialysis-RIA was chosen for monitoring them in rat brain during waking and sleep states.[168]

Angiotensin:

Angiotensin family include 4 types of peptides, generally known as hormone, can also be counted as neuropeptide. They cause vasoconstriction, increase blood pressure, and release of aldosterone from the adrenal cortex.[169] Lanckmans' group has made efforts to detect Ang IV *in vivo* with nano-LC-MS system. With a first development of a reliable quantification method with an internal standard[170], they have attempted to measure stimulated Ang IV level from rat brain dialysate samples.[171] However, the sensitivity was still a little low for measuring basal level of Ang IV so an estimation was made using zero-net-flux method.

Multiplexing from other species:

Besides mammalian neuropeptides, separation and analysis of neuropeptides from other species have also been conducted with analytical methods such as CE, LC with MS.

Sweedler group has contributed on detection of neuropeptide from a model Aplysia californica with CE-MALDI-MS[172] or nanoESI-MS[173]. Li and colleagues have been able to measure a series of neuropeptides from crustacean combining microdialysis with nanoLC-MS, and MALDI-TOF/TOF.[174, 175]

1.5. Improvements in capillary LC-MS

Capillary LC coupled on-line with MS has been chosen to study *in vivo* neuropeptides. Besides technical improvements to facilitate its combination with microdialysis, other efforts are also valuable to further enhance this technique. Although the current technique allows us to monitor some neuropeptides from *in vivo* samples, it is still time consuming. It is therefore desired to increase the analysis throughput, to save precious samples and to do multiple analyses on same samples. Thus, further effort is needed to expand the technique for even smaller samples, and explore method to preserve the separated chemicals from micro-scale separation method for additional off-line analysis with different instruments or with other manipulations. The challenge for saving the high-resolution separated effluents falls on the extremely small volumes and narrow bands involved. So herein, we will also describe a new concept based on the use of multiphase segmented flow to achieve fraction collection from capillary LC system and preserve separated components for off-line analysis with MS.

Multiphase flow in capillary or microfluidic systems has generated considerable interest as a way to partition and process many discrete samples or synthetic reactions in confined spaces.[176] A common arrangement is a series of aqueous plugs or droplets separated by gas or immiscible liquid so that each plug can act as a small, individual vial

or reaction vessel. Three ways to generate such segmented flow are illustrated in Figure 1.5. In the work of Chapter 5, the generation method with T junction was adopted to connect effluents from capillary LC column and immiscible oil solution. Depending on the channel dimension, viscosity and flow rate of the solutions, the size of fluid plugs can be varied from picoliter level to a few hundred nanoliters with frequencies of up to 1000 Hz.[177]

By generating segmented flow, aqueous samples were stored as plugs or droplets available for further analysis. Chemically analysis the contents of plugs have been challenging. Optical methods such as colorimetry and fluorescence are most commonly used.[178, 179] Systems for electrophoretic analysis of segmented flows have recently been developed.[180] Drawbacks of these methods are that they require the analytes be labeled to render them detectable and they provide little information on the chemical identity of plug contents. Therefore, MS becomes an attractive analytical technique for analysis of segmented flows because it has the sensitivity and speed to be practically useful for low volume samples analyzed at high throughput. Mass spectrometry has been coupled to segmented flow by collecting samples onto a plate for MALDI-MS[181] or a moving belt interface for electron impact ionization-MS.[182] Recently, a method to perform ESI-MS of a stream of segmented flow has been reported.[183] In this method, a stream of aqueous droplets segmented by immiscible oil was periodically sampled by using electrical pulses to transfer the droplet into an aqueous stream that was directed to an ESI source. This proof-of-concept report showed the feasibility of online droplet analysis; however, the LOD for peptide was ~500 μM. The high LOD was due at least in part to dilution of droplets once transferred to the aqueous stream and the high flow rate (~3 μL/min) for the

electrosprayed solution. The dispersion of droplets after transfer to the aqueous stream also limits the throughput of this approach. So in the part of Chapter 5, conditions and limitations of direct infusion of segmented flow is discussed to achieve dilution free detection.

1.6. Dissertation Overview

The research presented in this dissertation is based on some previous efforts in the Kennedy group on designing a capillary LC-MS system for monitoring endogenous enkephalins from rat brain. Efforts have been made to, firstly, improve the method to be a more routine tool for studying a variety of neuropeptides, secondly, focuse on opioid peptides, especially ENKs and exploring better quantification method, higher temporal resolution and some studies on pharmacological responses, and finally improve the analytical techniques for capillary LC separation by doing low volume fraction collection and off-line ESI-MS detection via segmented flow.

Chapter 2 discusses the possibility of storing neuropeptide samples with adding acetic acid for reliable off-line detection, which is also proven to improve the detection reproducibility. Practical aspects including sensitivity, specificity and reproducibility are discussed for a selection of 10 biologically important neuropeptides, showing a broadened application of the analytical system. BE had an LOD of 5 nM when detected directly, but it could be quantitatively determined by detecting a characteristic fragment produced by tryptic digestion with an LOD of 3 pM. This approach may prove useful for other large neuropeptide as well. The method is then used to determine 4 opioid peptide levels in rat brain striatum under basal and K^+ stimulated conditions. The presented work

has been published in *Analytical Chemistry* (2009, volume 81, page 2242).

Chapter 3 evaluates the system capability of reaching a higher temporal resolution for neuropeptide study. LE is chosen as a model sample in this part of study. Less dialysate collected with shorter sampling intervals leads to higher requirement of the accuracy for quantification, so an isotopic labeled internal standard (IS) is induced and the method is validated to achieve a higher reproducibility for detecting and quantifying such trace level samples. To demonstrate the advantages of monitoring neuropeptide with higher temporal resolution, comparison of dynamic changes of *in vivo* LE levels is done with 20 min or 5 min time resolutions under K^+ stimulation, showing more accurate information with the improved method. This part of work has been prepared for publication in *Journal of Neuroscience Methods*.

Chapter 4 shows some preliminary discovery, using the system as a tool for monitoring enkephalins, on dynamic changes of enkephalins in basal ganglia influenced by acute administration of amphetamine (AMPH) as a specific drug of abuse. We have found that subcutaneous injections of AMPH with doses higher than 2.5 mg/kg to naïve rats cause a substantial releasing of both ME and LE in the GP/VP region. And this releasing is dose dependent. This discovery offers further evidences of the relationship of AMPH injection – DA release – opioid peptide release in basal ganglia, especially srtiatopallidal and mesolimbic pathways. Our group will further investigate the projection pathways of this dynamic changes and the work will be published with the complimentary results.

Chapter 5 seems to steer away from the analysis of neuropeptides only, but offers a more common method to improve capillary LC-MS technique by achieving low volume

fraction collection and further off-line analysis of those fractions. Segmented-flow attracted scientists' interest because of its ability of manipulating samples at sub-nL levels with little dispersion. We have established a novel ESI-MS detection system for both air and oil segmented flows. The presented work in this chapter is based on initial work on ESI-MS detection of air-segmented flow published on *Analytical Chemistry* (2009, volume 81, page 6558), and the application of this system for high-throughput drug screening published on *Journal of the American Society for Mass Spectrometry* (2010, in press). The work on fraction collection and off-line analysis of oil-segmented flow has also been submitted to *Analytical Chemistry*.

Additionally, several possible future projects and some preliminary results are presented in Chapter 6.

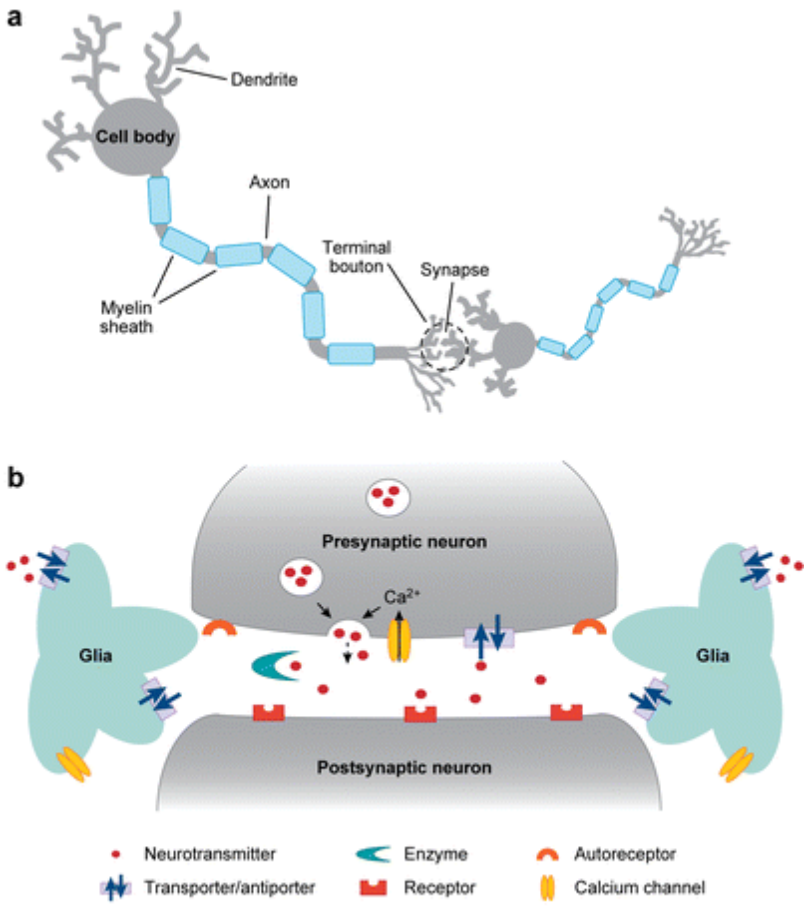

Schultz KN, Kennedy RT. 2008.
Annu. Rev. Anal. Chem. 1:627–61.

Figure 1.1: Cartoon of the sending neuron and receiving neuron (a) and the synaptic junction (b) during neurotransmitter releasing.

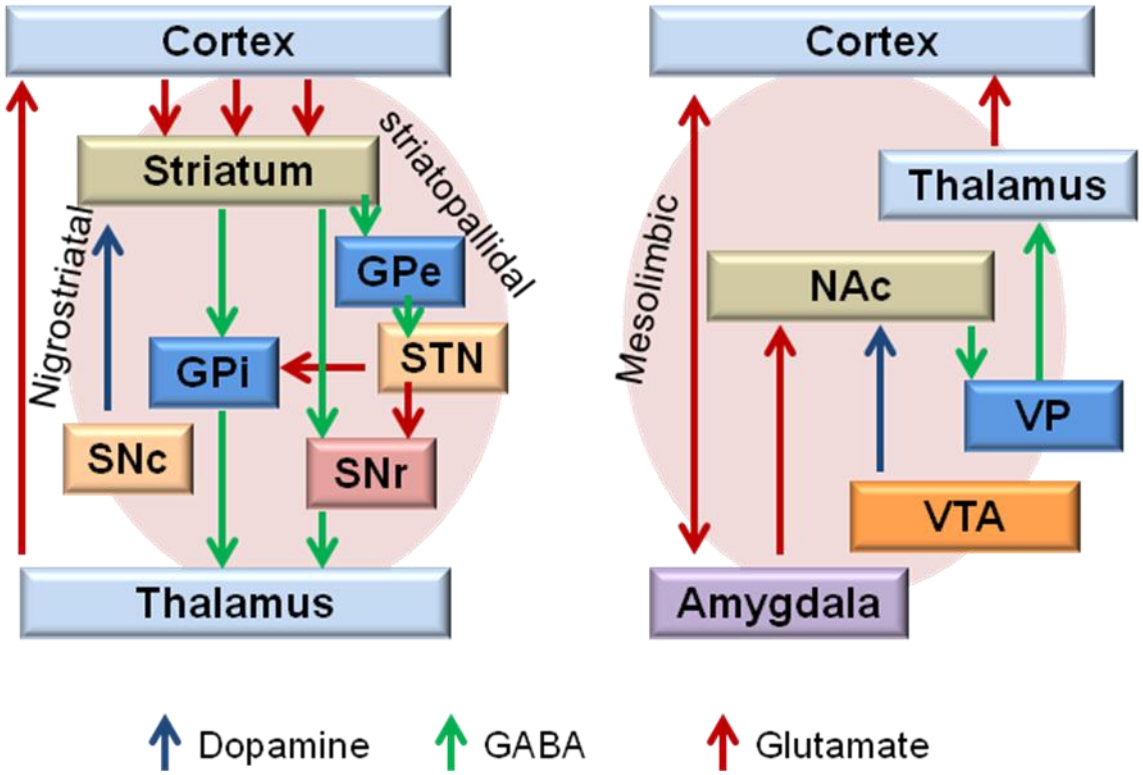

Figure 1.2: Nigrostriatal and striatopallidal pathways (left) and mesolimbic (right) pathways in basal ganglia. The substantia nigra is further divided into two parts: the *pars reticulata* (SNr) and *pars compacta* (SNc).

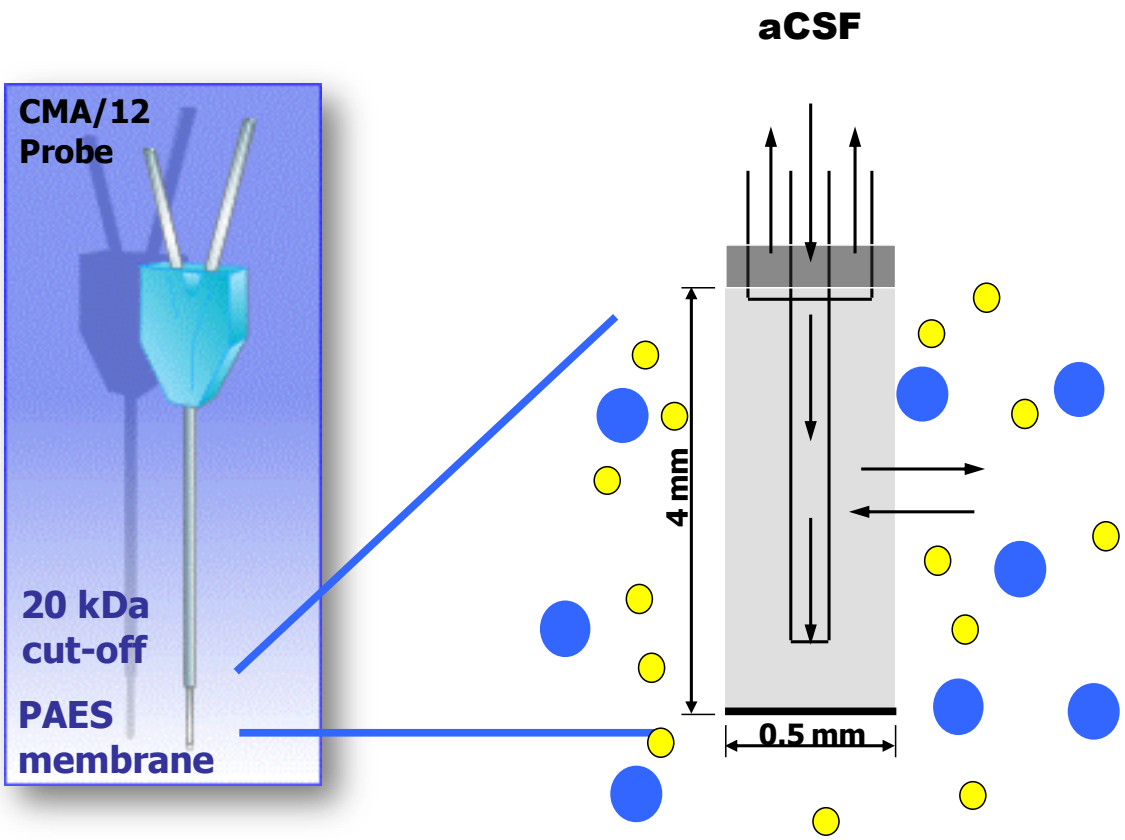

Figure 1.3: Scheme of the microdialysis probe utilized in this dissertation with 4 mm length and 0.5 mm diameter.

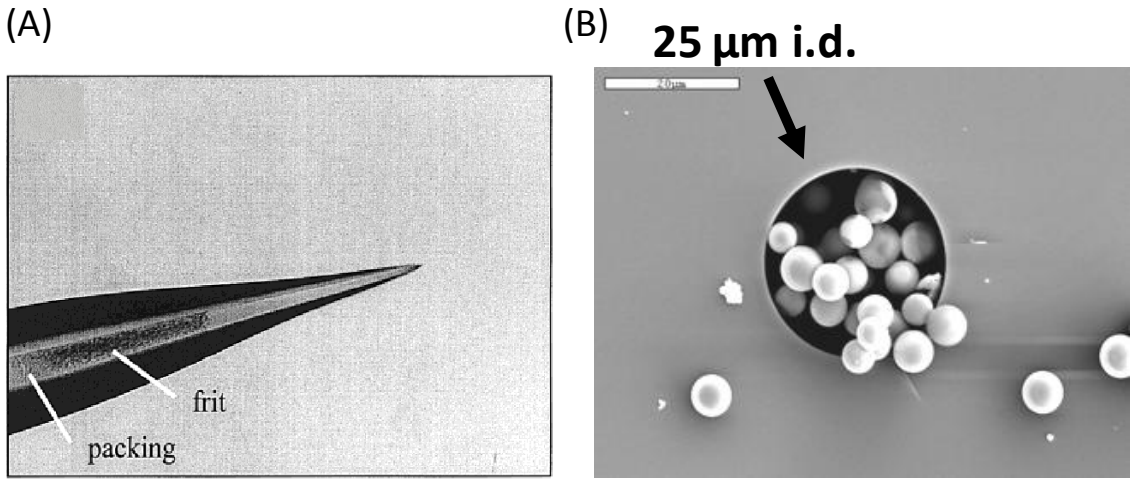

Figure 1.4: In-lab made reverse phase column with 25 µm i.d. (A) Picture of the integrated emitter tip at the end of the column, the photopolymerized frit and packing of column. (B) SEM photo of cross section of packed column with 5 µm diameter particles.

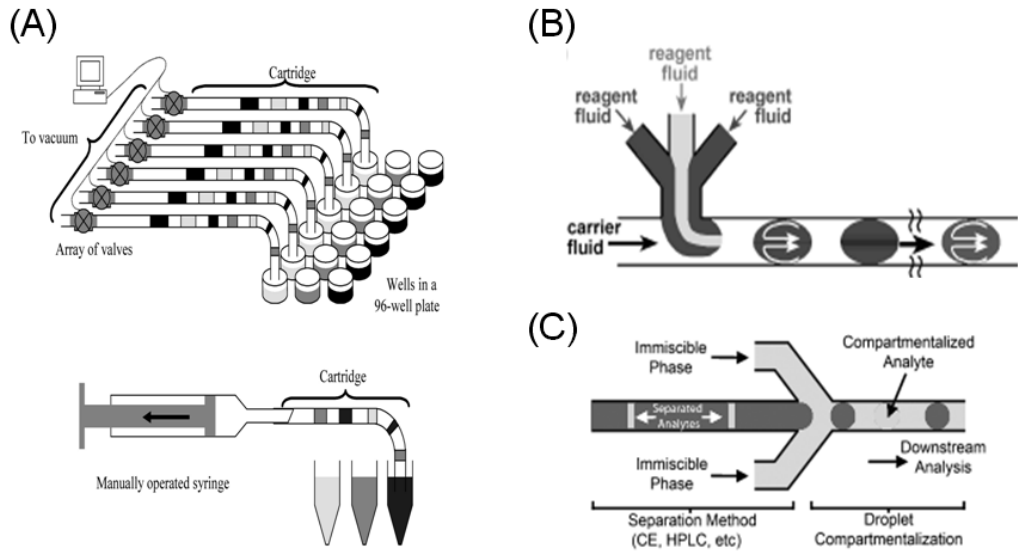

Figure 1.5: Three common methods of microfluidic segmented flow generation. (A) Generating droplets from a 96-wellplate with syringe pump in pulling mode.[184] Inlets of the tubing are inserted into sample and oil alternatively. (B) Droplet generation using a T-junction with oil as the carrier fluid.[185] Aqueous sample breaks off at the junction and forms sample plugs or droplets in the tubing. (C) Droplet generation using a flow-focusing geometry. In this example, effluents from a CE separation are compartmented into droplets containing separated components.[186]

Table 1.1: Summary of neuropeptide detection methods and their LODs

Analytes	Experiment Type	Method	Sampling technique (if applicable)	LOD with references
ME LE	Method development w/ testing in vivo	Capillary LC-electrochemical detection	microdialysis	20 pM (ME) [84]
	Method development w/ testing in vivo	HPLC-electrochemical detection	push-pull	0.15 pM (ME) 0.05 pM (LE) [85]
	Method development w/ testing in vivo	LC-MS2 or MS3	microdialysis	1 pM (ME) 0.5 pM (LE) [53, 86, 87, 187]
	Method development	CE		nM level[90-93]
Dyn	Method development w/ testing in vivo	RIA	microdialysis	3 nM[95]
	Method development w/ testing in vivo	LC-MS	microdialysis	40 pM[187]
BE	Method development w/ testing in vivo	LC-MS	microdialysis	5 nM (BE) 3 pM (BE10-19) [187]
EM1 & 2	Method development w/ testing in vivo	HPLC-electrochemical detection	push-pull	0.04 pM (EM 1) 0.15 pM (EM 2) [85]
OXT	Method development w/ testing in vivo	RIA	microdialysis	N/A[107]
VP/ CRH	Method development w/ testing in vivo	RIA	push-pull	N/A[108]
GHRH	Method development w/ testing in vivo	RIA	push-pull	N/A[115, 116]
TRH	Method development w/ testing in vivo	HPLC-RIA		N/A[117-119]
SOM	Method development w/ testing in vivo	RIA and ELISA	microdialysis	13.0 pM (RIA) 24.4 pM (ELISA) [120]

SP	Method development w/ testing in vivo	RIA		N/A[123]
	Method development w/ testing in vivo	CZE		250 nM[124]
	Method development w/ testing in vivo	CE-LIF		100 pM[125]
	Method development w/ testing in vivo	LC-MS		667 pM[126]
NKA NKB	Method development w/ testing in vivo	CE-LIF		0.04 nM (NKA) 0.2 nM (NKB) [130, 131]
NPY	Method development w/ testing on plasma sample	HPLC-ESI-MS		5 nM[136]
	Method development w/ testing in vivo	RIA	microdialysis	N/A[137]
VIP	Method development w/ testing in vivo	HPLC for sample purification CZE-UV		1 μM[141]
NT	Method development w/ testing in vivo	RIA	microdialysis	N/A[137]
	Method development w/ testing in vivo	CZE-UV		4.5 nM[145]
	Method development w/ testing in vivo	CE-ESI-MS		0.2 μM[146]
	Method development	capillary LC-UV-MS		600 pM[147]
	Method development w/ testing in vivo	CE-LIF		0.1 nM[131]
N/OFQ	Method development w/ testing in vivo	RIA	microdialysis	N/A[152]
CCK	Method development w/	RIA	microdialysis	0.3–0.6 pM[154, 155]

	testing in vivo			
GAL	Method development	LC-MS		3 nM[158]
	Method development w/ testing in vivo	RIA	microdialysis	7.9 pM[159]
	Method development w/ testing in vivo	HPLC-RIA	microdialysis	7 pM[160]
CGRP α and β	Method development	CEC	microdialysis	N/A[162]
a-MSH	Method development w/ testing at animal skin	EIA	microdialysis	N/A[166]
Hcrt	Method development w/ testing in vivo	RIA	microdialysis	10 pM[168]
ANG	Method development w/ testing in vivo	nanoLC-MS	microdialysis	50 pM[170, 171]

Table 1.2: Reported *in vivo* dialysate concentrations of neuropeptides as measured by microdialysis in rats unless otherwise noted.

Neuropeptide	*In vivo* concentration (all converted to pM)	Brain region
ME	127 ± 16 pM[187] 110, 50 pM[53]	striatum (rat)
LE	51 ± 9 pM[187] 36, 23 pM[53]	striatum (rat)
Dyn	78 ± 7 pM[187]	striatum (rat)
BE	109 ± 7 pM[187]	striatum (rat)
EM2	1259 ± 297 pM[85]	spinal cord (rat)
VP	~ 25 pM[108]	anterior pituitary (rat)
CRH	~ 25-40 pM[108]	anterior pituitary (rat)
GHRH	40 pg/mL[115, 116] ~ 8 pM	hypothalamus (cattle)
SOM	333 ± 8 pM[120]	striatum (rat)
SP	23.5 pM[123]	human CSF
NKA	2.31/2.24 nM[130]	human CSF
NPY	26.1 ± 3.5 pM[137]	ventral stiatum (rat)
VIP	25.5 ± 7.5 pmol per gram of tissue[141]	cerebral cortex tissue (rat)
NT	49.7 ± 7.0 pM[137]	ventral stiatum (rat)
N/OFQ	63 ± 12 pM / 60 ± 8 pM [152]	hippocampus/ thalamus (rat)
CCK	2.3 ± 0.1 pM[155]	anterior cingulated cortex (ACC) (rat)
GAL	7.9 pM[159]	spinal cord (rat)
Hcrt	~ 60 pM (BF) ~ 75 pM (HYP) ~ 45 pM (LC) [168]	basal forebrain (BF), perifornical hypothalamus (HYP), and locus ceruleus (LC) (rat)
Ang	46 pM [171]	globus pallidus/ventral pallidum (GP/VP) (rat)

CHAPTER 2

PRACTICAL ASPECTS OF IN VIVO DETECTION OF NEUROPEPTIDES BY MICRODIALYSIS COUPLED OFF-LINE TO CAPILLARY LC WITH MULTI-STAGE MS

2.1. Introduction

Neuropeptides constitute a large family of over 100 intercellular signaling molecules in the CNS. An important route to studying the function of peptidergic neurotransmitters and neuromodulators is to determine their concentration dynamics in the brain. Although measurements of mRNA or peptide content in tissue can be used for some studies, *in vivo* measurements allow direct detection of extracellular peptide rather than only peptide content, enable direct correlation to behavior, and use fewer animals. PET is one approach to estimate peptides *in vivo*; however, this method is expensive, not compatible with freely moving animals, and is presently limited to just a few peptides.[188] Microdialysis sampling combined with analysis of collected fractions is the most popular approach for *in vivo* neuropeptide studies;[189, 190] however, use of this method is challenging because of low *in vivo* concentration of peptides (1-100 pM) and low recovery of peptides by microdialysis (< 20% typically). Thus the assay method for neuropeptides must be sensitive enough to quantify picomolar concentrations in microliter volumes and robust enough to quantify peptide in many fractions collected.

Determination of endogenous peptides in microdialysis samples is often performed

using immunologic methods, in particular RIA.[159, 191, 192] Although RIAs can be developed with the requisite detection limits (100 amol), maintaining this sensitivity for routine measurements can be difficult. Immunoassays also have questionable specificity because of cross-reactivity between the target peptide and related peptides such as precursors and metabolites.[193, 194] Furthermore, RIAs are usually limited to measurement of a single peptide per sample. For these reasons, other approaches to peptide assay have been sought for dialysis samples.

One promising method for peptide determinations in dialysate is capillary LC coupled with MS^n.[195-198] This method has been shown to yield attomole detection limits, sequence specificity, and multi-analyte capability. Although LC-MS^n is promising, it has several limitations and unknowns for routine use. First, peptides in dialysates are unstable resulting in decreasing concentration as samples are stored. A second problem has been that the most sensitive peptide detection has been achieved on small bore columns (25 μm i.d.) which are not commercially available. Larger columns may be used if larger volumes of dialysate are collected; however, the relative merits and interaction of different dialysis flow rates and column inner diameters have not been quantified. Finally, the only endogenous peptides that have been quantified *in vivo* using capillary LC-MS are ME and LE,[198-200] NT[195] and Ang[170], although several others have been detected.[174, 200] The potential for monitoring of other peptides in brain has not been reported. We have addressed these issues by: 1) developing a sample storage method that stabilizes dialysate peptide, 2) quantitatively evaluating the effect of dialysis flow rate and column inner diameter on peptide detection in dialysate, and 3) exploring sensitivity for different neuropeptides. The latter study revealed that a large neuropeptide BE had

high LODs when detected directly but much better LODs could be achieved by digesting the peptide with trypsin and detecting a characteristic fragment. This approach may prove useful for other large neuropeptides as well. Overall, this collection of advances increases the practicality of using capillary LC-MS^n for *in vivo* neuropeptide measurements.

The method is demonstrated and validated for *in vivo* measurements of opioid peptides. The most important opioid peptides are enkephalins,[201] dynorphin,[202, 203] BE,[204] and the endomorphins.[12] These peptides, which are derived from the protein precursors proenkephalin, prodynorphin, and proopiomelanocortin (for both BE and endomorphins), exert their effects through binding to the μ, δ, and κ opioid receptors. Endogenous opioids have been implicated in many important functions including pain transmission, reward mechanisms, stress responses, food intake, and learning and memory. The ability to monitor this family of peptides *in vivo* may prove useful in elucidating their role in these processes.

2.2. Experimental Section

Chemicals and Reagents. Capillary LC solvents were purchased from Burdick & Jackson (Muskegon, MI). Enkephalins, Dynorphin A_{1-8} (Dyn A_{1-8}), other neuropeptides, and proteomics grade Trypsin were from Sigma-Aldrich. BE was from AnaSpec, Inc. (San Jose, CA). Ethanol, acetic acid, and hydrofluoric acid were purchased from Fisher Scientific (Pittsburgh, PA). The chemicals to prepare macroporous photopolymer frits, including isooctane, toluene, trimethylolpropane trimethacrylate, glycidyl methacrylate, and benzoin methyl ether (BME) were purchased from Sigma-Aldrich. Arificial cerebral

spinal fluid (aCSF) used for microdialysis perfusion consisted of 145 mM NaCl, 2.68 mM KCl, 1.10 mM $MgSO_4$, 1.22 mM $CaCl_2$, 0.50 mM NaH_2PO_4, and 1.55 mM Na_2HPO_4, adjusted pH to 7.4 with 0.1 M NaOH. High K^+ aCSF solution was the same as aCSF but with 75 mM KCl and NaCl reduced by a comparable amount to maintain ionic strength. Mobile phases and aCSF were prepared weekly and were filtered with 0.02 μm-pore filters (Whatman, Maidstone, England) to remove particulates. Fused silica capillary was from Polymicro Technologies (Phoenix, AZ).

Animals and *in vivo* Microdialysis. Adult male Sprague–Dawley rats (Harlan, Indianapolis, IN) weighing between 295 and 455 g were used for all experiments. The rats were kept in a temperature and humidity controlled room with 12 h light/dark cycles with food and water freely available. Each rat was used only once and euthanized on conclusion of the experiment. All animals were treated as approved by the University of Michigan Unit for Laboratory Animal Medicine (ULAM) and in accordance with the National Institute of Health (NIH) Guidelines for the Care and Use of Laboratory Animals.

Animals were initially given an intraperitoneal injection of 65 mg/kg ketamine (from Sigma) prepared in an isotonic salt solution with 33 mg/kg booster injections given as needed to maintain the surgical plane of anesthesia. 4 mm long microdialysis probes with polyarylethersulphone (PAES) membrane (CMA Microdialysis, North Chelmsford, MA, USA) were positioned and inserted into the striatum (1 mm anterior and 2.8 mm lateral of bregma to a depth of 8 mm from dura) using a stereotaxic instrument (David Kopf Instruments, Tujunga, CA, USA). The probes were perfused for at least 1 h after insertion prior to data collection.

For experiments requiring stimulation for neuronal depolarization, the aCSF perfusion syringe was switched by a connection with Teflon tubing to a 75 mM K^+ aCSF solution. All aCSF solutions were syringe filtered (0.02 μm, Anotop 10, Whatman, Maidstone, England) immediately preceding use. Following a recording session the animal was euthanized and the brain immediately removed and frozen at -80 C until histology. Probe position was verified by visual examination of 35 μm sections taken via microtome (Leica, SM2000R, Bannockburn, IL).

Trypsin Digestion of BE. 0.5 μL of 870 pM trypsin dissolved in NH_4HCO_3 buffer (pH = 7.8) was added to 5 μL of standard or dialysate sample. BE in dialysate was circa 100 pM, so the enzyme:substrate molar ratio was near 1:1 in the reaction mixture. (This ratio is higher than general trypsin digestion reaction for larger samples, but was found to yield best digestion with minimal background for the small samples with low concentrations.) The mixture was incubated at 37 C for 6 hours and then frozen at -80 C following addition of 0.5 μL glacial acetic acid until detection.

Neuropeptide Detection with Capillary LC-MS^3. Chromatography columns with integrated electrospray emitter tips were prepared in-house from 28 cm lengths of 25 μm i.d. fused silica capillary. To prepare columns, a ~500 μm long section of polyimide coating was removed 5 cm from one end of the tubing by rotating within the electric arc created it between two tungsten electrodes with 7.6 kV applied between them. An additional 1 cm coating nearer to the tip side was removed with a flame. Capillaries were filled with a photopolymer solution as described before[200] using He gas pressure and placed inside PEEK sleeves (Upchurch Scientific, Oak Harbor, WA) so that only the 500 μm section of bare fused silica was exposed. Polymerization was achieved by

illuminating the exposed region of the capillary with a UV lamp (Spectronics, Westbury, NY) for 30 min. (In practice, 20 capillary frits were prepared simultaneously.) Frits were flushed with acetone and dried for storage by passing He gas through the capillaries for 2 min at 500 psi. A P-2000 CO_2 laser puller (Sutter Instruments, Novato, CA) was used to create integrated electrospray emitters near the frit. The settings used on the laser puller were cycled once (line 1: heat 300, velocity 30, delay 128, pull 0; line 2: heat 300, velocity 30, delay 128, pull 125). The resulting pulled columns were etched with 49% hydrofluoric acid for 45 seconds to create sharp-edged electrospray emitters with 4 μm i.d., verified by scanning electron microscopy. Pulled columns were packed with an acetone slurry (5 mg/mL) of 5 μm Alltima C18 reversed-phase particles (Alltech, Deerfield, IL) at 500 psi as described elsewhere.[205] 4 cm of the total 20 cm length of fused silica was packed. Peptide samples were injected in weak mobile phases to allow the analytes to stack at the head of the column; therefore, the void at the head of the column did not contribute to extracolumn band broadening.

The capillary LC system utilizes a high pressure (4000 psi) pump (Haskel Inc., Burbank, CA) for sample loading and desalting, and a lower pressure (500 psi) micro HPLC pump (MicroPro, Eldex Laboratories, Napa, CA) for gradient separation (Figure 2.1). Switching between the two pumps gives a higher flow rate for loading and desalting and a lower flow rate for efficient separation and electrospray ionization without requiring equilibration of the pumping system at the different flow rates. Typically a 7 min sample loading time and 8 min desalting time was used for a 5 μL sample. The gradient program for separation consisted of an isocratic step of 10% B for 1 min, linear increase to 95% over 2.5 min, followed by isocratic at 95% B for 0.5 min.

Mobile phase A consisted of water with 2% acetic acid and mobile phase B consisted of methanol with 2% acetic acid. The final flow rate in the separation column (after flow splitting) was 90 nL/min, as measured using a SLG1430 l flow meter from Sensirion (Stäfa, Switzerland). The column was coupled to either a Finnigan™ nanospray ionization source (Thermo Fisher Scientific, Waltham, MA, USA) or a PV-550 nanospray ESI source (New Objective, Woburn, MA, USA) interfaced to an LTQ XL linear ion trap (LIT) MS (Thermo Fisher Scientific). A +3.0 kV potential was applied to a liquid junction prior to the column for electrospray.

Samples were injected using a WPS-3000TPL autosampler (Dionex, Sunnyvale, CA), which has the capability of operating different injection modes according to sample requirements. To inject 4 µL from a 5 µL volume the "microliter pickup" mode was used which sandwiches the sample volume between transport liquid (water) in a 10 µL sample loop. With this method, most of the *in vivo* sample could be injected with little waste. A washing program for the sample loop and injection needle between injections prevented carry-over between injections for concentrations < 1 nM.

The LIT-MS was operated in positive mode. All measurements were made with the following settings: automatic gain control (AGC) on, collisionally induced dissociation (CID), q = 0.25, isolation width 3 m/z, activation time 0.25 ms, micro scan number = 1 and default target count values. Collision energies were optimized for best sensitivity during constant infusion of each peptide. The MS^3 pathways for the 4 opioid neuropeptides were: 574→397→278, 323, 380 for Met-enkephalin (ME), 556→397→278, 323, 380 for Leu-enkephalin (LE), 491.5→435→417, 426, 694 for Dyn A_{1-8}, and 567→558→238, 450, 817 for tryptic fragment BE_{10-19}. Identification of

granddaughter peaks used for quantification was based on the method in a previous study.[206] Optimization of the ion optics for maintaining the best sensitivity of the instrument was achieved by tuning with direct infusion of 18 nM neurotensin$_{1-11}$ in 50% methanol 2% acetic acid at 100 nL/min every 2 weeks.

2.3. Results and Discussion

Neuropeptide Sample Storage and Handling for Reliable Off-line Measurement. Dialysis measurements may be performed off-line, where samples are collected in fractions and stored for later analysis, or on-line, where the analysis of fractions is performed serially as dialysate is removed. Off-line measurements of neuropeptides in dialysate are hampered by severe loss of peptide signals in dialysis samples stored for more than a few hours. The effect of peptide sample deterioration on quantification can be ameliorated by adding isotopically labeled standards to dialysis sample;[170] however, this does not avoid the problem of sample loss and subsequent effect on sensitivity. We previously avoided sample loss by using on-line analysis.[198, 200] Although on-line analysis limits degradation, it has the drawback of limiting temporal resolution to the chromatographic analysis time. Furthermore, a practical effect was that if a problem occurred with the analytical method during an experiment (such as column clogging or leaks), then it was difficult to recover and resulted in loss of the experiment.

In view of these persistent difficulties, we sought storage conditions that would stabilize peptides in dialysate samples and allow off-line measurements. Pilot experiments were performed by storing solutions of 600 pM LE in aCSF under different conditions and monitoring the LE content in the samples over time. As shown in Figure

2.2A, addition of acetic acid to a final concentration of 5% and storage at -80 C prevented the rapid degradation seen without this combination (Figure 2.2A). This method also proved effective for neurotensin$_{1-13}$ (NT_{1-13}) and $DynA_{1-8}$ standard samples (Figure 2.2B). We then determined the effectiveness of this procedure for ME, LE, and Dyn A_{1-8} in dialysis samples collected *in vivo*. As shown in Figure 2.2C, this method allows storage with minimal loss of sample for ~ 5 days. By day 10 however, degradation is significant.

The reason for the effectiveness of the acid treatment in aiding storage at -80 C was not explored; however, it can reasonably be attributed to inhibition of enzyme activity that might be associated with microbial contamination, minimization of oxidation rates of peptides prone to this reaction, such as those containing tyrosine, cysteine, or methionine residues[207], and prevention of adsorption by minimizing electrostatic attraction by protonating both the peptides and surfaces of capillary tubing and vials.[208]

Effect of Microdialysis Flow Rate and Column Size on Neuropeptide Detection. In designing a microdialysis experiment, the interaction of column i.d., dialysis flow rate, and sample volume must be considered. We have previously advocated use of small bore columns (25 μm i.d.) based on their better sensitivity compared to larger bore columns (e.g., 75 μm i.d.).[209, 210] On the other hand, larger bore columns are commercially available and presumably easier to use. The preferred column may be affected by the dialysis flow rate used. Low flow rates increase the concentration of peptide in dialysate (relative recovery), but also decrease both the total mass of peptide collected (absolute recovery) and the total volume available for analysis. This situation would be more suited to small bore columns. An alternative approach is to use high dialysis flow rates to generate larger volume samples and inject onto larger bore columns to gain the

convenience of working with larger collection volumes and bigger columns. This method would be especially advantageous if the sensitivity advantage of smaller columns can be offset by injecting and preconcentrating larger volumes on larger bore columns.

To gain a quantitative understanding of these relationships, we evaluated the recovery and sensitivity under a variety of conditions using LE as a model peptide. As shown in Figure 2.3A, the absolute recovery increases with flow rate; however, the effect is small with only a 9.5% increase over the flow rate range investigated. In contrast, the concentration collected has a dramatic increase of 3.7-fold with lowering of flow rate. (For these experiments we utilized a PAES probe, which we found in preliminary experiments to have good recoveries for a variety of peptides.)

We also determined the difference in sensitivity on 25 and 75 μm i.d. columns for a given injection volume and linear flow velocity (Figure 2.3B). These experiments revealed that the smaller columns had an approximately 10-fold improved sensitivity. The increase in sensitivity with small capillary i.d. can be attributed to: 1) more effective on-column concentration of the mass that is loaded onto the column, 2) reduced mass flow rate of solvents and other background constituents into the ESI source, which allows for greater analyte ionization efficiency, [211, 212] and 3) inherent decreased electrospray tip inner diameter which increases the ionization efficiency resulting from initial smaller droplets formed.[213] Although all these factors likely contribute, it appears that the majority of the enhancement can be accounted for by the 9-fold concentration enhancement expected for a 3-fold column i.d. reduction.

With the sensitivity and recovery data, we then calculated how varying column i.d. and dialysis flow rate would affect the measurements of peptide as summarized in Table

2.1. For this table, we assumed samples were collected for 20 min. We then calculated the relative amount of sample that could be injected onto the column and the relative signal that would be obtained based on the difference in sensitivity. (All calculated parameters were made relative to the smallest column and lowest flow rate.) Injection volume was a function of both the sample available and how much could be practically injected. With the autosampler used in these experiments it was possible to inject 3 μL from a 4 μL sample and 7 μL from a 10 μL sample. Another consideration was the maximal sample volume that could be loaded quantitatively loaded onto the column. If the injection volume becomes too large, analyte elutes from the column before injection begins resulting in non-quantitative injections.[214] In separate experiments we determined that the volume limit was 10 μL for a 25 μm i.d. column and assumed a 9-fold larger volume for the 75 μm i.d. column. Therefore, at higher dialysis flow rates even though 40 μL was available, only 10 μL was considered to be loaded onto the smaller bore columns.

Based on these considerations, we can see that at lower dialysis flow rates the same amount of sample can be loaded onto both sizes of column (Table 2.1). At higher dialysis flow rates, more sample can be loaded onto the bigger columns allowing more of the sample available to be used. Despite the better loading capacity of the bigger columns, the enhanced sensitivity of the smaller columns means that they yield the better relative signal under all conditions except at the highest flow rates. Furthermore, this difference can be as large as 10-fold.

These results help quantify the advantages of working with smaller bore columns and lower flow rate microdialysis. The effect observed will depend on the collection

time. If longer collection times were used, corresponding to lower temporal resolution for the measurement, then the smaller columns have less of an advantage. Conversely, the advantage of smaller columns will be greater when higher temporal resolution is desired. These results do not mean that only smaller columns and low flow rates can be successful for *in vivo* measurements, but they do illustrate the substantial benefits for sample limited analysis such as peptide dialysates.

25 μm i.d. Column Stability. As suggested by the above results, 25 μm i.d. columns are preferred for achieving high sensitivity. However, using such small columns leads to higher possibility of clogging which is initially detected as a decrease in peak area due to lower flow rate during column loading (all injections are based on loading for a fixed time). Indeed, in previous work we used a new column each day to prevent variability associated with gradual column clogging over longer periods.[198] We found that with filtering of all solutions that entered the column with every week and adding low dead volume (0.6 μL) in-line filters (Upchurch Scientific, INC.) to all lines that feed the column, such columns can be stable for 2-4 days with at least 10 injections each day.

Detection of a Variety of Neuropeptides with the cLC-MS^3 System. Previous work on *in vivo* detection of endogenous neuropeptides using LC-MS has been limited to ME, LE, NT_{1-13} and angiotensin. Therefore we sought to determine how widely applicable these procedures could be to different peptides by determining detection limits for a selection of 10 neuropeptides in 4 μL samples dissolved in aCSF (Table 2.2). For these experiments, we utilized MS^3 on a linear ion trap (LIT) MS, and in some cases a quadrupole ion trap (QIT) MS. MS^3 offered an ~5-fold improvement in LOD over MS^2 and was used for all experiments. As shown in Table 2.2, the LOD was generally better

when using the LIT than the QIT, although the difference was only substantial for peptides that had the worst LODs on the QIT.

Most of the peptides detected had LODs of 40 pM or better suggesting the potential to at least detect, if not quantify, peptides in dialysate. Two of the peptides were poorly detected though. Substance P is adsorptive and recent work suggests the possibility of obtaining much better detection limits for this peptide with procedures to mitigate this problem.[215]

BE was also found to have an LOD that would be too high for *in vivo* monitoring applications. The difficulties of detecting BE could be due to its hydrophilicity and size. BE is more hydrophilic than most of the other neuropeptides we examined, as estimated using the Bull and Breese index (B & B)[216, 217] (see Table 2.2), which tends to reduce ESI efficiency.[218] BE is also large enough that its signal is dispersed across many ions of different charge state reducing the abundance of the dominant ion chosen for collision and multiple stages of mass spectrometry.

We examined the possibility of detecting and quantifying BE based on detection of a characteristic peptide produced after tryptic digest. Of the ions detected in MS analysis of a BE tryptic digest (Figure 2.4A), the $[M+2H]^{2+}$ ion at m/z 567 corresponding to BE_{10-19} (as underlined in the amino acid sequence of BE_{1-31} YGGFMTSEKSQTPLVTLFK-NAIIKNVHKKGQ) is the most abundant. This peak was chosen for MS^3 and quantified for indication of intact BE concentration. Using this procedure we obtained an LOD of 3 pM for BE, representing an ~1,800-fold improvement over detecting the intact peptide. The improvement is likely due to both the smaller size of the fragment (and fewer charge states) and the greater hydrophobicity of the fragment (B & B index = -331 compared to -

99 for intact BE). Using this method, it was possible to detect and quantify BE in dialysate as illustrated by the mass chromatograms in Figure 2.4E. We also found that determination of BE by this method gave comparable reproducibility (RSD = ~13% for 58 pM sample, n = 3) to direct detection of other peptides. The calibration curve of BE resulted in an excellent linearity too with correlation coefficients of 0.99 from 58 to 580 pM (n = 3).

A trade-off for obtaining higher sensitivity by detecting the tryptic fragment is that some specificity is lost because the native peptide is not directly detected. As a negative control, we analyzed dialysate without tryptic digestion and found that the peptide was not detected (see Figure 2.4D) indicating that the peptide is not produced endogenously at detectable levels and therefore would not interfere with detection. A Basic Local Alignment Search Tool (BLAST) search revealed that the BE_{10-19} sequence is only found in proopiomelanocortin (POMC), the protein precursor of BE. Based on these results, we conclude that this peptide is a specific marker for BE or peptides that contain the BE sequence from POMC. We expect that this approach may also be useful for other larger neuropeptides as well.

***In Vivo* Monitoring of Opioid Peptides.** As a demonstration of this method, we used it to monitor 4 opioid peptides in microdialysis fractions collected off-line at 25 min intervals under basal conditions and during infusion of 75 mM K^+ aCSF through the probe in anesthetized rats. ME, Dyn A_{1-8}, and LE could be detected with one chromatographic separation as illustrated in Figure 2.5. Because BE required trypsin digestion, it was determined in separate experiments. Endomorphins were not detected despite the excellent LODs. These results suggest that even though these peptides are

produced from the same precursor as BE, their metabolism is such that they are present at lower concentrations. These peptides could be produced at lower amounts from the precursor, more rapidly degraded, or modified resulting in lower concentrations of the actual sequence tested.

The concentration of peptides in dialysate samples was determined by external calibration using standard solutions of peptide dissolved in aCSF as summarized in Table 2.3. Calibrations were performed by triplicate injections of 3 different concentrations (plus a blank) from 20-200 pM for ME and LE, 68-680 pM for Dyn A_{1-8} and 58-580 pM for BE. Calibrations were linear with correlation coefficients of 0.98 to 0.99. Peak area RSDs for standards were 7-9% across all calibrations for all analytes. To validate the use of external calibration, we performed a standard addition experiment by measuring the LE content of fractions collected *in vivo* before and after spiking 70 pM of standard LE to the dialysate. The spiked concentration increased the peak area of the LE peak by the amount predicted by the external calibration curve to within 9% (n = 6 fractions from 2 animals). Based on this result, we conclude that external calibration is adequate for quantification.

Our concentration of BE is ~66% lower than a previous report of 320 pM in dialysate measured by RIA [219]. This difference could be due to differences in sampling conditions and brain regions, but also could reflect the higher specificity of the LC-MS method. No direct measurement of Dyn A_{1-8} has previously been reported for comparison. For ME and LE, our data are in reasonable agreement to previous work in our lab although slightly higher (~15% increase for ME and 42% increase for LE compared to previous results)[198], which may reflect the use of off-line storage or different

dialysis probes. Our data show a ratio of ME and LE in striatum of ~2:1 under basal conditions, consistent with previous measurements of ME and LE in striatal tissue.[220] Interestingly, this ratio is different from the ratio of 6:1 for the copies of ME and LE in the precursor proenkephalin A indicating that processing of the precursor proteins (ME and LE can also be produced from other precursor opioid proteins) results in extracellular concentrations not directly predictable from copy number as previously noted.[221]

K^+ infusion evoked a substantial increase in all 4 peptides levels as expected due to depolarization of neurons (see Figure 2.6 and Table 2.3). The percent increase of ME and LE is comparable to previous reports.[198, 222] The dynamic information in Figure 2.6 illustrate that the release of peptide is not sustained for the entire time course of K^+ application. This likely reflects a limited supply of peptide available for release from neurons, but the potential that inhibition of secretion occurs over time cannot be ruled out based on this data.

One potential area for improvement for *in vivo* peptide measurements is reproducibility. Replicate measurements of standards had RSDs of 7% at 60 pM for LE. When standard solutions were sampled by microdialysis and collected into fractions, the RSDs were increased to 14% indicating additional variability associated with sampling, fraction collection, transport through the tubing, and manipulation of the small samples. RSDs measured in replicate fractions from a single animal (4 fractions per animal) under basal conditions averaged 15% for ME, 17% for LE, 24% for Dyn A_{1-8} and 18% for BE (n = 5 animals). For the enkephalins and BE, the RSD is comparable to the RSD of standards indicating that variability is mostly due to the analytical method. The comparable RSDs for BE and enkephalins support the conclusion that the trypsin

digestion procedure was reproducible and reliable for quantitative measurement. The higher RSD for Dyn A_{1-8} could be mainly due to the relatively high LOD for that peptide, indicating increased irreproducibility when measuring near the LOD. RSDs, especially for the more abundant peptides, could potentially be improved by using automated fraction collection or internal standards. Also, use of a triple quadrupole MS instead of an ion trap might also allow improvement of RSDs;[87] however, because of the limitation to MS^2 with such instruments, the LOD may not be as good as that achieved using MS^3 on the ion traps. Interestingly, the mean basal dialysate concentration of different rats tended to have larger RSDs for the enkephalins (42% for ME, 40% for LE, 15% for Dyn A_{1-8}, and 19% for BE), indicating that inter animal comparisons will have to account for these differences in individuals.

2.4. Conclusions

We have enhanced the potential for monitoring neuropeptides *in vivo* by microdialysis coupled with LC-MS^3. Treatment of collected fractions with acetic acid stabilizes samples so that they can be stored for days allowing off-line analysis. Study of different dialysis flow rates and column inner diameters reveal that best sensitivity is achieved with low flow rates and smaller bore columns. This advantage is not critical at low temporal resolution, but increases with the temporal resolution required. The approach is viable for a variety of peptides, based on sensitivity requirements; although some larger neuropeptides such as BE require detecting a tryptic fragment to obtain the requisite sensitivity. The method is demonstrated for 4 opioid peptides, including two previously undetected by LC-MS allowing initial *in vivo* concentration estimates to be

obtained. Further improvements in stability and availability of 25 μm i.d. columns as well as reproducibility are desirable to improve the utility of the method.

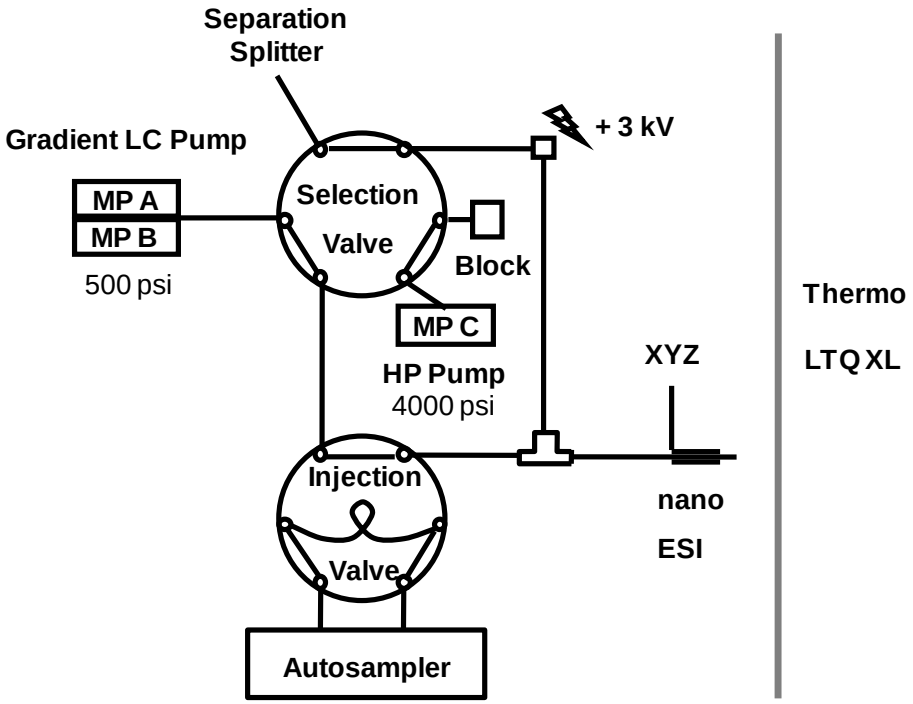

Figure 2.1: Diagram of the capillary LC system coupled with a linear ion trap MS. Mobile phase A (MP A) and mobile phase C (MP C) are both 2% acetic acid in H2O, while mobile phase B (MP B) is 2% acetic acid in methanol.

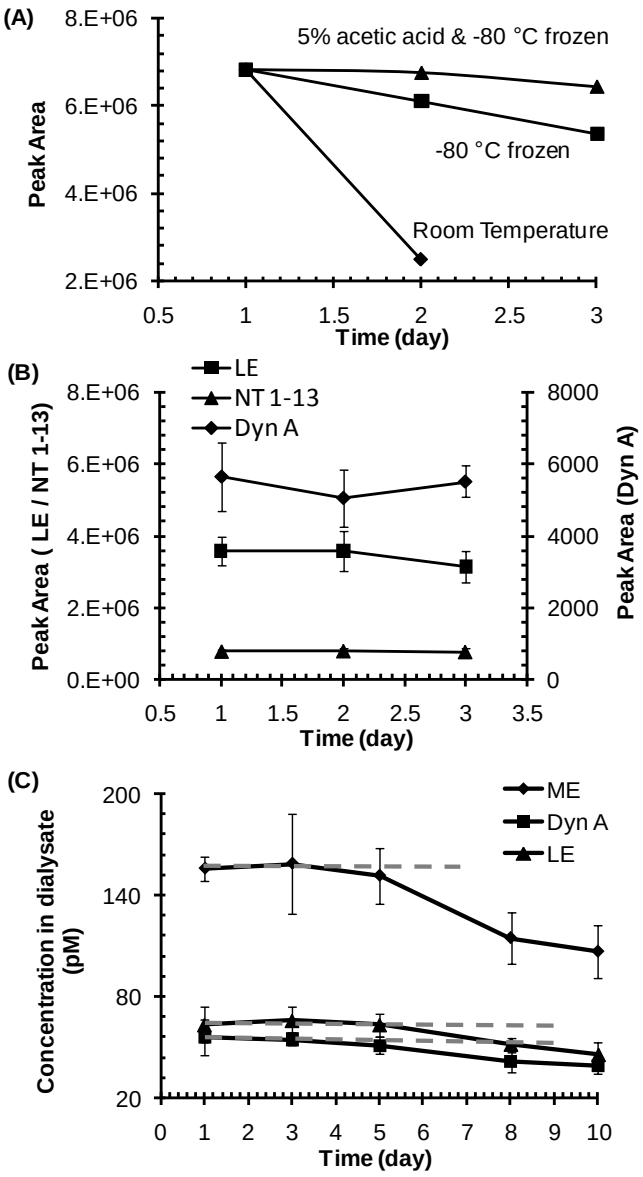

Figure 2.2: Effect of storge conditions on peptide detection. (A) Peak areas for 600 pM LE samples stored in aCSF at room temperature, -80 C, and -80 C with 5% acetic acid. (B) Peak areas of 60 pM LE, 66 pM NT1-13 and 68 pM Dyn A1-8 in aCSF with 5% acetic acid and stored at -80 C (n = 3, error bar = ± 1 standard deviation (SD)). (C) Measured concentration of ME, Dyn A1-8 and LE in dialysates stored over 10 days with 5% acetic acid at -80 C (n = 3, error bar = ± 1 SD). In this experiment, 15 basal *in vivo* dialysis samples were collected from an anesthetized rat at 25 min intervals with 0.2 µL/min aCSF perfusion rate. Acetic acid to a final concentration of 5% was added to the fractions which were then stored at -80 C. 3 of the 15 samples were chosen at random for analysis on the 1st, 3rd, 5th, 8th and 10th days after sample collection.

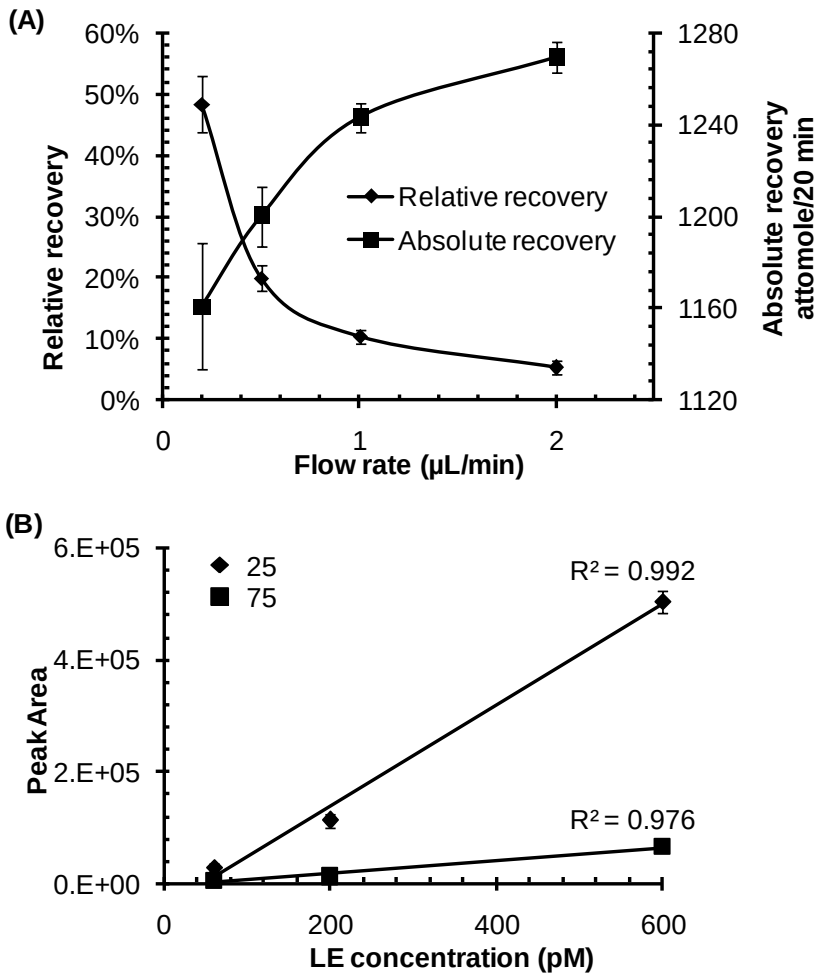

Figure 2.3: Effect of dialysis flow rate and column i.d. on detection of neuropeptides. (A) Relative and absolute recovery of microdialysis probe (CMA/12 Elite with PAES membrane, 4 mm long, MWCO 20 kDa) at 37 C with perfusion flow rate from 0.2 to 2 µL/min for LE. (B) Comparison of the calibration curve of LE on 25 µm and 75 µm i.d. columns (n = 3, error bar = ± 1 SD). Sensitivity is 10 fold higher on the smaller column.

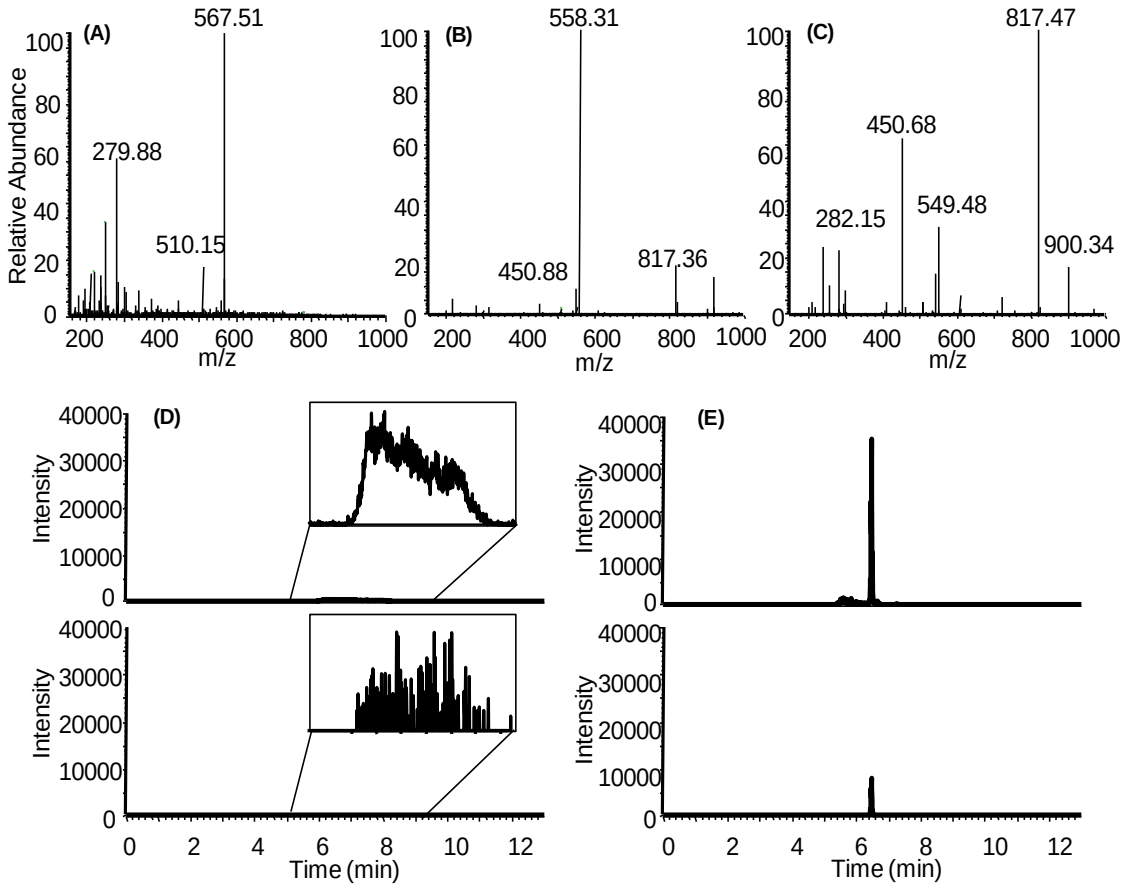

Figure 2.4: Detection of BE by a characteristic tryptic fragment. (A), (B), and (C) show MS, MS2 and MS3 spectra respectively of BE tryptic fragment BE10-19. Total ion chromatogram (TIC) and reconstructed ion chromatogram (RIC) of BE10-19 in an *in vivo* dialysate sample are illustrated without (D) and with (E) prior trypsin digestion. Lack of signal without digestion illustrates that this peptide is not present endogenously. Chromatograms in (D) and (E) are plotted on the same intensity scale for comparison. Inset in (D) shows the elution window for the peptide at ~1000-magnified scale on y-axis.

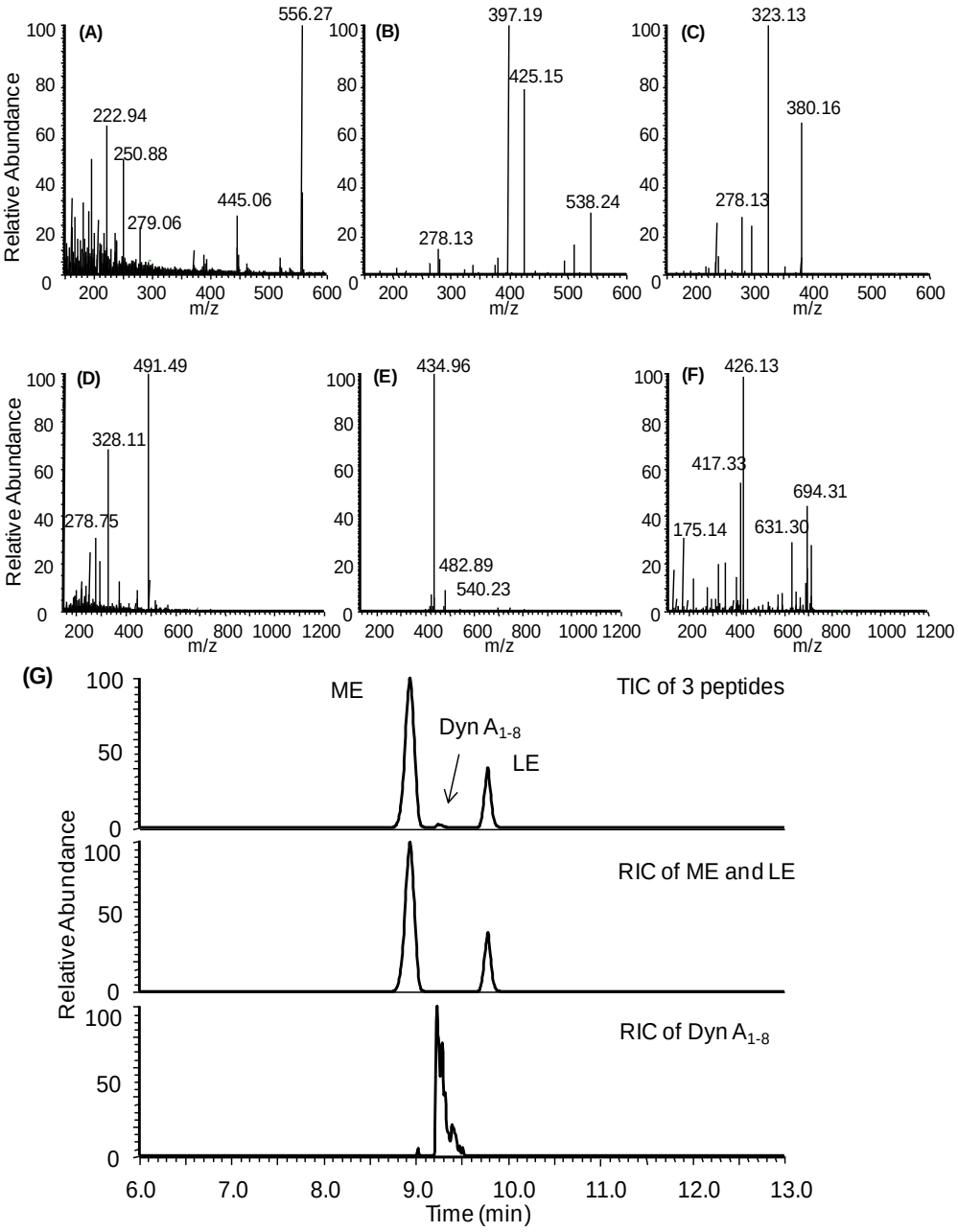

Figure 2.5: *In vivo* detection of enkephalins and Dyn A_{1-8}. (A), (B), and (C) show MS, MS^2 and MS^3 spectra of LE respectively. The ions chosen for CID were 556→397→278+323+380. (Spectra for ME are similar except the MH^+ peak is at m/z 574 in the first stage spectrum.) (D), (E), and (F) show the MS, MS^2 and MS^3 spectra respectively of Dyn A_{1-8}. The ions chosen for CID are 491→435→417+426+694. (G) Total ion chromatogram (TIC) and reconstructed ion chromatogram (RIC) of ME, Dyn A_{1-8}, and LE from an *in vivo* microdialysis sample. RIC were derived with the three most abundant MS^3 ions.

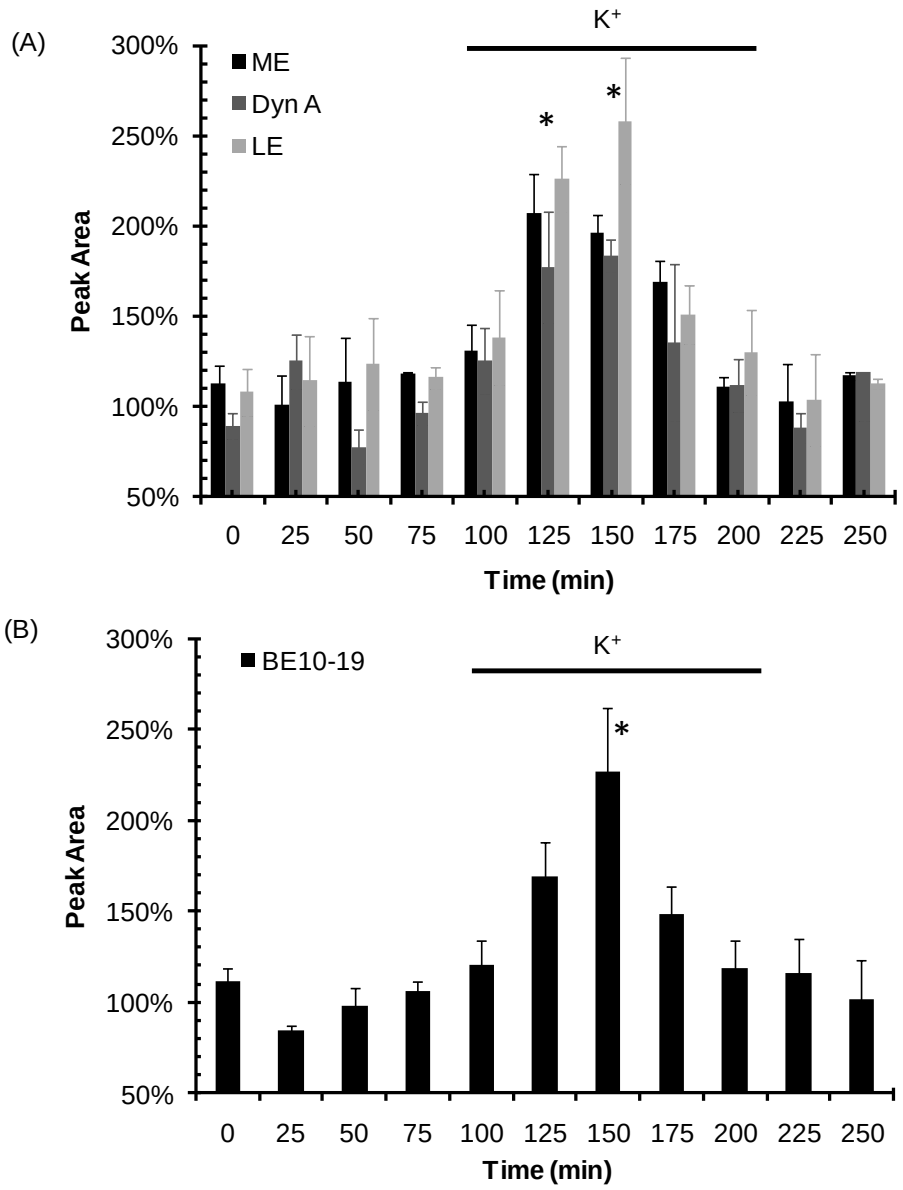

Figure 2.6: *In vivo* monitoring of opioid peptides. ME, Dyn A_{1-8} and LE were detected simultaneously (A) and BE, as a tryptic fragment, in separate rats (B). Fractions were collected at 25 min intervals and analyzed by LC-MS^3 (n = 3 rats, error bars = ±1 SEM). The bar indicates application of 75 mM K^+ to the microdialysis corrected for 25 min delay time due to the dead volume of connection tubing and the probe. The stimulated levels were significantly higher than baseline levels as determined by t-test (* $p<0.025$).

Table 2.1: Estimate of signal for LE with different microdiaysis flow rate on 25 and 75 μm i.d. columns. Calculations assume 20 min fraction collection times. Relative recoveries were used from Figure 3A. Calculation of amount loaded was based on the volume that could be injected onto a column (a function of column capacity and autosampler capability) and relative recovery. Amount was relative to the smallest column and lowest flow rate. Relative signal was calculated based on the amount loaded and the difference in sensitivity (10-fold as shown in Figure 3B). All values are relative to the lowest flow rate and smallest column.

Flow rate (μL/min)	**Sample volume for 20 min (μL)**	**Relative recovery**	**Column i.d. (μm)**	**Injection volume (μL)**	**Relative amount loaded on-column**	**Relative signal**
0.2	4	48.4%	25	3	1	1
			75	3	1	0.1
0.5	10	20.0%	25	7	0.96	0.96
			75	7	0.96	0.10
1	20	10.4%	25	10	0.72	0.72
			75	17	1.22	0.12
2	40	5.3%	25	10	0.37	0.04
			75	37	1.35	0.14

Table 2.2: LODs of 10 neuropeptides on our system. (EM 1 = endomorphin 1; EM 2 = endomorphin 2; Orp FQ = orphanin FQ; Oxy = oxytocin). LOD for BE is given for intact peptide and a characteristic tryptic peptide, BE_{10-19}, marked by *. Some peptides were also tested on a Finnigan LCQ Deca QIT. Bull and Breese index (B & B index) were calculated based on hydrophobicity scales of their amino acids, representing higher hydrophobicity with more negative value.[216]

Peptide	**Amino Acid Number**	**Molecular Weight**	**B & B index**	**LOD (concentrations in 4 µL volume)**	
				QIT	**LIT**
ME	5	573.7	-398	3 pM	1 pM
LE	5	555.6	-596	1 pM	0.5 pM
Dyn A_{1-8}	8	981.2	-381		40 pM
BE BE_{10-19}	31	3466.0	-99 -331	58 nM	5 nM (3 pM)*
EM 1	4	610.7	-1080		8 pM
EM 2	4	571.7	-1160		17 pM
Orp FQ	17	1809.1	261		60 pM
SP	11	1347.6	-121	100 nM	10 nM
NT_{1-13}	13	1672.9	-323	4 pM	4 pM
Oxy	9	1007.2	-146	6 nM	60 pM

Table 2.3: Summary of basal and stimulated dialysate concentration of ME, LE, Dyn A, and BE from striatum of anesthetized rats (n = 3). Stimulated results were obtained by perfusing 75 mM K^+ aCSF solution for 100 min. The stimulated levels were significantly higher than baseline levels as determined by t-test (* $p<0.025$). Corrected concentrations were calculated according to the average *in vitro* recovery and the dilution with addition of acetic acid and trypsin.

Concentration ± SEM (pM)	**ME**	**LE**	**Dyn A**	**BE**
Basal	127 ± 16	51 ± 9	78 ± 7	109 ± 7
Stimulated	223 ± 48*	106 ± 37*	109 ± 10*	206 ± 72*
Basal (corrected)	308 ± 40	110 ± 19	162 ± 15	299 ± 19
Stimulated (corrected)	542 ± 117	228 ± 80	228 ± 20	565 ± 197

CHAPTER 3

QUANTITATIVE *IN VIVO* MONITORING OF LEU-ENKEPHALIN IN RAT BRAIN WITH FIVE-MINUTE TEMPORAL RESOLUTION BY MICRODIALYSIS WITH CAPILLARY LC AND MULTI-STAGE MS

3.1. Introduction

Microdialysis sampling combined with analysis of collected fractions is a popular and versatile approach for *in vivo* neurotransmitter measurements.[223] Neuropeptide monitoring by this method is challenging because of low *in vivo* concentrations (1-100 pM) and low recovery of peptides by microdialysis (typically less than 20%). Thus, the assay method for neuropeptides must be sufficiently sensitive and robust to quantify picomolar (pM) concentrations of peptide in microliter (μL) volumes of a large number of fractions. One promising method for peptide determination in dialysates is capillary liquid chromatography (LC) coupled with multi-stage mass spectrometry (MS^n), which can achieve attomole detection limits and peptide sequence specificity.[53, 195-197]

A key figure-of-merit in the application of microdialysis to neurochemical analysis is temporal resolution, which affects the ability to record rapid changes of neurotransmitters in the brain with good accuracy and precision.[224-226] The temporal resolution possible with microdialysis sampling can be limited by several factors, including the mass detection limit of the quantification method, temporal broadening of concentration fronts as they are transported from the sampling probe to the fraction

collector or analyzer, and the time required for analysis (in the case of on-line measurements). Previous work with capillary LC-MS coupled on-line to microdialysis has shown that the analysis time, which includes preconcentration, desalting, gradient separation and column re-equilibration, limits temporal resolution to about 16 to 30 min. At 16-min temporal resolution, the reproducibility of the method was marginal, averaging 29% for *in vivo* basal LE detection.[53] In off-line detection, the temporal resolution for neuropeptides is usually determined by the time required to obtain sufficient sample for analysis.[51] Using radio immunoassay (RIA) for measurements, the temporal resolution has usually been limited to ~30 min [159, 227] or longer [228]. Using off-line capillary LC-MS^3, the best temporal resolution reported has been 25 min. However, the low detection limits should allow temporal resolution of about 3 min [52] in favorable cases. This improved temporal resolution has not previously been achieved, primarily because of the difficulty of manipulating the small fractions and the poor reproducibility of capillary LC-MS^3 near the limit of detection.[187]

In this work we demonstrate 5-min temporal resolution for monitoring leu-enkephalin (LE) by microdialysis coupled off-line to capillary LC-MS^3. Recent advances in commercial instruments for manipulating and injecting microliter samples onto capillary LC columns are used to solve sample handling problems, and incorporation of stable-isotope-labeled internal standards helps improve the reproducibility to acceptable levels for monitoring experiments. Although stable-isotope-labeled internal standards have recently found use for several proteomic applications [229-231], they have yet to be used with *in vivo* dialysis samples. The improved temporal resolution achieved in this work is demonstrated to allow more accurate observation of the dynamics of LE

concentrations during K^+-induced depolarization in rat brain.

3.2. Experimental Section

Chemicals and Reagents. Leu-enkephalin and fluorescein were purchased from Sigma-Aldrich (St. Louis, MO). Deuterated LE (dLE) with 8 deuterons on the phenylalanine residue was obtained from the Protein Structure Facility of University of Michigan (Ann Arbor, MI). Ethanol, acetic acid, and 49% hydrofluoric acid were purchased from Fisher Scientific (Pittsburgh, PA). The chemicals to make macroporous photopolymer frits (isooctane, toluene, trimethylolpropane trimethacrylate, glycidyl methacrylate, and benzoin methyl ether (BME)) were purchased from Sigma-Aldrich. The solution for photo polymerization was made with BME (1.5% w/w), glycidyl methacrylate (7% v/v) and trimethylolpropane trimethacrylate (16% v/v) in a 3:1 isooctane:toluene solvent. Capillary LC mobile phase (MP) solvents (methanol and water) were purchased from Burdick & Jackson (Muskegon, MI). Artificial cerebral spinal fluid (aCSF) used for microdialysis perfusion consisted of 145 mM NaCl, 2.68 mM KCl, 1.10 mM $MgSO_4$, and 1.22 mM $CaCl_2$, adjusted to pH 7.4 with 0.1 M NaOH. 75 mM K^+ aCSF solution contained 75 mM KCl with NaCl reduced by a comparable amount to maintain ionic strength. Mobile phase components and aCSF were prepared weekly and were filtered with 0.02 μm-pore filters (Whatman, Maidstone, England) to remove particulates. Fused silica capillaries were from Polymicro Technologies (Phoenix, AZ).

Fraction Collection from Microdialysis and Addition of Internal Standard. The apparatus depicted in Figure 3.1 was used for *in vivo* sample collection and

automated addition of IS to fractions. A syringe pump (CMA/102, CMA Microdialysis Inc., North Chelmsford, MA) with two channels was used to perfuse aCSF or 75 mM K^+ aCSF at 0.5 μL/min through a CMA12 Elite microdialysis probe with 4 mm membrane length (CMA Microdialysis Inc., North Chelmsford, MA). A six-port valve (Valco, Houston, TX) was used to switch between the two lines at the probe inlet. At the outlet of the probe, a tee junction with 100 μm i.d. (Cheminert® 360 μm, Valco) was used to add internal standard solution to dialysate. Internal standard solution consisted of 30 pM dLE in 10% acetic acid. The internal standard was added by a second CMA/102 pump at 0.5 μL/min so that the internal standard and dialysate were mixed in a 1:1 (v/v) yielding fractions with 5% acetic acid concentration. The mixed solution was collected into 250-μL polypropylene vials on ice. Fractions were stored at -80 ℃ prior to further analysis.

Testing the Limit of Temporal Resolution of the System. With short sampling intervals (a few minutes), the overall temporal resolution is influenced by band broadening associated with flow and diffusion effects (i.e., Taylor dispersion) within the perfusion system. To study these effects, the temporal response of the microdialysis system was examined by using fluorescein dissolved in aCSF as a test compound. Figure 3.2 shows the modified arrangement, having the same length (50 cm) of tubing for the inlet and outlet of the microdialysis probe and the same flow rate used for *in vivo* studies (0.5 μL/min), but with laser-induced fluorescence (LIF) detection for monitoring fluorescein. The detection point on the capillary was mounted on an epi-illumination inverted microscope (Axiovert 100, Carl Zeiss Inc.). Fluorescence was excited using the 488-nm line of an Ar^+ laser (Melles Griot, Carlsbad, CA), and collected at 1000 Hz using a LabView program written in-house. Igor Pro 6.01 (Wavemetrics, Inc., Lake Oswego,

OR) was used for data analysis and graphing.

Quantification of LE with Capillary LC-MS^3. Capillary columns with 25 μm i.d. were made in-house, according to the procedure described previously [187]. To prepare the column frits (20-28 per batch), a ~500 μm long section of polyimide coating from a 28 cm length of 25 μm i.d. fused silica capillary was removed by rotating within an electric arc between two tungsten electrodes with a 7.6 kV applied potential. An additional 1 cm coating nearer to the tip side was then removed with a flame. Capillaries were loaded with the photopolymer solution using He gas pressure and were placed inside PEEK sleeves (Upchurch Scientific, Oak Harbor, WA), so that only the 500 μm window was exposed. Polymerization was achieved by illuminating the exposed region of the capillary with a UV lamp (Spectronics, Westbury, NY) for 30 min. Frits were flushed with acetone and were dried for storage by passing He gas through the capillaries for 2 min at 500 psi. Prior to packing a column, a P-2000 CO_2 laser puller (Sutter Instruments, Novato, CA) was used to form an integrated electrospray emitter tip with the following settings (line1: heat 260, velocity 30, delay 128, pull 0; line 2: heat 260, velocity 30, delay 128, pull 125) to generate emitter tips with less than 1 μm orifices. The tip was then etched with 49% hydrofluoric acid for 1 min to create sharp-edged emitters of roughly 5 μm i.d. Pulled columns were packed to a length of 3 cm with an acetone slurry (5 mg/mL) of 5 μm Atlantis C18 reversed-phase particles (Alltech, Deerfield, IL) at 500 psi, as described elsewhere.[205] The Atlantis particles were found to have good compatibility with the 100% aqueous phase.

As described previously [187], the capillary LC system utilizes a high pressure (4000 psi) pump (Haskel Inc., Burbank, CA) for sample loading and desalting, and a lower

pressure (~400 psi) micro HPLC pump (MicroPro, Eldex Laboratories, Napa, CA) for gradient separations. A short solvent program was used for elution: isocratic at 10% B for 1 min, linear increase to 95% B over 2.5 min, isocratic at 95% B for an additional 0.5 min, where component A was 2% acetic acid in H_2O and component B was 2 % acetic acid in methanol. To shorten the sample run time, column re-equilibration times were overlapped with sample injection and desalting times, so that the total run time of a sample was reduced to 20 min compared to ~30 min in previous work.[187] The column was coupled to a PV-550 nanospray ESI source (New Objective, MA, USA) interfaced to an LTQ XL linear ion trap (LIT) MS (Thermo Fisher Scientific). A +1.5 kV potential was applied to the metal tee junction prior to the column to achieve nano electro-spray ionization (nanoESI).

The LIT-MS was operated in the positive-ion mode using the following settings: automatic gain control (AGC) on, activation type CID, q = 0.25, isolation width = 3 m/z, activation time = 0.25 ms, micro scan number = 1, and default target count values. Collision energies were optimized for highest sensitivity during constant infusion of 1 μM LE and dLE at 100 nL/min. The MS^3 transitions for LE were 556→397→323, 380, and for dLE were 564→405→330, 387. Identification of granddaughter peaks used for quantification was based on the method in a previous study.[206] Single reaction monitoring (SRM) of both LE and dLE was set in the instrument software (Xcalibur) with two scan events in the same time segment. In that way, the MS was switched between the LE and dLE pathways at 3 Hz to detect both species in the same analysis.

Samples were injected using a WPS-3000TPL autosampler (Dionex), which has the capability of different injection modes according to sample requirements. For *in vivo*

samples without IS, with 0.5 μL/min flow rate, the volume of each fraction was 2.5 μL. The "microliter pickup" mode on the autosampler was used to inject 2 μL from the 2.5 μL by sandwiching the sample between transport liquid (water) in a 5 μL sample loop. With this injection mode, most of the *in vivo* sample could be injected with little waste. When 2.5 μL internal standard was added, the volume for each dialysis fraction doubled to 5 μL, and the volume injected was doubled to 4 μL as well to counteract the 2-fold dilution of the LE and dLE. A washing program for the sample loop and injection needle between injections prevented carry-over between injections for concentrations < 200 pM.

Animals and in vivo Microdialysis. Adult male Sprague-Dawley rats (Harlan, Indianapolis, IN) weighing between 180 and 305 g were used for all experiments. The rats were kept in a temperature and humidity controlled room with 12 h light/dark cycles with food and water freely available. Each rat was used once and euthanized on conclusion of the experiment. All animals were treated as approved by the University of Michigan Unit for Laboratory Animal Medicine (ULAM) and in accordance with the National Institutes of Health (NIH) Guidelines for the Care and Use of Laboratory Animals.

For experiments performed on anesthetized rats, animals were initially given an intraperitoneal (i.p.) injection of 65 mg/kg ketamine (from Sigma) prepared in an isotonic salt solution with 33 mg/kg booster injections given as needed to maintain the surgical plane of anesthesia. Microdialysis probes were inserted into the striatum (1 mm anterior and 2.8 mm lateral of bregma to a depth of 8 mm from dura) using a stereotaxic instrument (David Kopf Instruments, Tujunga, CA, USA). The probes were perfused for at least 2 h after insertion prior to data collection. Following a recording session, the

animal was euthanized and the brain was immediately removed and frozen at -80 ℃ until histological examination was performed. The probe position was verified by visual examination of 40-μm sections taken via microtome (Leica, SM2000R, Bannockburn, IL).

3.3. Results and discussion

Simultaneous Detection of LE and dLE. Detection conditions for LE and dLE by MS^3 were first optimized by direct infusion of standard samples into the LIT MS. The resulting MS^3 spectra of LE and dLE are presented in Figure 3.3A and B, which show the shift of fragment peaks at m/z 323 and 380 of LE to m/z 330 and 387 due to the deuterons on the phenylalanine of dLE. Using a short gradient separation (see section 2.4), the LE and dLE co-eluted as shown in Figure 3.3C, indicating little isotopic effect on the separation.

Assay Precision. Previously we reported that the inter-column precision of measurements without an internal standard was variable, with some batches of columns giving relative standard deviations (RSD) of ~5% and others over 50% [187]. As a result, separate calibration was needed each time the column was changed. The situation improved dramatically with addition of internal standard, resulting in inter-column (inter-day) RSDs lower than 10% for a group of 4 different columns on different days within a range of 3 weeks. Therefore, repeated calibrations could be omitted to save time and labor.

Intra-column (intra-day) repeatability, determined by analyzing a standard containing 1:1 v/v 30 pM LE and 30 pM dLE with a final concentration of 15 pM for

each in a total injection volume of 4 μL, showed an RSD of 2% for sample signal, despite some shifts of the retention time of these peaks on a same column (RSD of retention times was 6%). Table 3.1 shows RSDs without and with the internal standard for three groups of samples: 30 pM LE standard samples, in vitro recovered microdialysis samples from 200 pM LE solution, and *in vivo* microdialysis basal samples from an anesthetized animal. As indicated in the table, the RSD was found to be over 30% for *in vivo* dialysates collected every 5 min from an anesthetized animal before adding the IS. The poor reproducibility was mainly due to three problems: increased variability of the injection volume using the "microliter pickup" mode compared to full-loop injection, increased variability in the sample collection time, and increased variability of manually pipetting (e.g. the acetic acid addition) of small sample fractions. Adding internal standard with the tee junction as shown in Figure 3.1 reduced all these three effects and thus reduced the final RSD for *in vivo* basal samples to approximately 10%.

Calibration and Sensitivity. Calibration curves, prepared by plotting the ratio of the peak areas of LE and dLE in reconstructed ion currents (RIC) of their mass chromatograms versus LE concentration before addition of the internal standard, indicate an LOD of about 2 pM in 2 μL for LE based on the amount that yielded a signal to noise ratio (S/N) of 3. The calibration curve had r^2=0.977 for LE samples from 10 pM to 120 pM, which covered the range of all *in vivo* dialysates.

It is known that co-eluting compounds may suppress each other's response in ESI-MS.[232] We observed an approximately 40% decrease in the 30 pM LE peak area when 30 pM dLE was added (n = 3, data not shown), indicating that the ion suppression effect occurred for these co-eluting peaks. As a trade-off, however, the co-eluting peak is the

best choice for improving reproducibility of quantification because both compounds experience the same ESI conditions. Therefore, despite suppressing sample signal to some extent, the method with dLE as internal standard was preferred.

Sample Stability. Addition of the isotopically labeled internal standard also corrects for sample stability problems [170]. In our previous work without the internal standard [187], sampled were stored with in 5% acetic acid at -80 ℃ to preserve *in vivo* samples. As shown in Figure 3.4, the LE signal in *in vivo* dialysate without treatment with acetic acid decreased over time, with approximately 50% LE decomposed after 10 h in the autosampler at 6 ℃. However, the ratio of LE/dLE in the same dialysates remained constant over a 12 hr period without treatment of acetic acid, indicating that dLE has a similar breakdown pattern as LE. Although in the final *in vivo* studies, all dialysates were stored in acetic acid and at -80 ℃ before detection, the addition of internal standard prolonged the stability of samples in the autosampler and made the procedure more efficient.

Microdialysis sampling temporal resolution. Although experiments can be performed with 5 min sampling interval, it is also possible that the temporal resolution could be limited by flow and diffusion effects (i.e., Taylor dispersion) within the fluidic system. To study these effects, signal transitions for fluorescein were examined at two points (#1 and #2 in Figure 3.2A). At detection point #1, the fluorescence signal was measured after switching the perfusate from water to 0.2 mM fluorescein to observe the pre-probe temporal resolution. This experiment mimicked the dispersion of a pharmacological agent or other stimulant (e.g., elevated K^+) prior to the probe. As shown in Figure 3.2C, the front was broadened to 60 s (10 to 90% rise time) in transport from

the valve to the probe. To observe the post-probe temporal resolution at point #2, the perfusion solution was fixed at 0.2 mM fluorescein, but the sample vial was rapidly altered from 0.2 mM to 2 mM fluorescein using pipettes to quickly change the solution surrounding the probe. This experiment mimicked a rapid change in concentration at the probe surface. As shown in Figure 3.2D, this experiment yielded a front with 120 s width. The dispersion in this experiment was limited primarily by mass transport across the probe membrane and Taylor dispersion during flow to the detection point, which is equivalent to reaching the fraction collector for an *in vivo* experiment. Finally, the overall temporal resolution was examined by switching the perfusion solution from water to 0.2 mM fluorescein and measuring the signal at point #2 of the recovered sample from a sample vial containing 2 mM fluorescein yielding a response of ~180 s (Figure 3.2E). These experiments show that for a pharmacological stimulation, the most rapid response that can be measured is 3 min, which is less than the 5 min sampling time. Therefore we conclude that the sampling time is the limiting factor in temporal resolution. If further improvement of temporal resolution is needed to be shorter than 3 min, supposing the mass sensitivity of the detection method is adequate, other methods, such as inducing segmented flow for sample collection [72], will be needed to reduce band broadening due to continuous flow.

Besides the temporal distortion, these experiments also showed that the delay time between the switching of the valve and the appearance of a change in the signal was 20 min. So for all *in vivo* experiments, the effective K^+ perfusion time is corrected for this system delay time.

Effects of temporal resolution on LE changes by K^+ stimulation. As a

demonstration of the potential for higher temporal resolution, the method was used to monitor LE in the microdialysis fractions collected off-line at both 20 min and 5 min intervals under basal conditions and during a 20 min infusion of 75 mM K^+ aCSF in the striatum of anesthetized rats. Figure 3.5 shows detection of endogenous LE and the added dLE from a dialysate sample. Four fractions of basal level were collected, with the first two points at a 20-min interval followed by two at 5-min interval. After switching to 75 mM K^+ aCSF, 10 more samples were collected every 5 min to cover a total of 50 min, and 2 additional samples were collected at 20 min intervals afterward. The injection volume was kept at 4 μL for all dialysis samples. In this way, the fraction number was limited to 16 for each animal, to make detection feasible within a single work day. The resulting mass chromatograms of LE and dLE comparing basal and maximal stimulated are shown in Figure 3.5A. The resulting dynamics of LE are shown in Figure 3.6. For comparison, we repeated the experiment but with constant collection of fractions at 20 min intervals with the results shown in Figure 3.5B and Figure 3.6. As shown, the larger fraction time yields a much reduced peak stimulation. Furthermore, the higher temporal resolution data reveals that the evoked peptide release rapidly peaks but then declines even the presence of elevated K^+. This result, which suggests either depletion of releasable peptide or activation of inhibitory mechanisms, cannot be observed with the 20 min temporal resolution.

The basal concentration of LE in dialysate samples was determined by external calibration to be 21.0±3.1 pM. Because of the excellent reproducibility and sensitivity, the method can be further applied to other neuropeptides with similar *in vivo* concentrations using the corresponding isotopically labeled compounds as internal

standards.

3.4. Conclusion

In this work, the minimum sampling interval for monitoring Leu-enkephalin, a model neuropeptide, by microdialysis was reduced from over 20 minutes to 5 minutes. In this method, fractions are analyzed via off-line capillary LC-MS^3 using isotopically labeled LE as the internal standard. Addition of the internal standard improves detection precision while keeps the LOD for LE at 4 attomole in aCSF. Moreover, the internal standard also corrects for the LE sample degradation in the dialysate for at least 12 hours. The analysis can easily be extended to other types of sampling methods, including brain tissue extraction, plasma and push-pull samples.

By lowering the temporal resolution to 5 min, dynamic studies of LE concentrations in rat brain under K^+ stimulation revealed a faster and larger change in the peptide level compared to detection with a more traditional temporal resolution of 20 min.

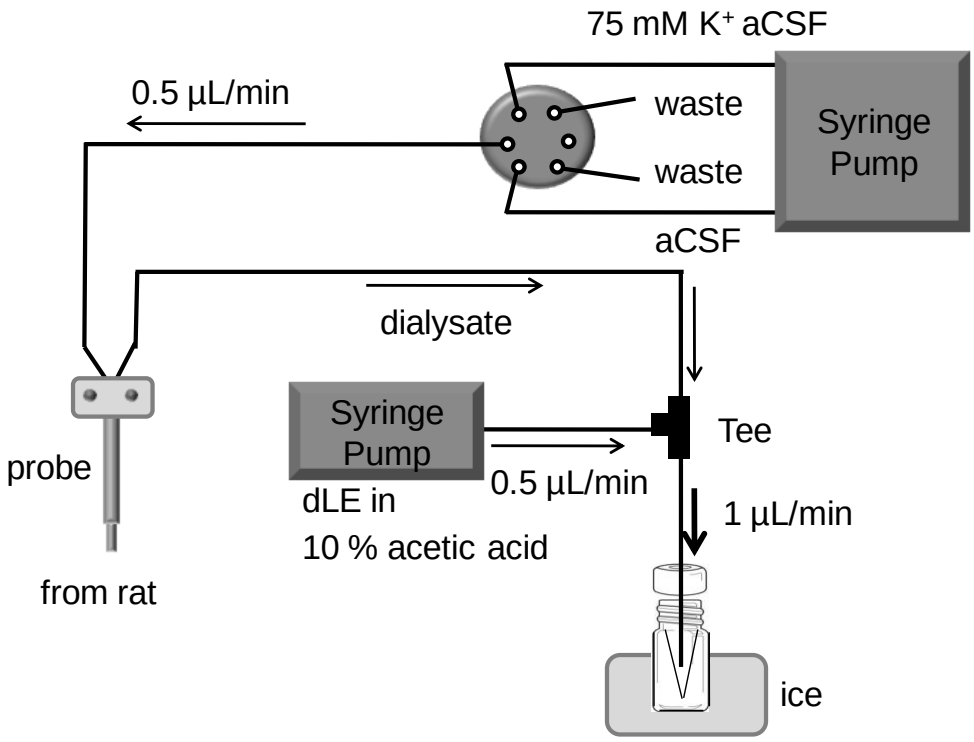

Figure 3.1: System configuration for *in vivo* sample collection. All connection are made with 100 µm i.d. fused silica capillaries. The inlet and outlet of the microdialysis probe are both 50-cm long.

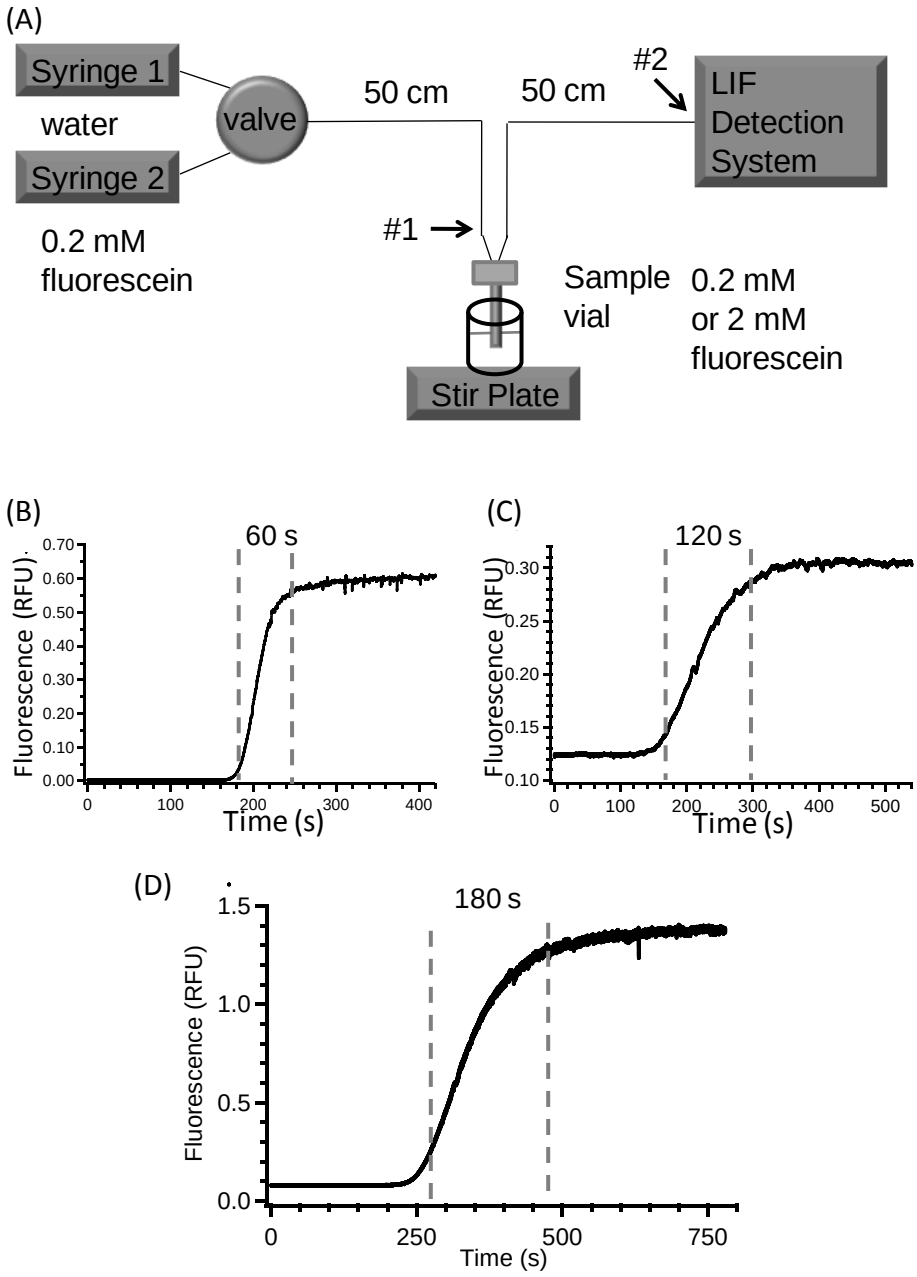

Figure 3.2: (A) System configuration for testing the temporal resolution with fluorescein mimicking a neuropeptide molecule. (B) Signal detected at point #1 when switching the valve from water to 0.2 mM fluorescein. (C) Signal detected at point #2 when the sample vial was switched from a low concentration (0.2 mM) to a higher concentration (2 mM) of fluorescein while keeping the perfusion solution constant at 0.2 mM. (D) Signal detected at point #2 after switching the perfusate from water to 0.2 mM fluorescein, in order to simulate the K^+ stimulation procedure. The temporal resolution in (B)(C)(D) were estimated as the time for the signal to increase from 10% above the minimum level to 10% below the maximum level.

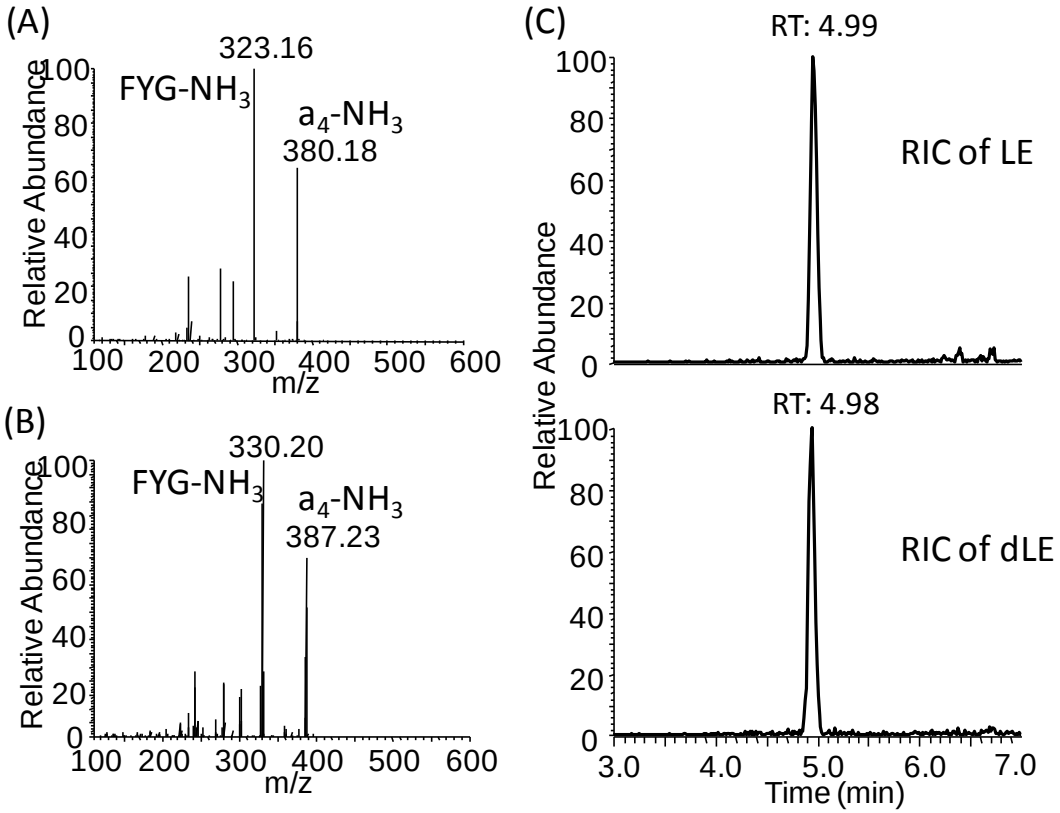

Figure 3.3: MS^3 spectra of LE (A) and dLE (B). (C) SRM chromatograms of a 1:1 volume ratio mixture of 30 pM LE (upper) and 30 pM dLE (lower) showing similar retention time (RT) of them.

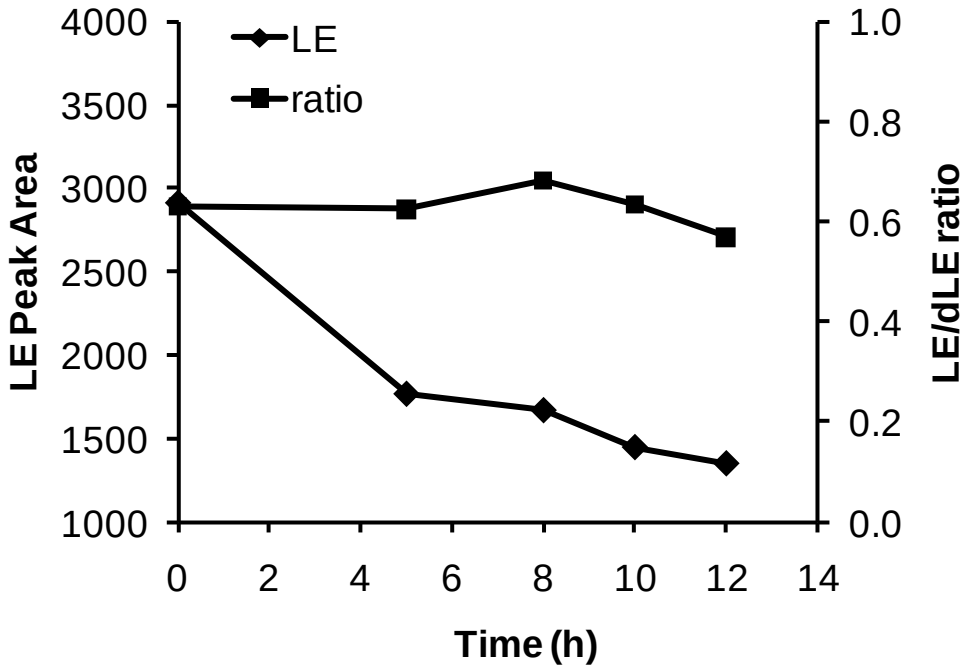

Figure 3.4: LE peak area and the ratio of LE/dLE peak areas for repeated injections of 4 µL from a total of 28 µL *in vivo* dialysate over a time period of 12 hours. Each time point represents a single analysis.

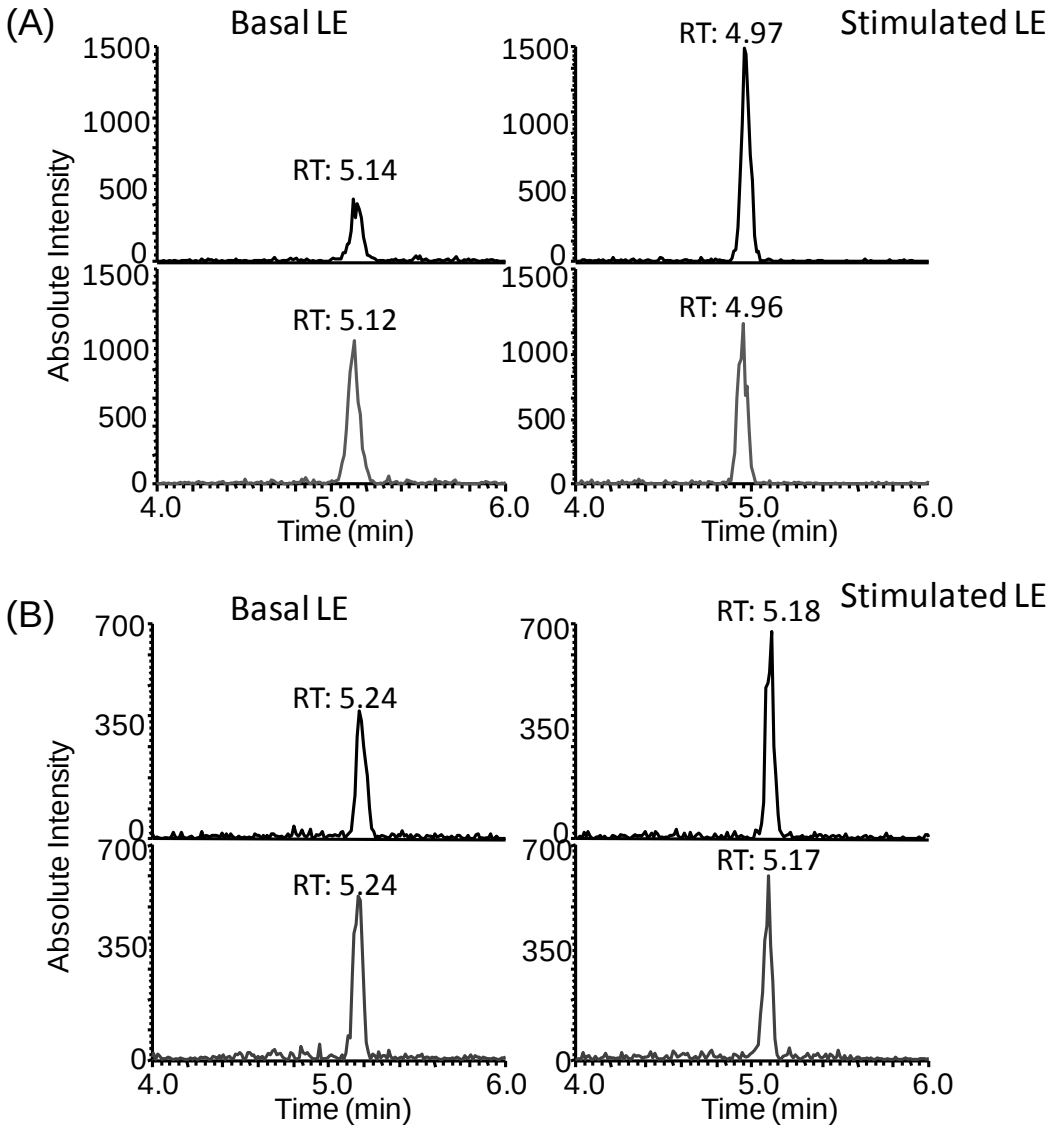

Figure 3.5: Comparison of LE and dLE peak areas in basal samples and after K+ stimulation in an animal experiment with 5 min (A) and 20-min temporal resolution (B). For both A and B, the upper panel shows the LE peak and the lower panel shows the dLE peak.

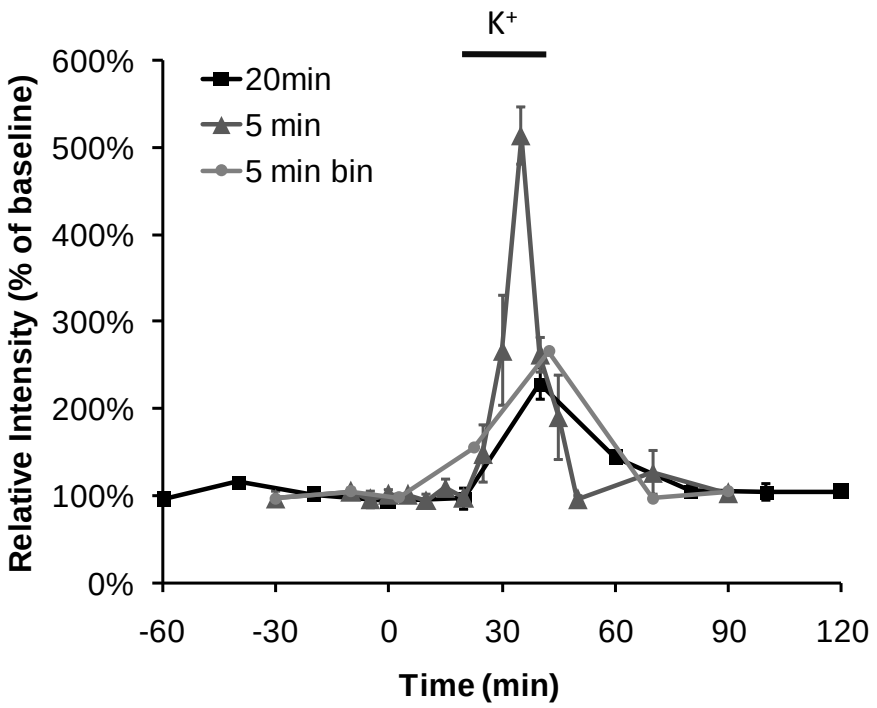

Figure 3.6: Effect of temporal resolution of sampling on LE dynamics over time with K^+ stimulation (n=3, error bar represents 1 standard deviation). Time point 0 min indicates the time at which the perfusate was switched to 75 mM K^+ aCSF, but the real time period of perfusion corrected for the measured 20-min delay time is shown by the bar above the plot. In the three replicates for 5-min detection, the stimulation peaks are aligned by fixing the highest point to the same time. The 5-min data were binned into 20-min samples by averaging all samples points except the first 2 and final 2 already detected with 20 min intervals.

Table 3.1: Comparison of RSDs for LE measurement without and with internal standard for standard 30 pM LE (n=4), *in vitro* recovery from 200 pM LE (n=6), and basal *in vivo* samples from rat brain striatum (n=6).

	Without internal standard	With internal standard
Standard (30 pM)	11.0%	2.0%
In vitro (from 200pM)	19.3%	9.6%
In vivo (from freely-moving animal)	33.5%	10.3%

CHAPTER 4

DYNAMIC CHANGES OF ENGOGENEOUS ENKEPHALINS FOLLOWING ACUTE AMPHETAMINE ADMINISTRATIONS

4.1. Introduction

Enkephalins, including ME and LE, along with endorphins and dynorphins constitute three types of major opioid peptides in the basal ganglia (BG). Structurally, these peptides share a YGGF amino acid sequence at their N-termini which causes cross reactivity[193, 194] when using traditional detection methods such as radioimmunoassay (RIA).[159, 191, 192] With our analytical chemistry system by coupling capillary LC with multi-stage mass spectrometry (MS^n)[195-198], the detection of ME and LE is possible down to attomole detection limits with both sequence specificity and multi-analyte capabilities.

With the ability to detect ME and LE *in vivo* as discussed in Chapter 2 and 3, we are interested in studying the influence of amphetamine (AMPH) on the dynamic changes of these neuropeptides in relevant brain nuclei. AMPH is a psychostimulant drug that is known to produce increased wakefulness and focus in association with decreased fatigue and appetite. However, prolonged use or high doses of the drug causes cravings, anxiety, and different grades of psychoses depending on the dose. The primary effect of AMPH is an excessive release of DA[233, 234] and chronic administration leads to neurotoxicity, particularly with the potent analog methamphetamine (METH).[235] This toxicity is likely

responsible for some of the behavioral abnormalities seen in frequent users.[236] At the molecular level, consequences of excessive DA release can cause abnormal regulation of DA receptor densities which may also contribute to the negative effects of the drug including dependence.[237] In order to fully understand events downstream of DA release and the underlying mechanisms of AMPH induced changes in biological and behavioral processes, studying neuropeptide dynamics is critical since they are closely linked to the regulation of the intact DA system.

Since their discovery ENKs have been known to play a role in DA systems.[238] In fact, in diseases such as Parkinson's disease, where striatal DA is completely lost, the expression of the precursor mRNA of ENK is elevated.[239, 240] This is thought to be a reflection of a lack of DA D2 receptor stimulation which causes excitation of cells containing ENK. Paradoxically, drugs which are known to increase striatal DA content such as cocaine[241] and AMPH[43] have also been shown to increase this expression. The latter indicated that DA D1 receptor mediate such increase in PPE expression caused by AMPH and METH injection. Taken together, researchers have hypothesized that the expression and eventual accumulation and release of ENK represents a compensatory mechanism to overcome DA dysregulation. Though these studies have mainly focused on ENK precursor mRNA measured in tissue, many researchers will take this to mean a final output or release of ENK at terminal regions (for instance GP/VP). This however has never been demonstrated because of a lack of sufficient analytical techniques. Additionally, behavioral consequences of ENK release have never been adequately explored for these same reasons.

Our current studies sought to explore the relationship between enkephalins and

AMPH-stimulated striatal DA release in striato-pallidal projection. We first examined the dynamic changes of enkephalins in striatum (CPu) and GP/VP regions, and then investigated potential dose-dependent patterns of such stimulation. We suspect a dose-dependent effect of such stimulations because the pattern of behavioral alterations is proven to be dose-dependent,[242, 243] and a quantitative relationship also exists between the dose of AMPH and the level of DA release.[234] The findings of the current study demonstrate, for the first time, that DA release induced by AMPH administration stimulates release of ME and LE in striatal and pallidal areas. These findings are consistent with the findings of Wang and McGinty[42, 43] that acute AMPH treatment increased levels of PPE expression. Indeed others have also seen such a pattern following AMPH treatment.[244-247] Thus, this is the first study demonstrating the ENK releasing effects of AMPH, yet the precise mechanism of this phenomenon has to be elucidated in future works.

Another line of investigation being undertaken in the field of ENK research is the study of their neuroprotective potential, that is, their ability to protect neuronal cells from damage. By enhancing natural cell protecting mechanisms or by inhibiting pathways leading to cellular damage are the aims of researchers studying neuroprotection. Numerous studies have demonstrated that ENK analogues have neuroprotective properties and the ENK δ-opioid receptor system is expressed in many of the same brain areas that AMPH and METH targets, including striatal areas. Systemic administration of ENK analogues such as [D-Ala_2,D-Leu_5]ENK have been shown to restore METH induced dysregulation in DA function.[248-250] It has been proposed by those authors that the endogenous ENK system might represent a natural mechanism to protect from

cellular death. Based on evidence of ENK induced neuroprotection, it is therefore of interest to further investigate the release of endogenous opioid peptides in response to METH induced cell death using the currently described analytical techniques.

4.2. Experimental Section

Chemicals and Reagents. LC and mass spectrometry grade solvents including methanol and water were purchased from Burdick & Jackson (Muskegon, MI). ME and LE were from Sigma-Aldrich and then made into 18 mM stock solution stored at -20 °. Ethanol, acetic acid, and hydrofluoric acid were purchased from Fisher Scientific (Pittsburgh, PA). Benzoin methyl ether, glycidyl methacrylate, toluene, trimethylolpropane, trimethacrylate, and 2,2,4-trimethylpentane were purchased from Sigma-Aldrich. D-Amphetamine was obtained from Prof. Edward F. Domino from the Department of Pharmacology of University of Michigan. Arificial cerebral spinal fluid (aCSF) used for microdialysis perfusion consisted of 145 mM NaCl, 2.68 mM KCl, 1.10 mM $MgSO_4$, 1.22 mM $CaCl_2$, 0.50 mM NaH_2PO_4, and 1.55 mM Na_2HPO_4, adjusted pH to 7.4 with 0.1 M NaOH. Mobile phases and aCSF were prepared weekly and were filtered with 0.02 μm-pore filters (Whatman, Maidstone, England). Fused silica capillary was from Polymicro Technologies (Phoenix, AZ).

Animals. Adult male Sprague–Dawley rats (Harlan, Indianapolis, IN) weighing between 440 and 570 g were used for all experiments. The rats were kept in a temperature and humidity controlled room with 12 h light/dark cycles with food and water freely available. Each rat was used only once and sacrificed on conclusion of the experiment. All animals were treated as approved by the University of Michigan Unit for

Laboratory Animal Medicine (ULAM) and in accordance with the National Institute of Health (NIH) Guidelines for the Care and Use of Laboratory Animals.

Recovery Surgery and *in vivo* Microdialysis. For experiments on freely-moving animals, aseptic surgical implantation of guide cannulae for the CMA/12 probe was performed 5-10 days before experiments. Animals were anesthetized with initially i.p. injection of 65 mg/kg ketamine (from Sigma) prepared in an isotonic salt solution with 33 mg/kg booster injections given as needed to maintain anesthesia. Cuide cannulae (CMA Microdialysis, North Chelmsford, MA) were positioned and implanted with a stereotaxic stage (David Kopf Instrument, Tujunga, CA) into GP/VP region (1 mm posterior, 3 mm lateral of bregma to a depth of 9 mm for the probe from dura) and secured with 4 skull screws and cranioplastic cement (Plastics One Inc., Roanoke, VA). The animals were then allowed for at least 5 days of recovery.

Microdialysis probes were then implanted on the day of the experimentation and the system setup for sample collection is shown in Figure 4.1. 4 mm long microdialysis probes with polycarbonate membrane (CMA Microdialysis, North Chelmsford, MA, USA) were first connected to the perfusion syringe with 75 μm i.d. fused silica capillary. The inlet and outlet capillaries of the probes were protected with polyvincylchloride (PVC) tubings (0.010" i.d. × 0.030" o.d., Small Parts Inc., Miami Lakes, FL) to prevent breakage during experiments. The CMA/12 probes were conditioned with 70% ethanol at 3.0 μL/min for 30 min before implatation, then flush with water for 20 min, then go to aCSF at 0.5 μL/min using a syringe pump (CMA 101). If air bubbles were observed inside the membrane, the probe was needed to be flushed at 5.0-8.0 μL/min flow rate when looking at the probe directly. Animals with enough recovery were temporarily

anesthetized with inhaling isoflurane and implanted the probe in the right position fixed in the guide cannula. Then animals were kept in a swivel-less system (Raturn, Bioanalytical Systems, Inc., West Lafayette, IN) during the experimental period. The probes were perfused for at least 1 h after insertion prior to data collection.

Following a recording session with sample collection, the animal was sacrificed and the brain immediately removed and frozen at -80℃ until histology was performed. Probe position was verified by visual examination of 35 μm sections taken via microtome (Leica, SM2000R, Bannockburn, IL). In this chapter, 9 of all animal brains were stored and examined with histology.

Capillary LC-MS^3. In order to prepare integrated chromatography column - electrospray emitter tips, ~500 μm long macroporous photopolymer frits were formed within 25 μm i.d. fused silica capillaries *in situ* 5 cm from one end. A section of polyimide coating was removed by rotating within the electric arc created it between two tungsten electrodes with 7.6 kV applied between them. An additional 1 cm coating nearer to the tip side was removed with a flame. Capillaries were filled with a photopolymer solution He gas pressure and the region to be pulled were concealed with PEEK sleeves (Upchurch Scientific, Oak Harbor, WA) so that only the 500 μm window for frit was exposed. This region of the capillary was exposed to a UV lamp (Spectronics, Westbury, NY) for 30 min to form the frit. (In practice, 20 capillary frits were prepared simultaneously.) Then the capillaries were flushed with acetone and dried for storage by passing He gas through the capillaries for 1-2 min at 500 psi. Columns were packed on the day of detections with first creating an integrated ESI emitter tip by pulling the capillaries with frits with a P-2000 CO_2 laser puller (Sutter Instruments,

Novato, CA). A two-line program was cycled once with line 1: heat 300, velocity 30, delay 128, pull 0 and line 2: heat 300, velocity 30, delay 128, pull 125. The resulting tips were etched with 49% hydrofluoric acid for 45 seconds to create sharp-edged electrospray emitters with 4 μm i.d., verified by scanning electron microscopy. Pulled columns were packed with an acetone slurry (5 mg/mL) of 5 μm Alltima C18 reversed-phase particles (Alltech, Deerfield, IL) at 500 psi as described elsewhere.[205] 4 cm of the total 20 cm length of fused silica was packed. While the photopolymerized frits can be batch produced and stored, the packed column was needed to be packed freshly in order to prevent column drying and tip breakage. As discussed in previous chapters, these packed columns are generally used for only 1-3 days.

The capillary LC system utilizes a high pressure (4000 psi) pump (Haskel Inc., Burbank, CA) for sample loading and desalting, and a lower pressure (500 psi) micro HPLC pump (MicroPro, Eldex Laboratories, Napa, CA) for gradient separation as in Figure 4.1B. This design was different from the system in Figure 2.1 in mainly two parts, one is the MS used in this chapter was a QIT rather than a LIT, another is that a gas pressure bomb was used for sample injection rather than an autosampler. The different pressures allowed for high flow rate for sample preconcentration and desalting, while keep a low flow rate (~100 nL/min) for a more efficient chromatographic separation and increased ESI sensitivity. Two six port valves (C2, Cheminert, Valco Instrument, Houston, TX) connected the system to realize pump selection and sample injection. Dialysate was loaded into a sample loop made by fused silica capillary. After each injection, the sample loop was flushed with water and then He air for cleaning, which is proven to reduce carry-over. All connections were constructed using 75 μm i.d. × 360

μm o.d. capillary except for the link between the injection valve and the splitting-tee immediately preceding the column, which had 50 μm i.d. instead.

Mobile phase A consisted of water with 2% acetic acid and mobile phase B consisted of methanol with 2% acetic acid. Sample loading and desalting were performed with Mobile phase C with 2% acetic acid in water for a total of 15 min. Then the gradient was started with an isocratic step of 10% B for 1 min, linear increase to 95% over 4.5 min, followed by isocratic at 95% B for 0.5 min. Column re-equilibration was necessary after each gradient for 8 min. The column was coupled to an QIT MS (LCQ Deca, ThermoFinnigan, San Jose, CA). A +1.5 kV potential was applied to the splitting Tee prior to the column for electrospray. The emitter tip was positioned ~1 mm from the MS inlet using a micromanipulator operated in x,y,z directions as previously described.[52]

The QIT-MS was operated with the following conditions: positive mode, automatic gain control (AGC) on, collision induced dissociation (CID), q = 0.25, isolation width = 3 m/z, activation time = 30 ms, micro scan number = 1 and default target count values. Normalized collision energies were optimized at 40 and 33% for ME, and 42 and 33% for LE, with mass range 150-600 m/z. Optimization of the ion optics was achieved by tuning with direct infusion of 18 nM neurotensin$_{1\text{-}11}$ in 50% methanol 2% acetic acid at 100 nL/min every 2 weeks. The MS^3 pathways were 574→397→278, 323, 380 for ME and 556→397→278, 323, 380 for LE. The collision energies were optimized with constant infusion of enkephalins in 50% methanol 2% acetic acid with a flow rate of 100 nL/min. Identification of granddaughter peaks used for quantification was based on the method in a previous study.[206]

4.3. Results and Discussion

Sensitivity of Enkephalin Detection with MS^3. Although as discussed in the chapters above, we have validated the detection method for neuropeptides. With addition of 5% acetic acid and storage at low temperature, reliable off-line detection has been achieved. However, we started with MS^3 for detection of all neuropeptides, but there was no direct evidence showing a better sensitivity with such high stage of MS for peptide quantification on our system. In previous report, the comparison was also ambiguous for MS^2 and MS^3 methods showing no significant difference in sensitivity by looking at high concentration samples,[53] thus require a further investigation on the necessity of using MS^3 for detection. In principle, further improvements in sensitivity and selectivity could be achieved by using higher stages of mass spectrometry.[251] With addition of each stage of mass spectrometry, both signal and noise decrease; however, the noise decreases faster. So signal to noise ratio (S/N) should increase with higher MS stage as long as the signal is enough for detection.[84] To test the sensitivity of both methods, sample level near the LOD was chosen. On our instrument, for a 2.5 μL 2 pM LE injection, S/N in the chromatogram detected by MS^2 is only 4, while it increased to 21 for MS^3. (see Figure 4.2) Therefore, direct evidence was obtained that the MS^3 reached a higher sensitivity for enkephalins, which was important for *in vivo* monitoring in the following experiments. With external calibration, the LODs of our cLC-MS^3 system with QIT instrument, calculated as the sample amount would generate S/N = 3 in the RIC, were about 4 attomole for ME and 1 attomole for LE, which is superior to previous studies with other methods.

In this study, simultaneous detection of both ME and LE were achieved with time-

segmented detection by changing the scan method from ME to LE between the two peaks because ME elutes before LE in all experiments. However, as the retention times of them shifted among different columns, the first sample on a new column was always serving as a test sample by only measuring LE, and then the time segmented detection method can be reset accordingly. The retention times of ME and LE on a same column were found to be reproducible with RSD < 8% in general, however, if a partial clogging happened, the retention time would shift dramatically and a new column was needed in those cases.

Figure 4.3 showed detected ME and LE from an *in vivo* dialysate from GP/VP brain region, acquired with time-segmented scan method. While RSD for standard 60 pM sample was found to be commonly less than 10%, the RSDs for basal *in vivo* dialysates were averaged to 23% for ME and 19% for LE (n = 14 in the experiments of this chapter).

Dynamic changes of ME and LE levels in CPu. Although we have been able to expedite the detection temporal resolution to 5 min, given the large numbers of sample fractions collected from one animal, we still fixed the temporal resolution at 20 min in this study. Because the pharmacological effects fall in a time range of generally more than one hour, this temporal resolution is adequate to reveal dynamic information of the neuropeptide levels in brain. System delay time was calculated with the dead volume of the outlet tubing from the microdialysis probe and was determined to be 10 min. To detect ME and LE levels over time from an animal, injection of the AMPH was given 10 min before the fourth sample collected so the first four fractions from on animal are considered as basal samples, following with stimulated ones.

First 3 series of samples were collected from CPu region of rat brains. After 4 baseline samples, a single injection of 5 mg/kg amphetamine dissolved in aseptic saline was administrated subcutaneously to the rat and samples were continuously collected for 2 more hours. We found that the amphetamine evoked a substantial increase of both ME and LE to about 17% above baseline, as shown in Figure 4.4. This elevated level was proven to be statistically significant by t-test. The observed elevation of ME and LE releasing in CPu was lower than previous study with a similar dose of AMPH (30 μmol/kg = 5.6 mg/kg) revealing a 97.8% above control increase in PPE mRNA level 3 hours after AMPH injection.[43] Our study with the ability of studying time resolved dynamic chnages of neuropeptide releasing, ministered to build a bridge between pharmacological treatment and many previous studies with histochemistry method on mRNA levels.

Dose-dependent Dynamic changes of ME and LE levels in GP/VP. Taken that this change in ME and LE releasing in striatum, might cause amplified changes in the downstreams of ENK projections, we then studied the ENK release in the palidum as the output of basal ganglia, which contains mainly the GP and VP areas. (see Figure 1.2) A practical reason to choose this brain region is the size of this area is suitable for our microdialysis probe utilized.

The *in vivo* ENK levels were monitored in GP/ VP with same method for administration of amphetamine and sample detection revealing a stronger release of both ME and LE, with a maximal level to about 100% above baseline for the same dose of AMPH (see Figure 4.5B) These results indicate that the ENK system associated with GP/VP responded to AMPH differently than that in striatum, possibly due to the

involvement of higher dense of ENK projections from striatum to pallidum. The time course of such stimulation though showed a similar manner of the alteration of ENK levels from the two brain regions, with the maximal point achieved at 40-60 minutes after the injections. ENK levels were back to baseline generally after 2 hours.

We next evaluated the dose dependency of the changes. Lower doses at 0.1, 1 and 2.5 mg/kg were given in a repeated injection way to reduce experimental complexity while the higher doses of 10 and 12 mg/kg were examined in separate animals. 0.1 or 1 mg/kg changed neither the ENK levels nor the behavioral activity of the animals by observation during the experiments (but animal behavior was not quantitatively evaluated). 2.5 mg/kg injection started to cause a release of ME and LE, in a similar time course as other doses, however showing an averagely lower stimulation compared to 5 mg/kg. Both 10 and 12 mg/kg AMPH caused this substantial releasing as well. Even higher dose, such as 20 mg/kg has also been tested, however resulting in severe toxicity to animal living conditions.

To compare the stimulated level caused by all these doses of AMPH, the peak areas and peak heights for the traces of ME and LE over time under different doses were calculated. Peak area was calculated by summing up the values of all points higher than baseline, and peak height was counted as the highest point in the plots of Figure 4.5. As summarized in Figure 4.6, sigmoidal fits of these curves were established for both peak areas (A) and peak heights (B), with each figure showed three traces for ME, LE individually and a sum of both peptides as an indication of total ENK contents. Our results with distinct ENK responses to lower and higher doses of AMPH are consistent to the differential behavioral responses to METH treatment ranging from minor increase in

locomotor activity after low dose of METH to intense stereotypic responses after high doses METH treatment.[243]

The time courses of ENK responses to all doses were similar, reaching maximal stimulated points at 40-80 min for all doses, and descending back to baseline after 2 hours. Compared to previous study on DA releasing by i.p. injection of 5 mg/kg AMPH,[234] where revealed DA release after the injection to a 30-fold increase at 45-60 min after administration, and coming back to basal line after 4 hours, the ENK response to AMPH showed a shorter and lower enhancement. This is probably because of easier depletion of neuropeptide storage in pre-synaptic neurons. Therefore, PPE mRNA and tissue ENK levels might be elevated to compensate such release, consistent with previous reports.[42, 43, 246]

Due to multiple projections from striatum to GP and VP, the mechanism of this transient releasing is still unclear. It can be speculated that since the GP/VP receive DA projections from the SN/VTA, respectively, that elevated DA acting locally on DA D2 receptors on pallidostriatal GABAergic projections causes a reduction of inhibition of striatopallidal neurons and thereby increasing ENK transmission as illustrated in Figure 4.7. D1 receptor might also play roles in this circuit via unclear pathways. Though it has yet to be tested, our group is currently working on this by examining such release when blocking individual pathways. We will discuss about these future directions in the last chapter.

Experimental Complications. One potential area for improvement of *in vivo* ME and LE measurements in this chapter is absolute quantification. Although we have talked about continuous improvement of column stability during my PhD research period, all of

the measurements in this chapter were finished before many of those improvements. Thus, because of the home made columns generally last for only 1 day, it became extremely difficult to make calibration curves on each new column. For a complete external calibration, standard samples with 3 replications at 3 different concentrations are required and detection of all these standard samples following by all *in vivo* samples on a same column in a same day is generally not feasible with our system. So in most of the measurements in this chapter, we basically focused on the relative dynamic changes of the neuropeptides rather than the absolute concentrations due to lack of calibration for samples from each animal. External calibration curves, however, have been made on separate columns, showing linear range from 20-200 pM of 5 μL samples for ME and LE, and the sensitivity for LE was 4-folds higher than ME, due to different properties of these two peptides. LE is more hydrophobic than ME, resulting in higher ESI efficiency and thus higher signals in MS. Although without the data showing absolute concentrations of ME and LE from GP/VP dialysates, we were able to calculate the ratio of ME and LE from these basal samples and this ratio varied from 1.8:1 to 3.7:1 for all animals, corrected with the differential detection sensitivity. This variability might be the result of inter-column variability for the measurements and variable probe positions from different animals. As discussed in Chapter 2 of this dissertation, the ratio of ME and LE was found to be ~ 2:1 in striatum, and it seems to be higher in average in GP/VP, which might be the results of discrepancy in striatopallidal projections of these two peptides. Further investigation on such discrepancy will be interesting because previous immunoassay method had difficulties to differentiate these two similar peptides.

Second potential area for improvement of this study is the spatial resolution.

Previous studies have indicated different pathways projected to GP and VP as we discussed in the introduction part, and different manners of DA release have also been found in these two regions.[252] In the present study, by doing histology on 9 of the rat brains after experiments, the probe position was found to generally cover both GP and VP regions. Although this 4-mm long probe is suitable for CPu, it is relatively large to either region of GP or VP and we have also observed partial coverage of the probe in striatum and other surrounding areas. The requirement for enough recovery prohibited us from moving to smaller probe to achieve better spatial resolution. A 2-mm long CMA/12 probe with the same polycarbonate membrane has been tested, but signals of some *in vivo* samples were lost due to lower recovery. Therefore, future works on design and build of smaller microdialysis probes with other membrane materials having higher recoveries will be valuable.

4.4. Conclusions

In summary, the capillary LC-MS^3 method utilized here demonstrates its ability to measure enkephalins at basal level and after treatment of AMPH from freely-moving animals. By monitoring the microdialysis samples over time, we found that acute injection of AMPH stimulates a substantial release of ME and LE in striatum and GP/VP. GP/VP as the output of basal ganglia, showed a higher increase of these neuropeptides when compared to striatum, specifically CPu in this study. Such stimulation was found to be dose-dependent, showing no response with doses lower than 1 mg/kg and reaching a maximal level with doses higher than 5 mg/kg. This study is an initial step to explore the relationship between enkephalins and AMPH-stimulated striatal DA release in striao-

pallidal projection. Future efforts will be made to reveal the specific DA receptors mediating such ENK release.

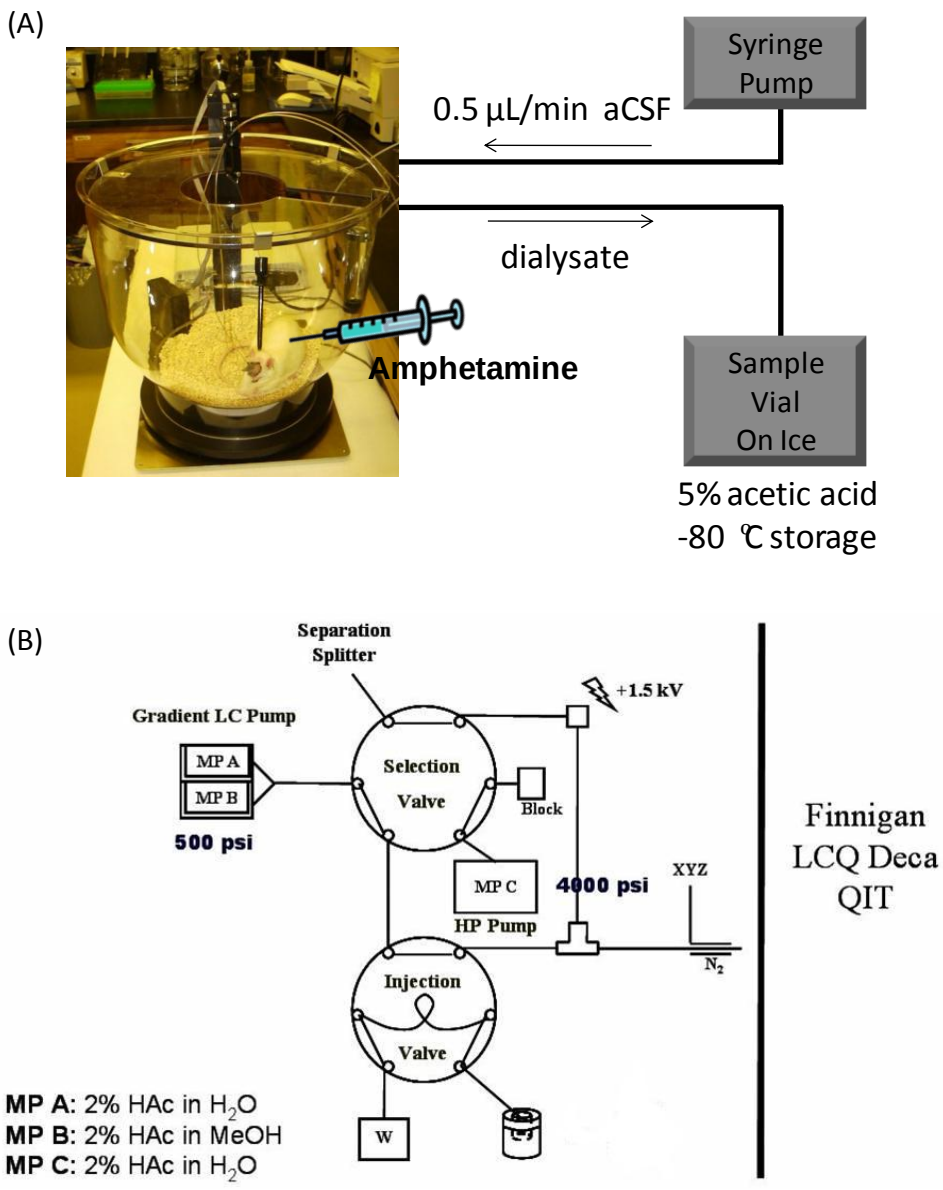

Figure 4.1: System configuration of microdialysis sampling from freely-moving animals and the detection instrumentation. (A) Sample collection with 0.5 µL/min flow rate with 75 µm i.d. fused silica capillaries for all connection tubings. Dialysate fractions are added with 0.5 µL acetic acid and then stored at -80 ℃ until detection. (B) The detection system with a gas pressure bomb to inject 5 µL from each sample fraction.

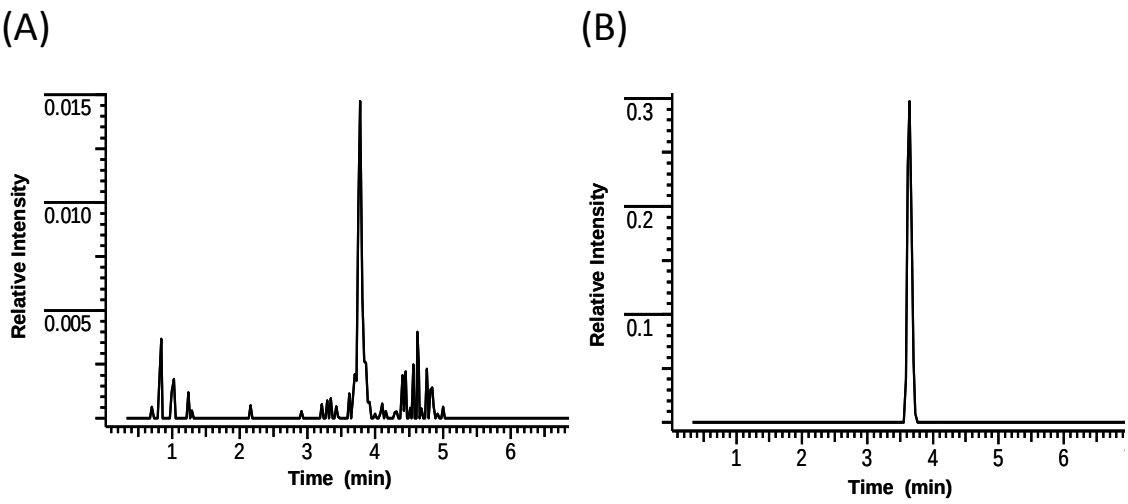

Figure 4.2: Comparison of reconstructed ion chromatograms for 2.5 µL 2 pM LE detected with LC-MS^2 (A) and LC-MS^3 (B). S/N improves from 4 to 21 from LC-MS^2 to LC-MS^3.

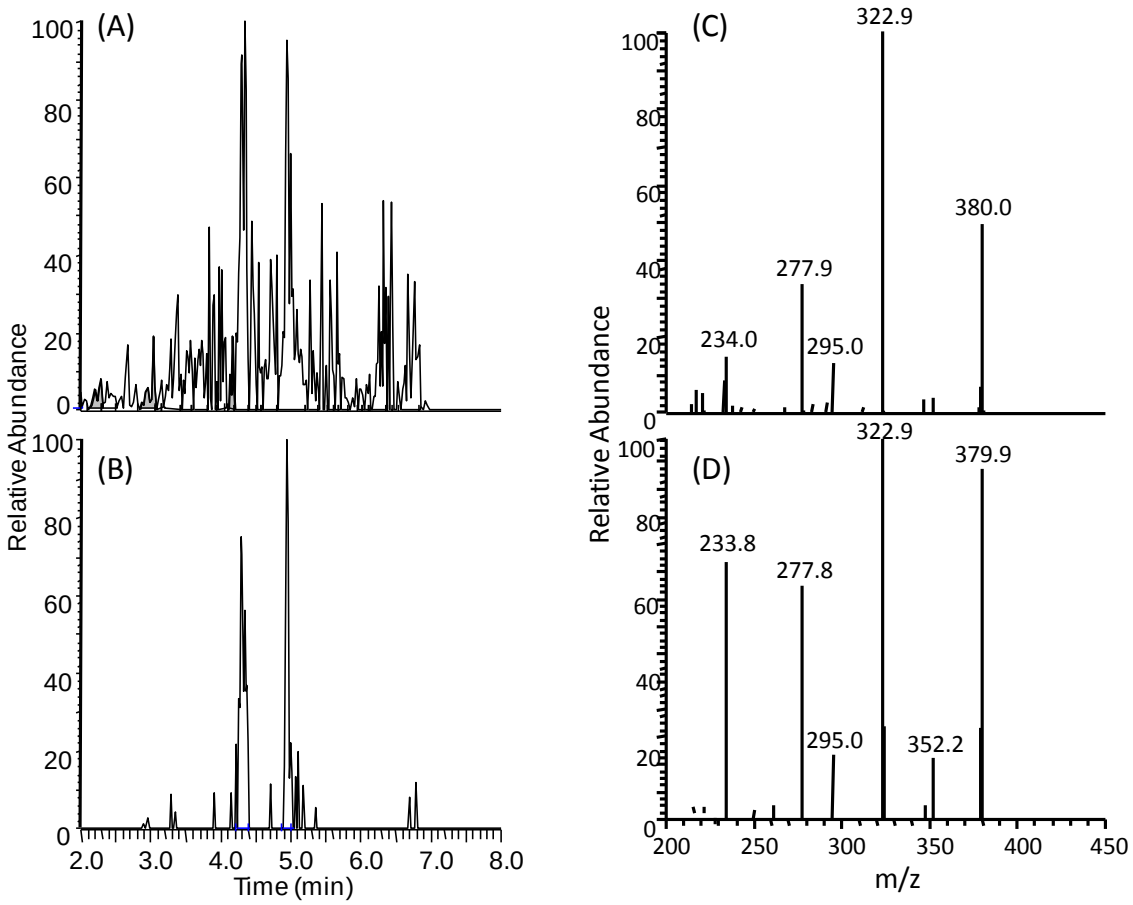

Figure 4.3: Mass chromatograms from separation of basal dialysates from GP/VP of a freely-moving animal. (A) TIC of the separation from 2 to 8 min. (B) RIC with characteristic peaks in MS^3 spectra for ME and LE. (C) MS^3 spectrum of ME. (D) MS^3 spectrum of LE.

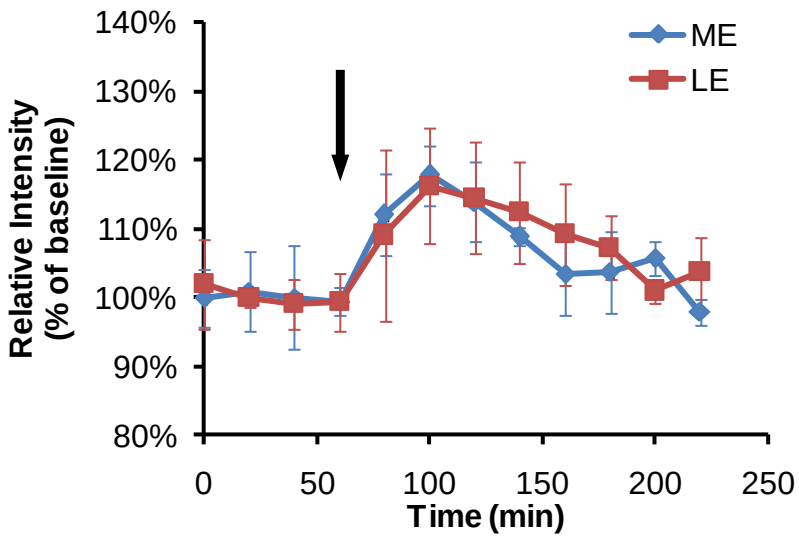

Figure 4.4: Dynamic changes of ME and LE level over time in CPu with injection of 5 mg/kg AMPH. The black arrow indicates the time of giving AMPH injections corrected with 10 min system delay time. The maximal stimulation was proven to be statistically significant compared to baseline by t-test. (n=3, error bar= SD)

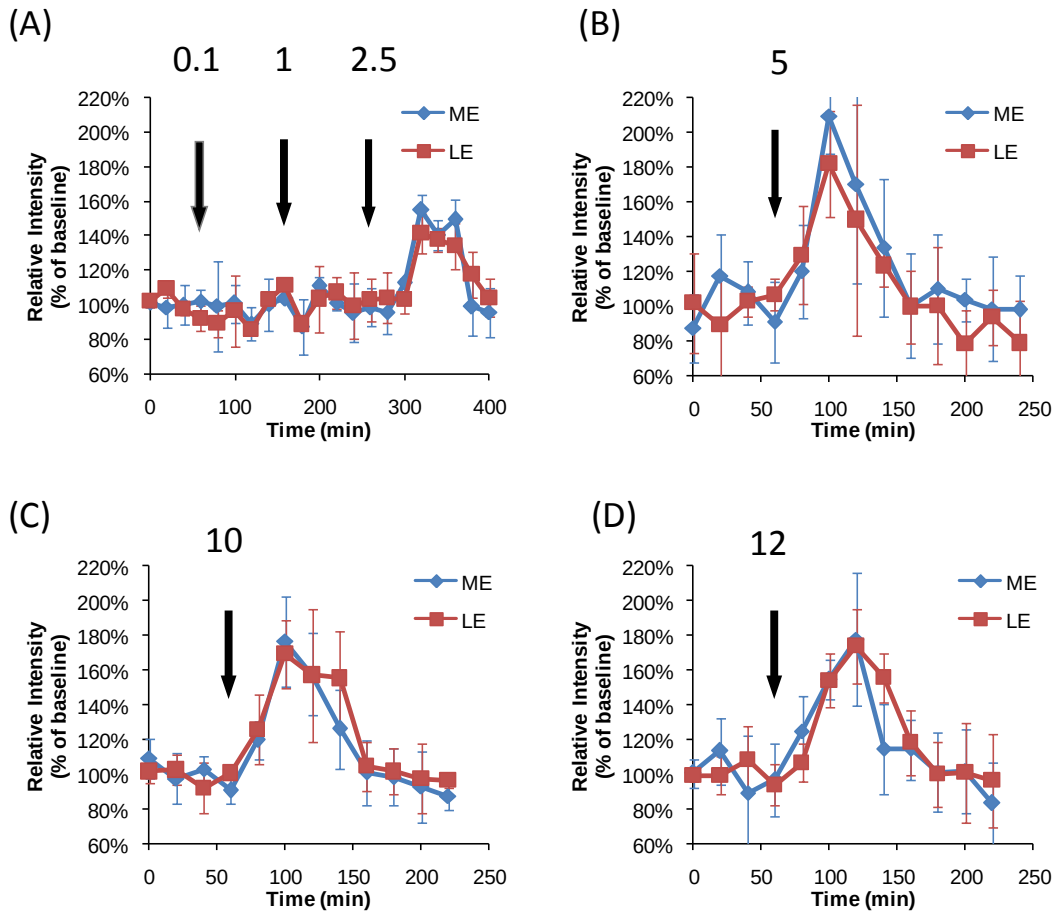

Figure 4.5: Dynamic changes of ME and LE level over time in GP/VP with injections of different doses of AMPH. Overlap injections of 0.1, 1, and 2.5 mg/kg AMPH are shown in (A), and 5, 10 and 12 mg/kg results are shown in (B)(C)(D) respectively. n=4 for 5 and 10 mg/kg, n=3 for other doses, error bar=SD.

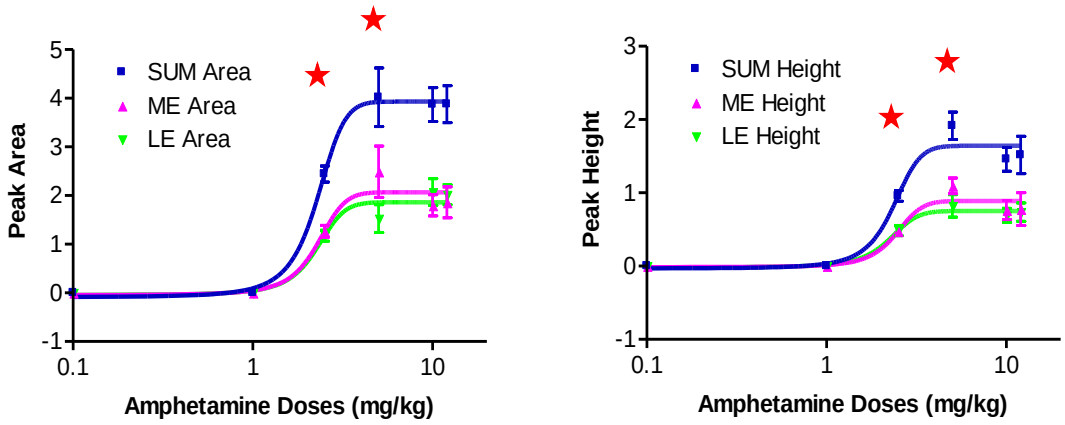

Figure 4.6: Dose-dependent response curve for ME, LE and the sum of the two neuropeptides. ★p<0.1 with t-test.

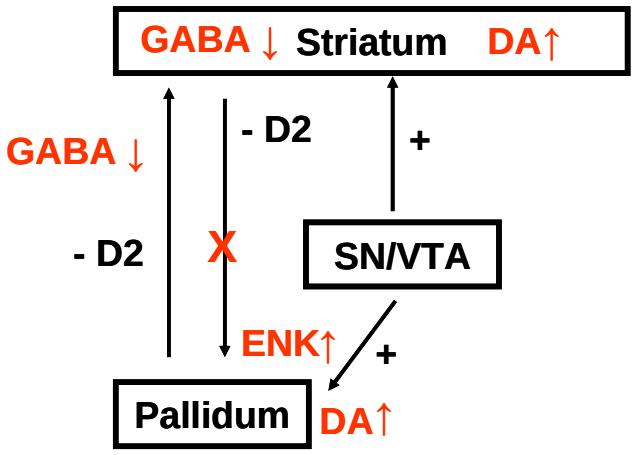

Figure 4.7: Schematic illustration showing the proposed mechanism of the DA excitation (+) to both Striatum and pallidum regions. Pallido-striatal projection via D2 receptor caused reduced GABA level in striatum. While GABA serves as an inhibitory neurotransmitter for the striato-pallidal pathway, this reduction dis-inhibits (hence excites) the stiato-pallidal projection of ENK, resulting in an increase level of them in Pallidum region.

CHAPTER 5

FRACTION COLLECTION FROM CAPILLARY LIQUID CHROMATOGRAPHY AND OFF-LINE ELECTROSPRAY IONIZATION MASS SPECTROMETRY USING OIL SEGMENTED FLOW

5.1. Introduction

Microscale separations methods such as capillary liquid chromatography (LC) and capillary electrophoresis (CE) are well-recognized as powerful methods that can provide numerous advantages including high resolution, high sensitivity, and effective coupling to mass spectrometry (MS).[253, 254] A limitation of such methods has been the relative difficulty of collecting fractions for storage and further characterization off-line. This difficulty stems chiefly from the problems of storing and manipulating nanoliter and smaller fractions that would be generated. Conventional methods for fraction collection from a separation method commonly involve transferring samples to wells or vials; however, this approach is limited in practice to fractions no smaller than a few microliters. In this work we demonstrate fraction collection from capillary LC based on flow segmentation i.e., collecting fractions in a tube as plugs or droplets separated by an immiscible oil, followed by off-line electrospray ionization (ESI)-MS of the segmented samples.

Although on-line ESI-MS is generally effective, fraction collection and off-line ESI-MS may be desirable in many situations including when: 1) using off-site mass

spectrometers; 2) using multiple mass spectrometers for analysis of a single sample; 3) only a portion of the chromatogram requires MS analysis; and 4) multiplexing slow separations to rapid MS analysis. Off-line analysis is also desirable when certain fractions of a chromatogram require MS analysis time that is longer than the peak width. This latter situation may arise in analysis of complex samples generated from proteomics or metabolomics studies where multiple stages of mass spectrometry (MS^n) may be used to gain chemical information on several overlapping or co-eluting compounds. When using on-line analysis, these problems may be avoided by slowing the entire chromatographic separation; however, this unnecessarily increases analysis time and it may dilute compounds. Alternatively, "peak parking" may be used wherein mobile phase flow is stopped or slowed to allow more time to collect mass spectra when compounds of interest elute.[255] Peak parking is infrequently used because of the complexity of varying flow rate during chromatographic separation and deleterious effects on the separation.

Off-line analysis provides a convenient approach to avoid these limitations. A commercial system for fraction collection and off-line ESI-MS based on a microfabricated chip has been developed. This system uses fraction collection onto well-plates and requires 1-10 μL fractions for ESI-MS analysis.[256]

Compartmentalization of effluent into segmented flow has emerged as a novel way to collect fractions from miniaturized separations such as chip electrophoresis[186] and capillary LC[257]. For capillary LC, fractions were collected as segmented flow to facilitate interfacing to CE for 2-dimensional separation. Both of these examples used on-line analysis and did not explore off-line analysis or interface to mass spectrometry.

Performing off-line ESI-MS of fractions required development of a method of

interfacing oil-segmented samples to the ionization source. One approach to analyzing segmented flow using ESI-MS has been to use a microfluidic device to extract sample plugs from oil and transfer them to an aqueous stream interfaced with MS.[183, 258] This approach has limitations such as unavoidable dilution and spreading of sample zones during extraction and transfer to the ESI emitter tip. As a result, the sensitivity, throughput and quantification possible by this approach are compromised. We have previously reported that sample plugs segmented by air can be directly infused into a metal-coated nano ESI emitter tip to achieve high-throughput, low carry-over between samples, and sensitive ESI-MS analysis.[259] Use of air-segmented samples also has limitations however. Segments can merge, allowing mixing of fractions, because of the compressibility of air under pressure required to pump the sample plugs through an ESI emitter. Segments can also merge during storage due to evaporation of the air through Teflon or polydimethylsiloxane containers. In this work, we demonstrate ESI-MS of oil-segmented samples and application to fraction collection from capillary LC with subsequent off-line ESI-MS.

5.2. Experimental Section

Chemicals and Reagents. Capillary LC solvents, including acetonitrile, methanol and water were purchased from Burdick & Jackson (Muskegon, MI). FC-72, FC-77, FC-40 and perfluorodecalin were from Sigma-Aldrich. Acetic acid and hydrofluoric acid were purchased from Fisher Scientific (Pittsburgh, PA). Mobile phases were prepared weekly and were filtered with 0.02 μm-pore filters (Whatman, Maidstone, England) to remove particulates. Fused silica capillary was from Polymicro Technologies (Phoenix,

AZ). Small molecule metabolites samples malate, citrate, phosphoenolpyruvate (PEP) and fructose 1,6-biphosphate (F1,6P), fumarate, succinate and cyclic adenosine monophosphate (cAMP) were from Sigma-Aldrich. Corticotropin releasing factor (CRF) was from Phoenix pharmaceuticals, Inc. (Burlingame, CA).

Sample Preparation. Metabolite sample stock solutions were made in water at 5 mM concentration then stored in -80 ℃. Samples were then diluted from stock using 80% methanol and 20% water for injection on HILIC column.

Analysis of oil-segmented flows with MS. For initial tests of ESI of oil-segmented flow, segmented samples were formed by pumping sample (50 μM cAMP dissolved in 50% acetonitrile 50% ammonium acetate at pH 9.9) and oil into two separate arms of a tee junction with 100 μm i.d. at 500 nL/min using a syringe pump (Fusion 400, Chemyx, Stafford, TX, USA). In this way, ~7 nL sample plugs separated by 7 nL oil plugs were formed and pumped into 150 μm i.d. by 360 μm o.d. high purity perfluoroalkoxy plus (HPFA+) tubing (Upchurch Scientific, Oak Harbor, OR) connected to the third arm of the tee.

For off-line ESI-MS detection, the HPFA+ tubing containing sample was connected with a Teflon connector to a Pt-coated, fused silica ESI emitter (PicoTip^{TM} EMITTER FS360-50-8, New Objective, Woburn, MA, USA) with 8 μm i.d. at the tip (see Figure 5.1B). The emitter was mounted into a nanospray ESI source (PV-550, New Objective) interfaced to a linear ion trap (LIT) MS (LTQ, Thermo Fisher Scientific, Waltham, MA). Unless stated otherwise, samples were pumped at 200 nL/min with the emitter tip poised at 1.5 kV. Full scan MS was used in such experiments showing cAMP sample signal at m/z 328. All the other metabolite samples were also detected with negative mode ESI.

Capillary LC Separations. Fraction collection and off-line ESI MS analysis were performed for two different applications each using a different chromatography mode. The first was separation of polar metabolites by hydrophilic interaction liquid chromatography (HILIC). To prepare capillary HILIC columns, a frit was first made by tapping nonporous silica (Micra Scientific, Inc., Northbrook, IL) into one end of a 15 cm length of 75 μm i.d. fused silica capillary. The particles were briefly heated with a flame to sinter them in place. The capillary was then packed from a slurry of 8 mg Luna NH2 particles (Phenomenex, Torrance, CA) in 4 mL acetone as described elsewhere.[260] The ESI emitter tip was pulled from a separate capillary with 10 μm i.d. and 360 μm o.d. using a 2 cycle program (Cycle 1: HEAT 330, FIL void, DELAY 128, PULL void. Cycle 2: HEAT 330, FIL (void), DELAY 128, PULL 125) on Sutter P-2000 pipette puller (Sutter Instruments, Novato, CA). The tip was then etched with 49% hydrofluoric acid for 100 s to create sharp-edged electrospray emitters. Separations were performed using a UPLC pump (NanoAcquity, Waters, Milford, MA). Mobile phase (MP) A was acetonitrile, while MP B was 5 mM Ammonium acetate in water with pH adjusted to 9.9 by NaOH. Separation of metabolites was realized with a linear mobile phase gradient from 30% to 100% MP B over 22 minutes. For on-line detection, the column was interfaced to a triple quadrupole (QQQ) MS (QuattroUltima, Micromass/Waters, Milford, MA) using a Waters Universal NanoFlow Sprayer ESI source. Off-line detection was performed with the LIT.

Malate (m/z = 133), citrate (m/z = 191), PEP (m/z = 167) and F1,6P (m/z = 339), were separated on a 15 cm long HILIC column with 75 μm i.d. at a flow rate 500 nL/min. Full scan MS was utilized on detection of 1 μL injection of 20 μM of these four fully

resolved molecules. For MRM detection, another set of metabolites were used, including fumarate (m/z 115), succinate (m/z 117), malate, cAMP and F1,6P, and the sample concentration were lowered to 10 μM due to higher sensitivity with MRM detection compared to full scan analysis. Both the QQQ and LIT MS were operated in negative mode. With QQQ, transitions used for MRM detection of these five metabolites were determined to be: m/z 115→ m/z 71 for fumarate, m/z 117→ m/z 73 for succinate, m/z 133→ m/z 115 for malate, m/z 328→ m/z 134 for cAMP, and m/z 339→ m/z 96 for F1,6P. With LIT MS, daughter ion scans used for MRM of these samples were obtained by setting 5 different scan events to 5 parent ions of different molecules and detecting all daughter ions in a range of 50 to 1000 m/z.

The second application was separation of a tryptic digest of corticotropin-releasing factor (CRF) using reverse phase capillary LC. Instead of using a separate emitter tip, the reverse phase columns were made with integrated emitter tips as described before.[187, 200] Columns were then packed with an acetone slurry (10 mg/mL) of 5 μm Atlantis C18 reversed-phase particles (Alltech, Deerfield, IL) at 500 psi to 3 cm length as described elsewhere.[261] 2 μL of 1 nM of the tryptic CRF samples were injected by WPS-3000TPL autosampler (Dionex, Sunnyvale, CA) in weak mobile phases (2% acetic acid in H_2O) to allow the analytes to stack at the head of the column. The capillary LC system utilizes a high pressure (4000 psi) pump (Haskel Inc., Burbank, CA) for sample loading and desalting for 12 min, and a lower pressure (500 psi) micro HPLC pump (MicroPro, Eldex Laboratories, Napa, CA) for gradient separation. MP A was water containing 2% acetic acid, while MP B was methanol with 2% acetic acid. The gradient went from 10% to 90% of MP B for 7 min. Both on-line and off-line detection used the LIT MS, operated

in positive mode.

Fraction Collection. For off-line analysis, LC effluent was collected into fractions using the system shown in Figure 5.1. In this approach, effluent from the column is directed into a tee with an immiscible fluid, typically a perfluorinated oil, flowing through another arm of the tee. As described elsewhere, within a certain flow rate range, alternating and regularly spaced plugs of sample and oil are formed.[262-265] Polyether ether ketone (PEEK) tees with 50, 100 and 150 μm i.d. (Valco, Houston, TX) were used for this work. The oil-segmented fractions collected into a 60 cm length of 150 μm i.d. by 360 μm o.d. HPFA+ tubing for storage. A picture of the tubing containing such fractions is shown in Figure 5.1C.

5.3. Results and Discussion

ESI Conditions for Oil Segmented Flow. Initial studies were directed towards identifying conditions for successful direct infusion ESI-MS of oil-segmented samples. Preliminary studies identified the immiscible fluid used for segmenting samples, electrospray voltage, and infusion flow rate as critical parameters for achieving stable and sensitive direct ESI-MS analysis.

Five different liquids, hexane, FC-72, FC-77, FC-40 and perfluorodecalin (PFD), were evaluated as possible immiscible fluids to segment samples. We observed that hexane, FC-72 and FC-77 all generated a visible electrospray at voltage > -1 kV, which is similar to the lower voltage needed for electrospray of aqueous sample. Attempts to analyze aqueous cAMP samples segmented by these fluids during direct infusion did not yield a series of segments but instead a low and fluctuating ion current as illustrated by

the example in Figure 5.2A. In contrast, FC-40 and PFD did not yield electrospray up to -1.5 kV. Instead, these oils formed droplets at the emitter tip that then migrated along the outside of the tip away from the emitter. With these oils, no signal was observed when the oil plug flowed through the tip (Figure 5.2B) and only sample signal was detected thus allowing detection of cAMP as a series of discrete current bursts corresponding to the plugs exiting the emitter tip. These results suggest that the electrospray of immiscible segmenting fluid interferes with formation and detection of ions from adjacent aqueous sample plugs. The difference in oil performance can be attributed, at least in part, to their viscosity. Higher viscosity fluids are more difficult to electrospray[266, 267] and it was the higher viscosity fluids (see Table 1) that could be successfully used in this case.

Because PFD did not interfere with spray of sample, further experiments were performed with it as the oil phase. The effect of ESI voltage was tested while infusing a series of aqueous samples of 50 μM cAMP in full scan mode. As illustrated in Figure 5.3, at voltage less than -1.2 kV no signal for cAMP was observed. At this voltage, neither the aqueous sample nor the oil generated visible electrospray. When the voltage increased to -1.5 kV, signal for the analyte was detected as discrete bursts in the reconstructed ion current (RIC) trace. The total ion current (TIC) revealed a similar pattern showing that no signal was obtained as the oil was pumped through the emitter. In agreement with these observations of the signal, we observed electrospray only for the aqueous plugs in this voltage range. At -1.8 kV, the TIC increased; however, signal for the analyte was reduced in the RIC suggesting that the increase in TIC was due to signal from the oil which begins to electrospray at this voltage. The signal for cAMP also becomes erratic with the onset of oil electrospray. Above -1.8 kV this trend continues

and no signal for analyte is detected and the TIC remains noticeably elevated between aqueous plugs. Optimal ESI voltage was thus determined to be around -1.5 kV on our instrument and used for the following experiments.

These results further support the conclusion that detection of samples in the aqueous fractions is best if oil does not generate electrospray. For a given oil, the results will be obtained in the range that the aqueous sample generates electrospray but the oil does not. For low viscosity oils such as FC-72 and FC-77, there are no voltages that generate only aqueous spray so these oils did not yield good results under any conditions.

Effect of Flow Rate. To explore the influence of infusion flow rate, we monitored ESI signal for cAMP from a series of plugs while varying the infusion flow rate. As shown in Figure 5.4A, increasing flow rate from 50 nL/min to 200 nL/min, had little effect on the signal, except samples were introduced more rapidly allowing higher throughput. At flow rate lower than 400 nL/min, the traces are stable with occasional spikes which had inconsequential influence on average peak heights. As the flow rate was increased to 400 nL/min however, signal was eliminated. Observation of the emitter tip revealed that this loss of signal coincided with accumulation of oil on the tip. Thus, at the higher flow rates oil phase exiting the tip was not removed fast enough and blocked the emitter tip.

To prevent oil accumulation on the emitter tip, we attempted to siphon the oil away from the tip by placing a 20 cm length of 50 μm i.d. Teflon tubing next to the emitter about 1 mm from the tip as shown in Figure 5.4C. With the Telfon tubing in place, oil droplets that began to accumulate were drawn away from the tip. In this case, alternating 10 nL aqueous and oil plugs could be infused at a flow rates up to 2 μL/min without loss

of signal (Figure 5.4B). With the Teflon siphon tubing, the stability of spray of oil-segmented flow could be maintained from 20 to 2000 nL/min.

At the highest flow rate used, the droplets were analyzed at a rate of 2.2 Hz. While high-throughput sample analysis was not the focus of this work, these results do suggest that ESI-MS of segmented flow may be a useful route to high-throughput analysis. Higher flow rates were not attempted because the throughput became limited by the MS scan rate, which was 0.13 s per scan for this experiment. To reach higher throughput, a faster detector, such as a time-of-flight MS, would be needed.

Reproducibility of Plug Deteciton. Although direct ESI-MS of the oil segmented plugs did yield stable peak heights, we observed that the width of plugs had RSDs as high as 38% over stretches of 30 plugs. This variability is not due to variation in plug generation because the RSD of plug lengths formed in the tee junction was 3% as measured by visual observation under a microscope. The variability is also not due to complete coalescence of plugs within the ESI tip because the number of plugs generated always equaled the number detected by MS. Thus, it appears that this variation is cause by an effect of flow through the emitter tip. Possible causes include partial coalescence of plugs within the tip and fluctuations in flow rate associated with segmented flow through the emitter.

Fraction collection from capillary LC by oil-segmented flow. Fractions from a capillary LC column were formed by pumping column effluent into a tee with oil flowing perpendicular to the mobile phase as illustrated in Figure 5.1A. It is possible vary the fraction size by varying the relative flow rates and tee dimensions. Using a 100 μm i.d. tee, 500 nL/min mobile phase flow, and 300 nL/min oil flow generated ~7 nL LC fraction

plugs segmented by ~5 nL oil plugs (Figure 5.1C). When using tees with 50 and 150 μm i.d., the sample droplet sizes were 2 nL and 35 nL respectively. For this work, we used 7 nL droplets which generated 5 to 18 fractions per chromatographic peak depending on the separation. Consistent sample plug sizes (RSD of 4% for 30 plugs visually observed) were obtained for all fractions collected under our LC separation conditions. No obvious difference was observed for sample plugs generated at the beginning of gradient with 70% acetonitrile and at the end of gradient with 0% acetonitrile.

Detection of LC Separated Components Offline. To compare off-line detection of fractions with on-line LC-MS detection, we analyzed a 20 μM mixture of 4 small molecule metabolites (malate, citrate, PEP and F1,6P) using HILIC interfaced to MS both on-line and off-line. For on-line analysis, the components were detected by full scan with a QQQ MS (Figure 5.5A). For off-line analysis, the fractions were collected as segmented plugs and 1 hour later infused through a nanoESI emitter tip to a LIT MS operated in full scan mode. In the off-line trace (Figure 5.5B), the individual LC peaks were cleaved into 10-18 fractions. This number of fractions is sufficient to prevent loss of resolution.[268] As discussed above, it is possible to adjust conditions to yield different fraction volumes depending upon the experiment.

In comparing on-line and off-line analysis, the peak shapes and relative sizes are the same indicating no extra-column band broadening occurred during fraction storage and analysis. Resolution is also unaffected, e.g. resolution (R_s) for citrate and PEP was calculated to be 2.0 for both on-line and off-line detection. The most obvious difference in the traces is that the overall times for all four sample peaks are longer in the segmented flow sample (5 min for off-line compared to 8 min for on-line). This difference occurs

because the flow rates were kept the same in both methods at 500 nL/min; but, the ratio of oil to sample volume is 3:5, so that infusion of the oil added 3/5 analysis time compared to sample analysis time in the off-line detection. These results illustrate that detection of the chromatogram was unaffected by the storage of those samples in oil-segmented flow and that capillary LC separated components can be preserved for additional analysis off-line.

In agreement with the observation of collected fractions, the widths of the ion current signal for individual fractions was independent of the organic solvent content of the mobile phase. Thus at the beginning of the gradient the average peak widths were 0.036 ± 0.011 min (n = 26) and at the end of the gradient were 0.035 ± 0.013 min (n = 26). The RSDs of plug widths during detection was similar to that when detecting standard sample plugs. Despite the variation in plug widths, the resulting peak shape in chromatograms was unaffected. This observation suggests that substantial coalescence did not occur within the emitter tip because coalescence would lead to peak tailing and fronting because of cross-contamination f the fractions.

Peak parking. We next tested the off-line system for extending the MS analysis time of selected components, analogous to peak-parking, for two examples. The first was to obtain multiple MS^2 spectra (i.e., multiple reaction monitoring) for co-eluting peaks using a relatively slow mass spectrometer. For complex samples, MRM is a common method for simultaneous detection and quantification of targeted components.[269-271] Triple quadrupole MS is generally used for MRM detection because of its ability to rapidly switch between different MS-MS transitions; however, quadrupole ion traps can be advantageous for MRM because they usually have better full scan sensitivity in MS^2,

and can be used for MS^n analysis, which cannot be done by QQQ. A limitation of this approach is that MRM on an ion trap is relatively slow due to longer scan time. For demonstration of off-line ESI-MS with MRM, we analyzed a test mixture of five metabolites, fumarate, succinate, malate, cAMP and F1,6P at 10 μM each. Fumarate, succinate and malate were allowed to co-elute to illustrate the challenge of MRM for co-eluting compounds. In the experiment, fractions were collected at 0.84 s intervals corresponding to 7 nL samples.

On-line detection of the three co-eluting compounds gave RICs as shown in Figure 5.6A. In the first case of off-line detection, the sample was analyzed by pumping the fractions at 500 nL/min while monitoring MS-MS transitions on a linear ion trap for all 5 analytes yielding the RICs shown in Figure 5.6B. Under this condition, the total time for the 3 co-eluting analytes was about 30 s but the MRM scan time was 1.8 s for each point of one analyte; therefore, it was possible to only obtain 1 scan for each MS-MS transition over a sample plug as illustrated in Figure 5.6B. Furthermore, not all compounds could be detected in each plug so for some sample plugs, no signal of a particular compound was detected. For example, the middle RIC in Figure 5.6B showed a total of 6 spikes, which were 6 points detected for succinate (m/z 117) peak. However, no signal was detected between the fourth and fifth spike, while a sample plug was seen at the same time, indicating a missing signal for that plug.

The off-line experiment was then repeated but the flow rate was reduced from 500 nL/min to 50 nL/min during the detection of the co-eluting peak (Figure 5.6C). Under this condition, the peak width, and detection time, is increased by a factor of 10. This allows many more scans to be acquired per sample plug and per chromatographic band.

For succinate, only 6 scans with S/N > 3 were obtained at 500 nL/min as shown in Figure 5.6B, while over 80 scans were obtained with the reduced flow rate as shown in Figure 5.6C. With the greater scan number, it was also possible to detect the analyte in all the plugs. Meanwhile, the advantages of capillary LC are preserved such as high resolution, improved sample concentration and increased ionization efficiency.

As a second demonstration of the utility of off-line analysis for peak parking, we examined acquiring multiple spectra for compound identification using analysis of a tryptic digest of the peptide CRF as an example. In the separation of CRF tryptic peptides, the flow rate of LC separation was reduced to 100 nL/min to reach better nano-ESI sensitivity. So the oil flow rate was lowered to 60 nL/min to maintain a fixed ratio at 5:3 as well. Compared to the experiment above, despite of different flow rates, droplet sizes were the same at 7 nL. With on-line separation at 100 nL/min and full scan MS, the most dominant peak in the chromatogram corresponds to the fragment with m/z 623 (Figure 5.7A), but the peak was only about 0.3 min wide which was insufficient to acquire multiple stages of MS with optimized CID manually. To confirm the sequence of this fragment peptide, fractions were collected and off-line ESI analysis performed at 100 nL/min. During elution of the peak of interest, the flow rate was reduced to 25 nL/min. In this way, a 0.3 min wide peak was extended to about 1.8 min width which allowed manual selection of parent ions for MS^2 and MS^3 analysis. During this time, a series of 8 fractions (i.e., sample plugs) were pumped through the emitter. The parking event was terminated after the MS^3 analysis was accomplished. With the spectra, we found the most abundant tryptic fragment of CRF is the peptide CRF1-16 with sequence SEEPPISLDLTFHLLR by comparison with Protein Prospector MS-product database.

(This software is freely available on the web at http://prospector2.ucsf.edu/.)

This approach offers a simple alternative to on-line peak parking. To achieve peak parking with on-line capillary LC-MS, specially designed LC-MS systems were needed to be used that allow the flow rate to be reduced during separation.[255, 272, 273] Thus, when a peak of interest elutes into the MS, the LC flow rate is switched from normal to reduced flow for the extension of analysis time for selected peaks. While this approach is feasible, it has several difficulties. Successful flow rate switching for gradients at low flow rates requires considerable engineering of the flow system. Also, because larger emitter tips yield unstable sprays under these conditions, the best results have typically been obtained from small emitter tips (1-2 μm), which are unfortunately the easiest to be clogged.[273] With the off-line approach however, it was easy to change the flow rate for peak parking by only changing the flow rate of the syringe pump for infusion of the segmented flow into MS. These flow rate changes had little effect on signal intensity over a range of 20 nL/min to 2 μL/min. By decoupling the separation and MS detection, it is possible to maintain the optimal flow rate for separation and MS analysis.

The system described here is also a useful alternative to collecting fractions in a multi-well plate. A primary advantage for this approach is the ease of collecting, manipulating, and analyzing nanoliter volume fractions which is extremely difficult when using multi-well plates.[274]

Other applications of the fraction collection and off-line analysis can be envisioned. By splitting plugs, using established methods,[275, 276] it would be possible to analyze plugs by different mass spectrometers, NMR[277], a second dimension of separation[257], or other methods. Furthermore, plugs could be stored as long as they are stable for later analysis

or re-analysis. The system may also be useful for multiplexing a MS. If the chromatographic separation is relatively slow, it may be possible to perform several separations in parallel and then rapidly infuse them into a fast scanning MS, e.g. TOF-MS, for improved throughput.

5.4. Conclusions

In this study, we have established a method for direct ESI-MS analysis of oil-segmented flow. When coupled with fraction collection from capillary LC, the method allows off-line ESI MS analysis with no extra column band broadening and no mixing of fractions collected. The system was shown to yield mass chromatograms that are equivalent to on-line analysis. With off-line analysis however, it is possible to better match the MS analysis time to the chromatographic peak widths. In this case, we demonstrated the equivalent of peak parking wherein flow rate is slowed for longer MS analysis of selected fractions. The system was demonstrated to be suitable for both reverse phase and HILIC separations. The method illustrates a general approach for preserving low volume components from microscale separation for further manipulation and study. Other applications are possible such as performing multiple assays on collected fractions. The capability of segmented flow ESI-MS for analysis rates over 2 Hz was also demonstrated. This suggests the potential for using ESI-MS for high-throughput screening in drug discovery and other applications.

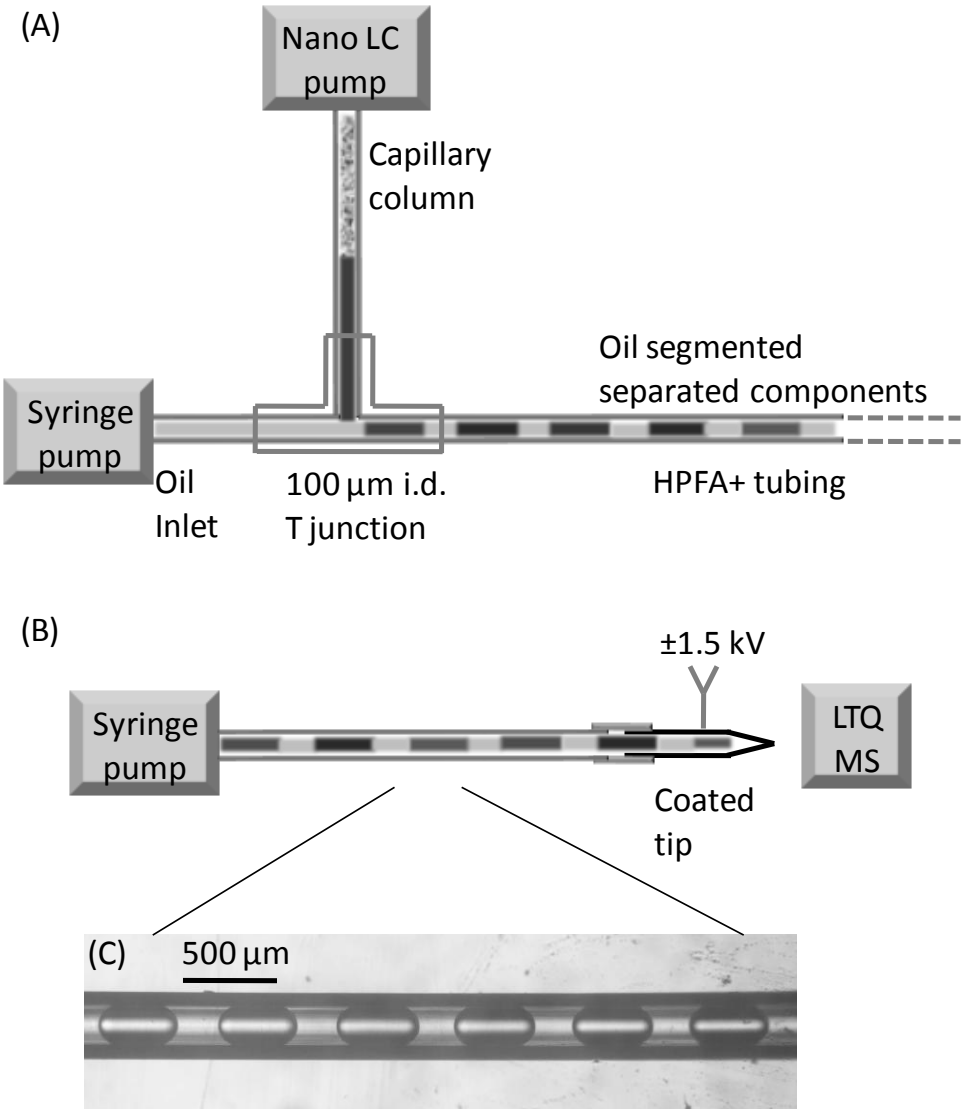

Figure 5.1: Illustration of scheme for fraction collection from capillary LC and off-line ESI-MS using segmented flow. (A) Segmented flow was generated with a tee junction that connected an oil stream and effluent from capillary LC. (B) Oil-segmented fractions collected could be stored in HPFA+ tubing and then be infused into MS off-line by a syringe pump. (C) Picture of the oil-segmented flow in 150 µm i.d. tubing showing ~400 µm long sample plugs (LC fractions) separated by ~240 µm long oil plugs.

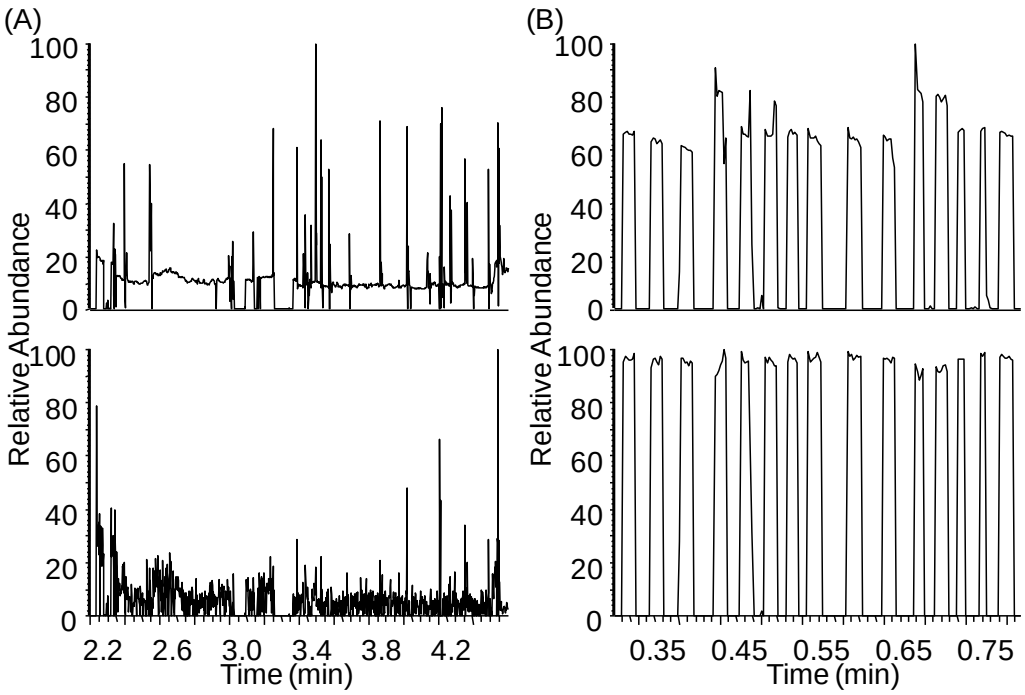

Figure 5.2: (A) TIC (upper) and RIC (lower) of 50 μM cAMP (m/z = 328) sample droplets infused at 200 nL/min with FC-72 as oil phase, showing noisy signal all over the chromatogram and little signal of samples. (B) TIC (upper) and RIC (lower) of the same cAMP sample droplets with PFD as oil phase, showing discrete segmented signals of cAMP sample plugs.

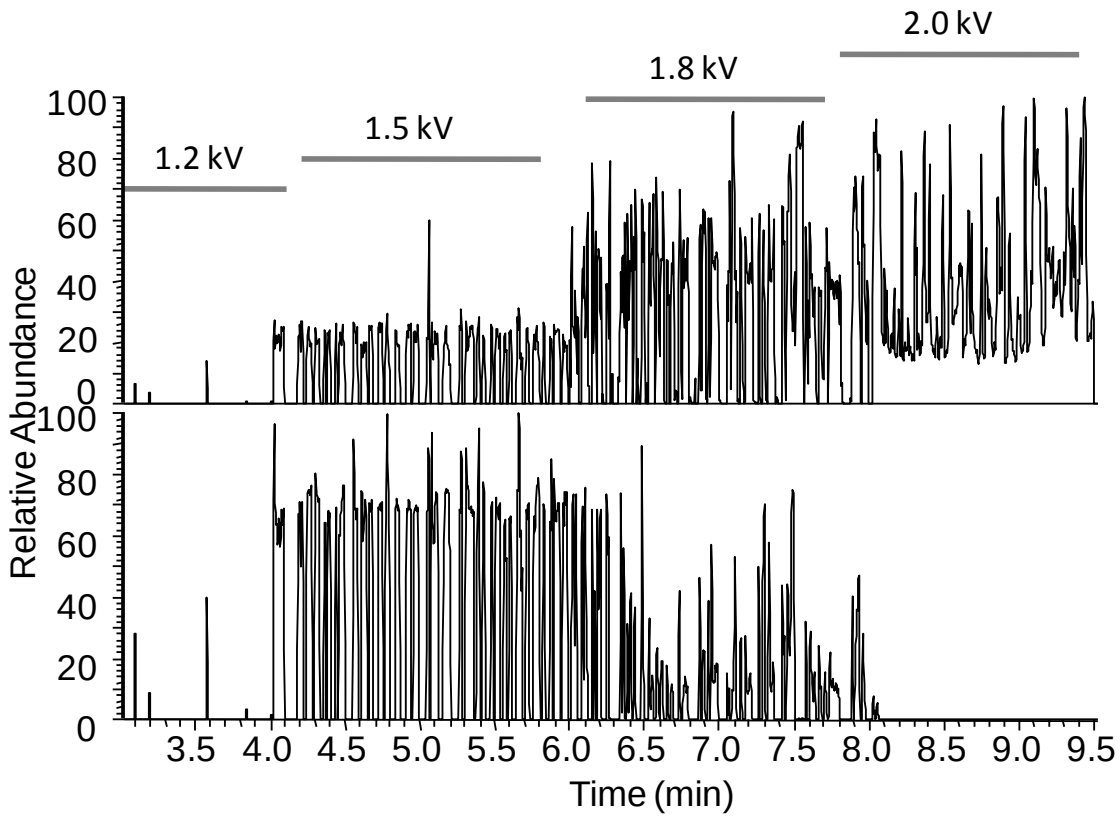

Figure 5.3: (A) TIC (upper panel) and RIC (lower panel) of oil segmented droplets of 50 µM cAMP sample infused at 200 nL/min, with different spray voltage from 1.2 to 2.0 kV. (B) Oil coming at the tip at 1.5 kV just dripped off the tip. (C) Oil underwent ESI at 2.0 kV. When the oil sprayed, the TIC signals were higher due to more signal of oil, but the RIC for aqueous samples were lower, which means the spray of oil interfered with the sample ions.

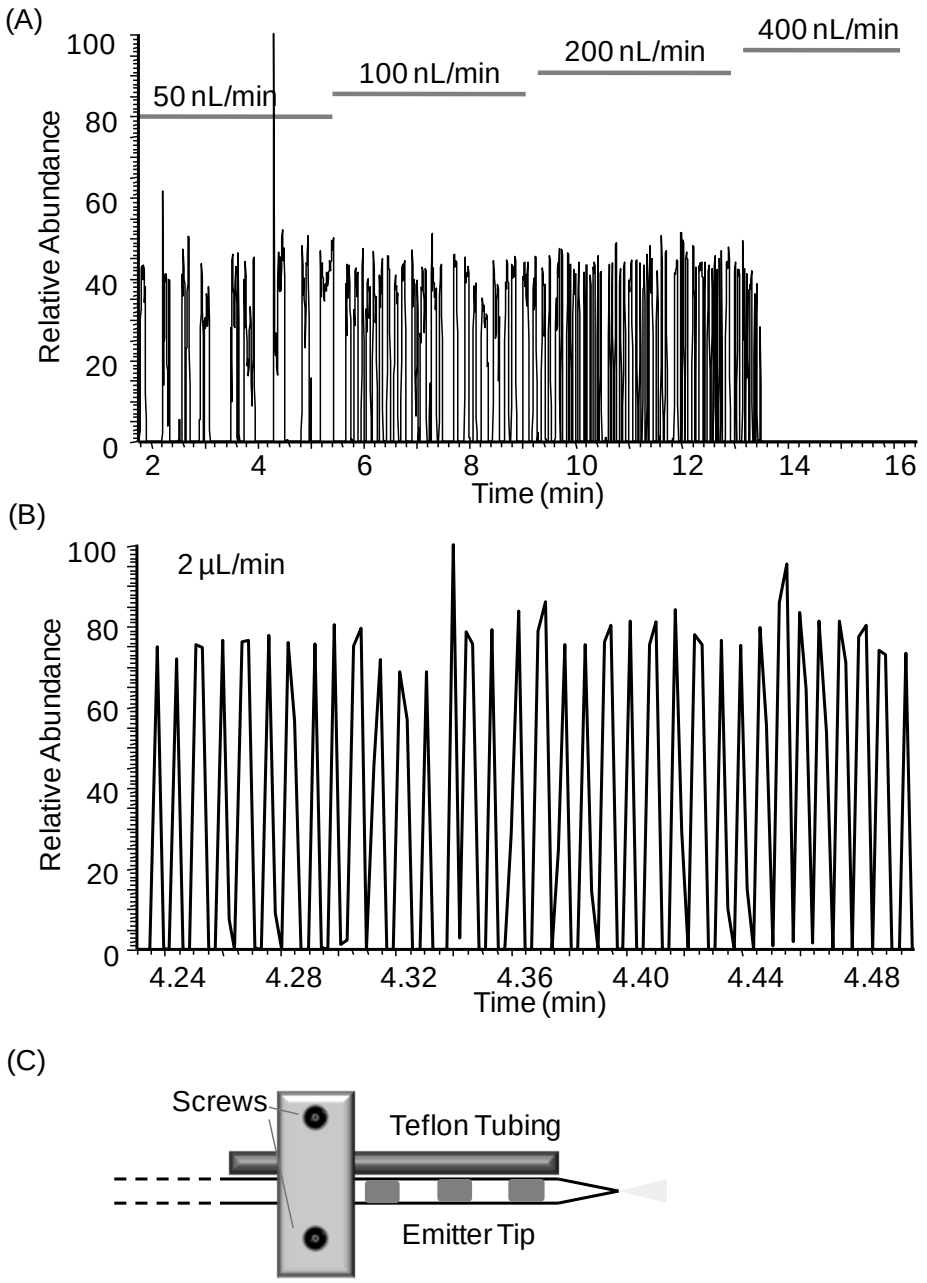

Figure 5.4: (A) RIC of oil segmented droplets of 50 µM cAMP sample infused at different flow rate from 50 to 400 nL/min. At 400 nL/min, no signal was seen because oil accumulated at the emitter tip too fast to be removed so it blocked the voltage causing no signal. (B) RIC of oil segmented droplets infused at 2 µL/min. In this case, with a side Teflon tubing to extract oil out (shown in C), such high flow rate could be used and fast detection of droplet signal was achieved. This chromatogram showed detection of 35 droplets in 0.26 min, which is a frequency at about 2.2 Hz.

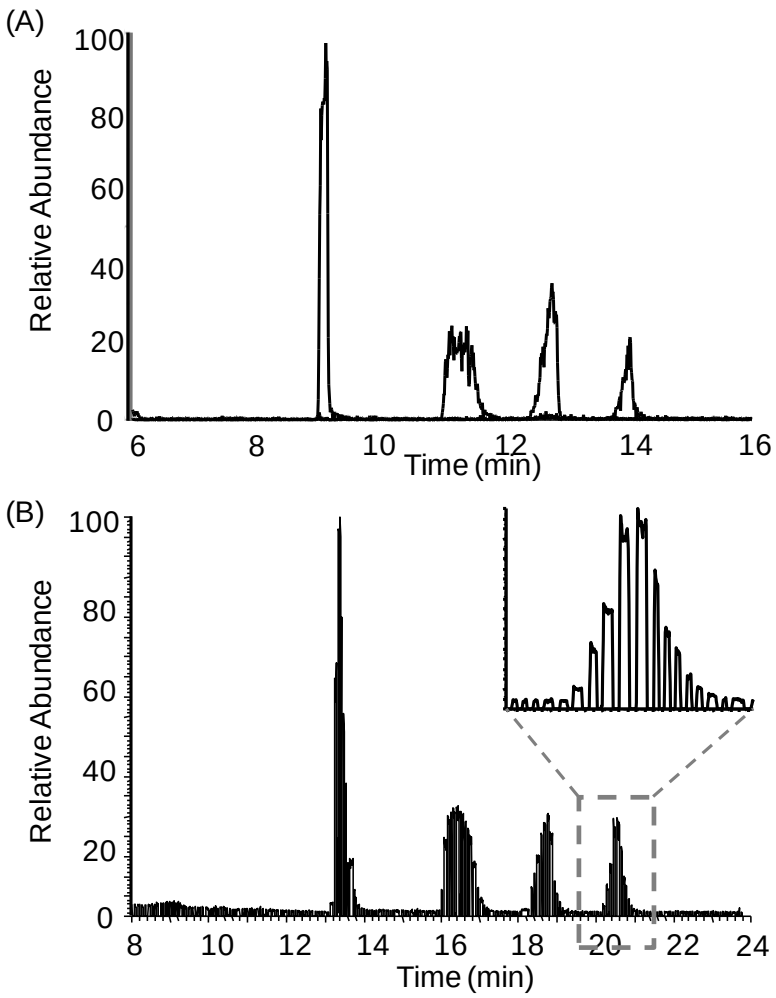

Figure 5.5: Overlap of RICs for 4 metabolite components. (A) On-line detection of 4 sample on micromass QQQ MS, showing peaks of malate, citrate, PEP and F1,6P in a row. (B) Raw RICs of the 4 sample in droplet format obtained using the LIT MS. Using the same flow rate at 500 nL/min, it took 16 min to analyze 10 min of LC effluent because the oil in the final segmented flow accounts for 3/8 of total volume. A zoomed look of the detection of fractions over the F1,6P peak was shown.

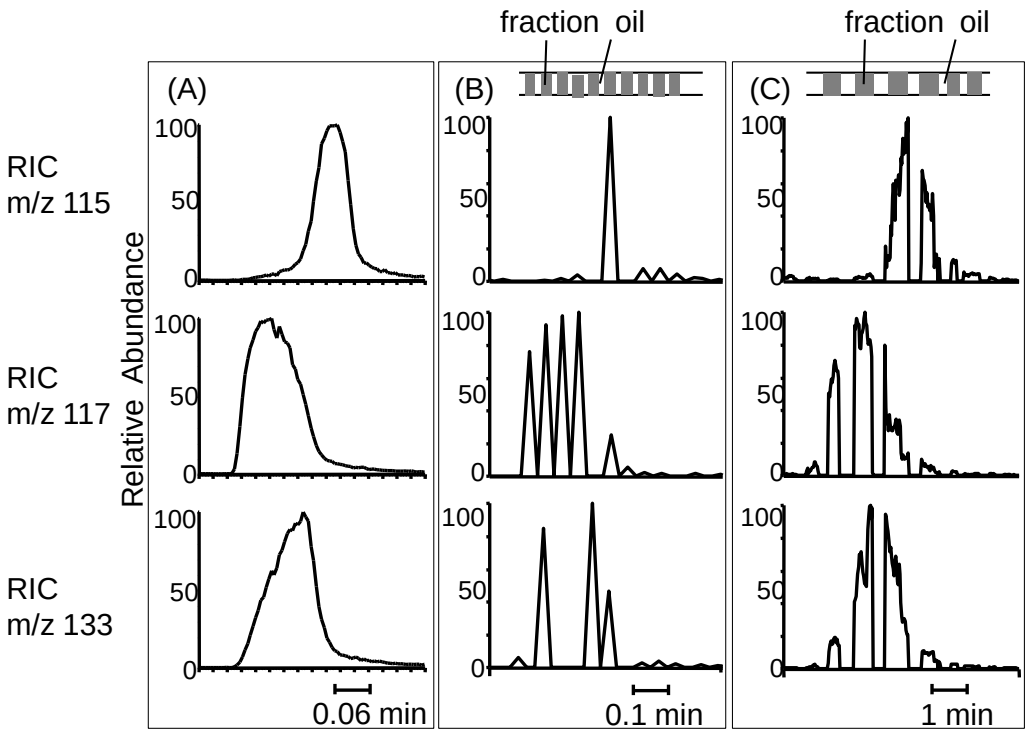

Figure 5.6: Comparison of RICs of 3 co-eluting components fumarate (m/z 115), succinate (m/z 117) and malate (m/z 133) without and with peak parking. Different time scales for three groups of chromatograms were marked at the bottom of each figure. (A) On-line detection of the 3 compounds with QQQ-MS. (B) Off-line detection of the 3 compounds in segmented flow at 500 nL/min, the same flow rate as the original on-line detection. These peaks were narrow, resulting in only 1-5 scans covering each sample peak. Top figure showed rough sample droplets distribution. (C) Off-line detection of the 3 compounds in segmented flow by reducing flow rate to 50 nL/min right before the three peaks, resulting in more scan numbers over each sample peak.

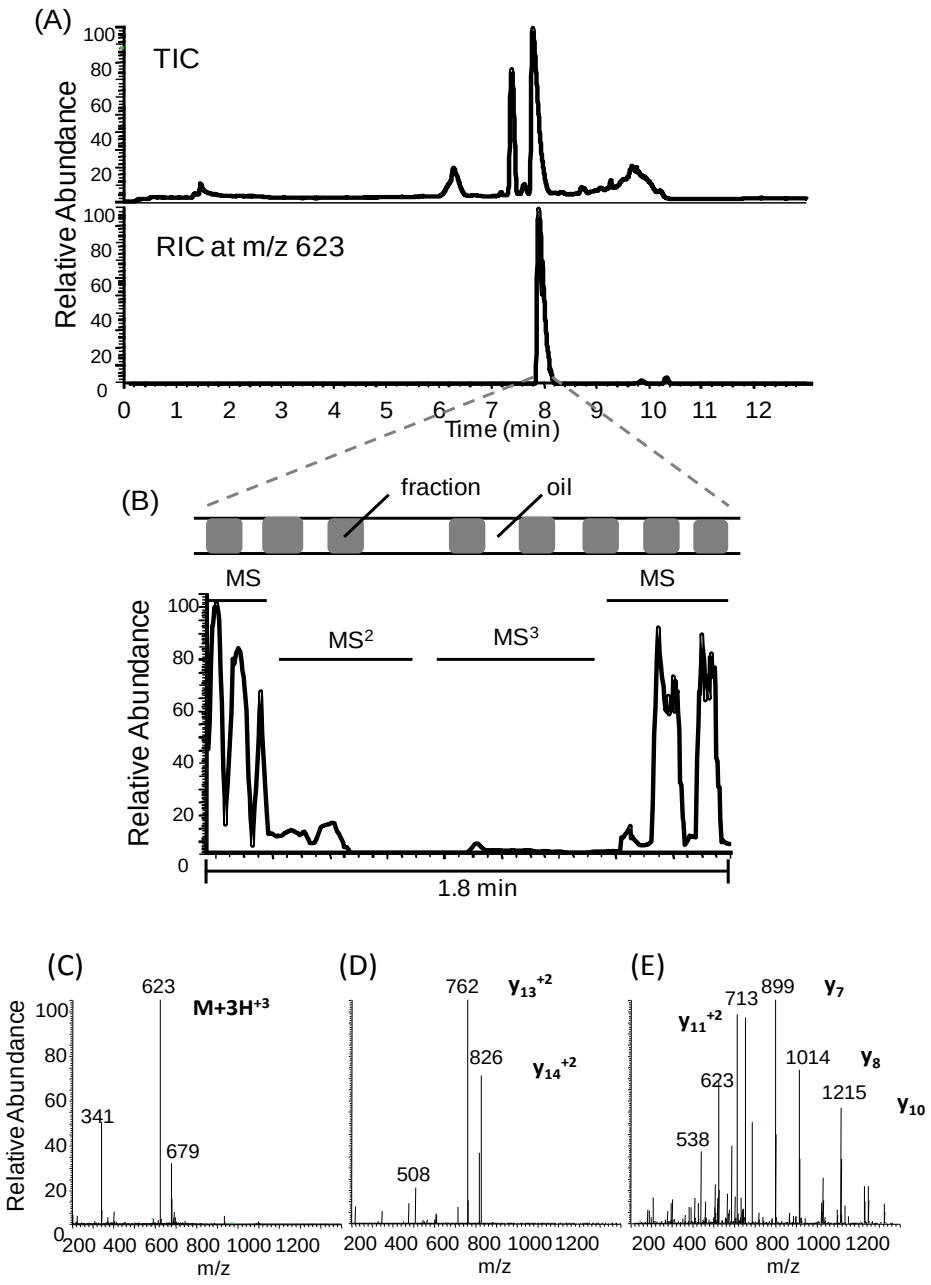

Figure 5.7: (A) TIC and RIC of trypsin digested CRF. RIC showed the peak of the most abundant fragment peptide at m/z 623. (B) The expanded region of the TIC corresponding to the peak parking event initiated when first peak at m/z 623 was seen for MS detection of segmented flow of the separation. MS^2 and MS^3 analyses were performed manually by selecting the most abundant parent ion. Sample droplet distribution was indicated, which was uneven due to unstable perfusion flow rate at 25 nL/min generating by the syringe pump. TIC for MS^2 and MS^3 were lower compared to MS signal. (C),(D), and (E) show mass spectra corresponding to the MS, MS^2 and MS^3 event respectively in the peak parking region.

Table 5.1: Dynamic viscosities of five tested oils at 300 K and comparison to commonly used ESI solvents water and methanol.

	Hexane	**Methanol**	**FC-72**	**Water**	**FC-77**	**FC-40**	**PFD**
Dynamic viscosity (mPa s)	0.3	0.56	0.64	0.89	1.3	3.5	5.1

CHAPTER 6

FUTURE DIRECTIONS

In this dissertation, we improved the capillary LC-MS system in two aspects. In terms of method development, several novel approaches have been added to the analytical technique performed previously in the Kennedy lab. A simple but effective way for storage of neuropeptide in dialysate was developed and proven to maintain the samples for up to 5 days allowing reliable off-line detection. The robustness of the system has been improved by adding inline frits and extensive filtration of all solutions flowing into the column. Efforts have also been made to improve the quantification ability by inducing an isotopically-labeled internal standard, which reduced the detection RSD of *in vivo* samples collected every 5 min from over 30% to ~10%. The temporal resolution with microdialysis sampling for enkephalin detection was improved from more than 20 min to 5 min. The capillary LC-MS system has also been tested for neuropeptides other than enkephalins, especially larger peptides with low sensitivity by MS detection. BE, a model analyte, has been measured *in vivo* with high sensitivity detection (LOD at 3 pM) for its characteristic tryptic fragment. Four opioid peptides have been detected under basal and 75 mM K^+ stimulation and their extracellular concentrations have been calculated with external calibration. In addition, a novel design to collect nanoliter-level fractions via segmented flow from the capillary LC effluent was developed and tested off-line with nano ESI-MS. Using a 100 μm i.d. Tee junction,

effluent from a capillary LC separation was segmented by oil. With this approach, chemically-separated components were preserved as nanoliter-level plugs and could be stored and transported easily. The segmented flows were then analyzed off-line on a linear ion trap MS, leading to consistent results similar to traditional on-line analysis. At an optimal ESI voltage of 1.5 kV and within a flow rate range of 20 to 2000 nL/min, aqueous plugs interspersed in the oil-segmented flow were ionized via ESI while oil plugs were dripped off the emitter tip or were extracted with hydrophobic Teflon tubing connected to the side of the tip when using higher flow rates. A sample analysis rate of 2.2 Hz was achieved, and peak parking of selected peaks was realized by changing the infusion rate of the segmented flow to obtain more structural information of the samples.

In terms of application, this method now has been used routinely for addressing pharmacological problems. We have demonstrated the use of the system for reliable analysis of *in vivo* opioid peptides, particularly Met- and Leu-enkephalin (ME and LE) by coupling it to microdialysis sampling with fraction collection from freely-moving rats. A preliminary study revealed a substantial release of these neuropeptides in the GP/VP region caused by acute administration of amphetamine (AMPH), a dopamine-stimulating drug. This study for the first time indicated a relationship between dopamine and ENK release as well as a possible correlation between ENK precursor expression levels and ENK release to the extracellular space in certain brain regions.

Future work based on this dissertation can be directed towards both improvement of the analytical method and further application for more pharmacological studies.

6.1. Detection of larger peptides or proteins with quantitative measurement of their tryptic fragments

By coupling microdialysis with LC-MS analysis, one problem is that the technique is limited to relatively small peptides due to poor fragmentation of larger peptides or proteins by the mass spectrometer and poor recovery of larger molecule by the microdialysis probe. However, Chapter 2 of this dissertation proposed a promising method for quantitative analysis of such larger peptides or proteins, by detection of a trypsin-digested peptide fragment with the capillary LC-MS system. BE as a model molecule was proven successful.

In future work, other larger neuropeptides such as corticotrophin-releasing hormone (CRH) and Gastrin-releasing peptide (GRP) would be of interest as they are implicated in a number of physiological and pathophysiological processes. The ability to sample and measure larger peptides would also allow trophic factors to be monitored for the first time. For example, brain-derived neurotrophic factor (BDNF) is a growth factor that has been implicated in evoking changes in neuron structure that lead to enduring adaptations such as in learning and addiction as well as the survival of dopaminergic neurons of the developing substantia nigra.[278, 279] Growth factors have also been implicated as possible treatments for neurodegenerative diseases;[280] as such, measuring the concentration *in vivo* is important in assessing their transport and effectiveness. Due to the difficulty of detection and measurement, there have been no reports of the extracellular concentration of BDNF in brain. The protein level has been estimated by the mRNA expression levels as have most of the other neuropeptides or hormones.

The molecular weight of BDNF is 13.6 kDa, which is suitable with the current

CMA/12 probes of 20 kDa or 100 kDa MWCO; therefore, it should be possible to recover it from extracellular space. After sample collection, an in-solution trypsin digestion will be done to generate fragment peptides as markers of the BDNF molecule. With optimization of the MS methods to detect one or more fragment peptides, we will be able to achieve quantitative measurement of this protein from dialysis samples. This method will provide the first opportunity to monitor the dynamics of trophic factors in the brain and potentially their role in learning, addiction, and disease treatments.

6.2. Monitoring neuropeptides with better spatial resolution

In Chapter 2 of this dissertation, efforts to improve the temporal resolution of the neuropeptide of interest have been introduced. Another important factor on evaluating an *in vivo* microdialysis study is the spatial resolution. Limited by the requirement of sufficient recovery, commercial microdialysis probes with 4 mm long and 500 μm o.d. were used in the experiments, limiting the spatial resolution of this study to the probe size at 4×0.5 mm. In Chapter 4, the probe used was found to sample not only GP/VP regions but also some surrounding brain regions including part of striatum. Neuropeptides in those different brain regions might have differential responses to stimuli, thus, requiring better spatial resolution for more accurate study, especially for solving pharmacological problems. Moreover, the commercially-available probes are also expensive, which may limit their extensive usage to reveal more biological information.

Recently, smaller probes with 2.0 to 2.5 mm sampling length have been made in the Kennedy lab by Dr. Mabrouk. Two types of membrane materials have been tested. One is acrylonitrile sodium methallyl sulphonate from Hospal (Bologna, Italy); the other is

polyarylethersulphone (PAES, the same membrane as on CMA/12 probes used in this dissertation) from Gambro (Lakewood, CO). Microdialysis probes were made with diameters of ~250 μm and implanted into the GP with coordinates Anterior-Posterior (AP): -1.3, Medial-Lateral (ML): -3.2, Dorsal-Ventral (DV): -7 from dura and the VP with coordinates AP: -0.3, ML: -2.4, DV: -8.2 from dura for collecting samples from these two different brain regions from the same animal. Preliminary studies with these probes have shown sufficient recovery of enkephalins, although lower compared to the larger probe, which allows us to use these probes for microdialysis sampling. It will be very interesting to reveal the neuropeptide levels and dynamic changes in these brain regions at higher spatial resolution in future.

6.3. Exploration of the effect of dopamine receptor on enkephalin dynamics

As described in Chapter 4, our preliminary discovery of ENK release in the basal ganglia caused by AMPH injection further confirmed the relationship between drugs of abuse and the endogenous opioid system. Future efforts will be made to understand more details of such influences.

Our long-term goal is to demonstrate which factors prompt such ENK release and finally to confirm the protective mechanism of the opioid peptide against neuronal injury. The hypothesis is that endogenous ENK release and subsequent δ-opioid peptide receptor stimulation represent a natural compensatory mechanism when projection of DA is dysregulated in basal ganglia. To elucidate this question, further efforts can be made in two directions. The first direction is to determine how ENK release is changed in striatal and pallidal regions during different phases of AMPH intoxication. Our preliminary

findings filled the gap between DA signaling and ENK release partially. In order to elucidate the potential role of DA receptors in the striatal and pallidal response of ENK systems to the AMPH treatment, DA D1 and D2 receptors will be blocked by adding antagonists with reverse microdialysis or systematic administration. D1 receptor antagonist SCH 23390 or D2 receptor antagonist haloperidol will be prepared at an optimal dose to inhibit these receptors while keeping the other neurotransmitter systems at a normal level. The ENK levels will be measured under such inhibition, but with systematic injection of AMPH. In this way, the main factors that mediate such projections from striatum to pallidum will be revealed.

The second direction is to determine how manipulating endogenous ENK levels or direct stimulation of the δ-opioid peptide receptor influence the AMPH-induced neural degeneration. Because AMPH and related drugs have been shown to cause neuronal damage in multiple animal models as well as in humans, the release of ENKs caused by AMPH injection has indicated a possible transient response of such neuropeptides as a protective effect to the drugs based on our studies. Once we are able to better understand the relationship between the ENK systems and neuronal degeneration in the brain, it will be possible to target these systems for potential neuroprotective therapeutics.

6.4. LC fraction collection coupled to additional chemical manipulation or detection

As discussed in Chapter 5, fraction collection of capillary LC effluent and generation of separated components in segmented flow has been developed. In other work, we have shown that sample plugs segmented by oil can be prepared in Teflon tubing by dipping the tubing end into a multi-well plate to form different sample plugs

(see Figure 6.1). Direct MS analysis of such plugs has advantages, such as peak-parking (shown in Chapter 5) or high throughput screening (HTS).[181, 281] Further development of droplet manipulation will expand the scope of applications of this approach. Examples of manipulations that would be of interest include droplet splitting and reagent addition. Some work has already been done on developing such methods. The combination of fraction collection and droplet splitting would allow multiple assays to be performed on fractions. For example, both fluorescence detection and MS detection could be used on protein samples. Fluorescence detection is more convenient to profile and quantify the total amount of proteins while mass spectrometry is a powerful tool to identify and reveal structural information of isolated proteins.[282] Therefore, these two techniques can offer complementary information for protein analysis. Alternatively, two or more different MS instruments can be applied for analysis of the same series of samples, such as a QQQ for accurate quantification and a QIT or LIT for multi-stage fragmentation.

The use of droplet splitting and reagent addition could allow HTS at the nanoliter-scale with MS detection. A series of potential test compounds (i.e., a chemical library in a multi-well plate) could be "reformatted" using the approach in Figure 6.1A. To screen the test compounds, a portion could be split off (Figure 6.1C). Reagents necessary for the screening assay could be added as shown in Figure 6.1D. Reagent 1 in the figure could be the enzyme added into each inhibitor sample plug while reagent 2 could be the substrate solution to be added downstream. After that, the mixture sample plugs will be allowed to react for a certain incubation time by either controlling the flow rate of the segmented flow or adjusting the tubing length after the second Tee junction. Finally, reagent 3 can be added to quench the reaction and facilitate subsequent ESI by inducing

some organic solution, and the segmented flow could go directly into an ESI emitter tip for MS detection and analysis. This experimental scheme will not only work for such enzyme inhibitor screening assays, but it could also work for other reactions by changing the reagents. Finally, the plugs could be passed through the MS for detection. With this experimental scheme, HTS and other assays could be performed.

The droplet/plug approach could also be used for post-column manipulation of fractions. One difficulty of doing pre-column reactions lies on the complexity of the sample resulting in confusing identification of the reaction product. For example, trypsin digestion of one protein analyte in a protein mixture would generate non-specific fragments similar to other proteins resulting in false positive measurements. Thus, it will be more specific to do the digestion reaction in the plugs of the chosen sample band after LC separation, and the downstream MS detection of that fragment peptide will be more accurate.

The micro-scale LC fraction collection method described here can also allow second dimensional analysis as was first proposed by the deMello group.[257] With better second dimension separation efficiency using CE separation of sample droplets that our group has proposed,[180] we believe that we improve the 2-D separation. The second dimension can also be another capillary LC run with further development to load such sample droplets onto an LC column.

6.5. Hyphenation of pump-free LC or SPE with MS detection of salty sample

One important step of LC separation is desalting. Biological samples such as *in vivo* dialysates or cell extracts contain large amounts of inorganic salts, which have

severe ion suppression effects that interfere with ESI signal of the samples. We have demonstrated the ability of desalting using a reverse-phase LC column with traditional LC pumps in this dissertation. In future work, formation of a series of sample and solution plugs to mimic such procedure is promising to miniaturize the system.

This idea can be demonstrated as in Figure 6.2 where pumping samples and eluting solutions, shown as a series of plugs separated with air gaps, are transferred to a short (1-2 cm) packed column of reverse-phase C18 particles in capillary. Only a single syringe pump is needed to push the samples and solutions through the column realizing sample loading, desalting with water, eluting with high organic mobile phase, and re-equilibrating with water in a row as well as mimicking the rather complicated LC pump functions but at a smaller scale and in a simpler way. The outlet of the column is connected to an ESI emitter tip for the ESI-MS analysis.

A preliminary result is shown in Figure 6.2 with a serial injection of four 100 nL 18 nM LE sample plugs dissolved in aCSF, followed by around 1 μL water for desalting, another 1 μL 60% methanol and 2% acetic acid in water for elution, and then additional 1 μL water for re-equilibration. All these sample and solution plugs were separated with about 100 nL air in 150 μm i.d. Teflon tubing, and peaks of these four samples were appeared with an about 7-min intervals with continuous MS detection. The infusion flow rate was 500 nL/min. The system was proven to have low carry-over between samples as shown in Figure 6.2 by the tiny peak in a subsequent blank aCSF sample. One drawback of the preliminary experiment was that by using air to separate sample plugs, the air can be compressed over time resulting in mixing of sample and eluting solution and missed signal after 4-5 injections. Using immiscible oil to separate these plugs can be an

alternative way to prevent such mixing; however, the oil plugs were found to interfere with the sample elution on the short reverse-phase column resulting in poor chromatograms. Therefore, to solve such problems, an effective method to remove the oil phase completely prior to the column will be needed. At this point, preliminary chip designs to extract oil off with hydrophobic side channels have failed due to high back-pressure generated at the short packed column tended to force aqueous solution passing through the microfluidic channels as well. If this system can be further designed, such a novel pump-free, automated and high-throughput sample desalting and ESI-MS detection device could serve as an on-line desalting method for a large number of samples.

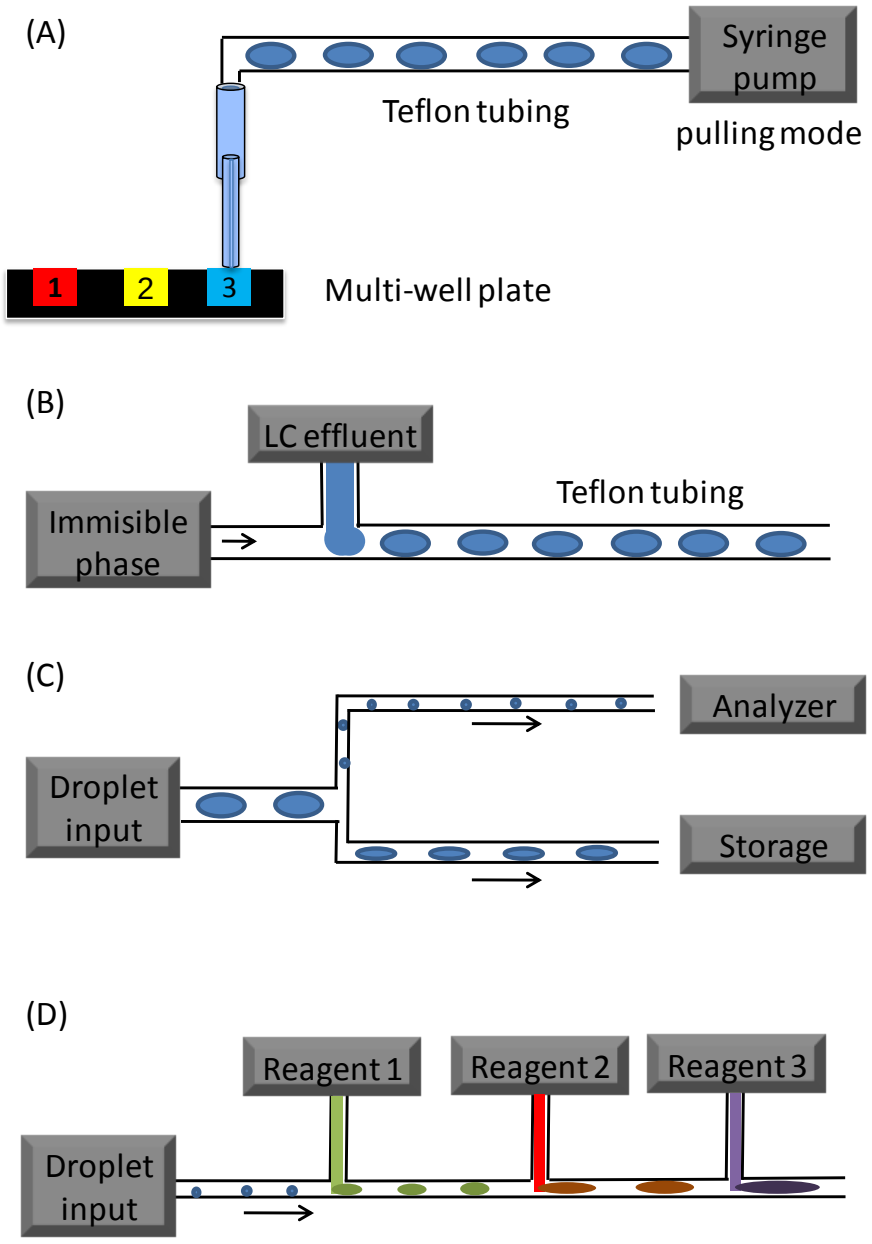

Figure 6.1: Segmented flow generation and post-separation fraction processing. (A) Segmented flow generation from a multi- well plate. (B) Segmented flow generation with fraction collection from micro-scale LC separation. (C) Droplet splitting used to produce two or more identical cartridges containing the same series of sample plugs. (D) Derivatizing agents added into previously collected or splitted droplets using Tee junctions.

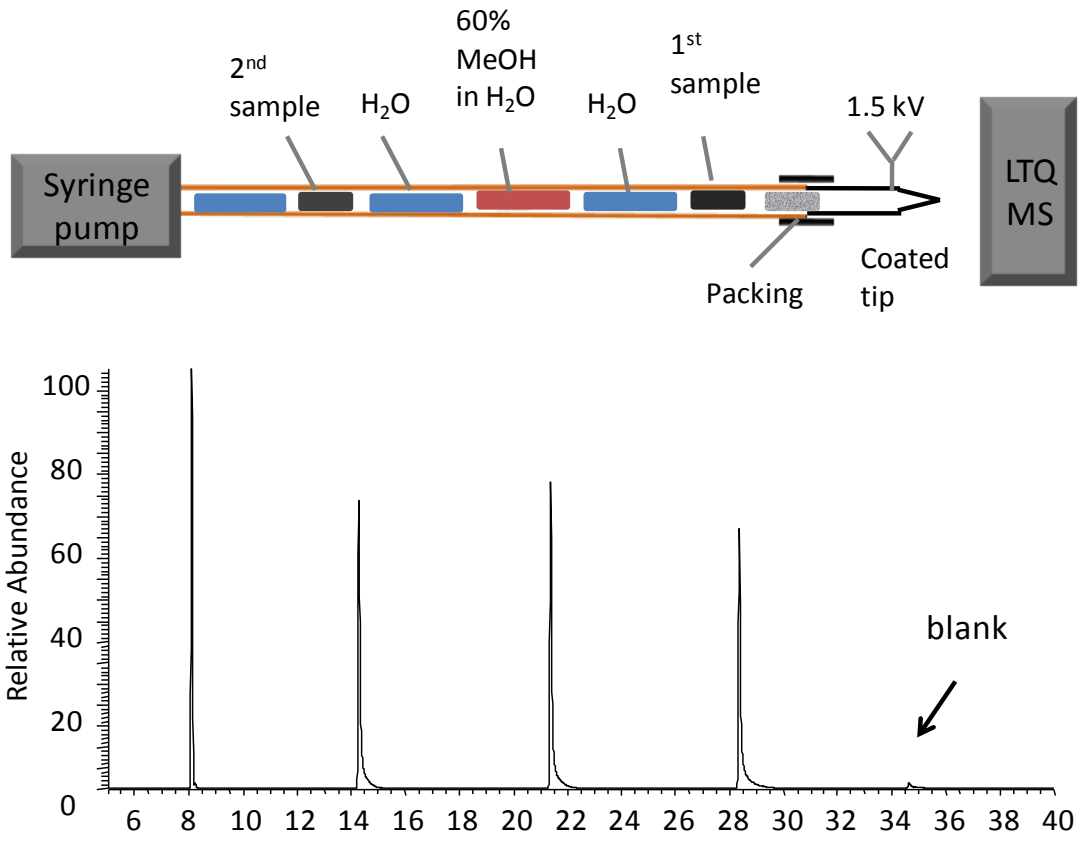

Figure 6.2: Droplet-based LC separation for desalting. A sample droplet, a wash droplet followed by eluting solution, and re-equilibrating solution segmented with air gaps are pumped through a reverse-phase packed short column sequentially. The chromatogram showed a preliminary result of four 18 nM LE samples in aCSF and 1 blank sample detected with this system.

BIBLIOGRAPHY

(1) Blanton, M. G.; Kriegstein, A. R. *Journal of Neurophysiology* **1992**, *67*, 1185-1200.
(2) Macintosh, F. C. *Canadian Journal of Biochemistry and Physiology* **1959**, *37*, 343-356.
(3) Parsons, S. M.; Prior, C.; Marshall, I. G. In *International Review of Neurobiology, Vol 35*; Academic Press Inc: San Diego, 1993; Vol. 35, pp 279-390.
(4) Lesch, K. P.; Bengel, D. *Cns Drugs* **1995**, *4*, 302-322.
(5) Krieger, D. T. *Science* **1983**, *222*, 975-985.
(6) Burger, E. *Arzneimittel-Forschung/Drug Research* **1988**, *38-1*, 754-761.
(7) Bolles, R. C.; Fanselow, M. S. *Annual Review of Psychology* **1982**, *33*, 87-101.
(8) Cooper, S. J. In *Mesolimbic Dopamine System : From Motivation to Action*; Willner, P., Scheelkruger, J., Eds.; John Wiley & Sons Ltd: Chichester, 1991, pp 331-366.
(9) Douglas, A. J.; Dye, S.; Leng, G.; Russell, J. A.; Bicknell, R. J. *Journal of Neuroendocrinology* **1993**, *5*, 307-314.
(10) Van Bockstaele, E. J.; Menko, A. S.; Drolet, G. *Molecular Neurobiology* **2001**, *23*, 155-171.
(11) Przewlocki, R.; Przewlocka, B. *European Journal of Pharmacology* **2001**, *429*, 79-91.
(12) Zadina, J. E.; Hackler, L.; Ge, L. J.; Kastin, A. J. *Nature* **1997**, *386*, 499-502.
(13) Wichmann, T.; DeLong, M. R. *Current Opinion in Neurobiology* **1996**, *6*, 751-758.
(14) Peterson, B.; Riddle, M. A.; Cohen, D. J.; Katz, L. D.; Smith, J. C.; Hardin, M. T.; Leckman, J. F. *Neurology* **1993**, *43*, 941-949.
(15) Carlsson, M.; Carlsson, A. *Trends in Neurosciences* **1990**, *13*, 272-276.
(16) Lee, M. S.; Marsden, C. D. *Movement Disorders* **1994**, *9*, 493-507.
(17) Gerfen, C. R.; Engber, T. M.; Mahan, L. C.; Susel, Z.; Chase, T. N.; Monsma, F. J.; Sibley, D. R. *Science* **1990**, *250*, 1429-1432.
(18) Thompson, R. C.; Mansour, A.; Akil, H.; Watson, S. J. *Neuron* **1993**, *11*, 903-913.
(19) Meng, F.; Xie, G. X.; Thompson, R. C.; Mansour, A.; Goldstein, A.; Watson, S. J.; Akil, H. *Proceedings of the National Academy of Sciences of the United States of America* **1993**, *90*, 9954-9958.
(20) Mansour, A.; Thompson, R. C.; Akil, H.; Watson, S. J. *Journal of Chemical Neuroanatomy* **1993**, *6*, 351-362.
(21) Kalivas, P. W.; Churchill, L.; Klitenick, M. A. *Neuroscience* **1993**, *57*, 1047-1060.
(22) Maneuf, Y. P.; Mitchell, I. J.; Crossman, A. R.; Brotchie, J. M. *Experimental Neurology* **1994**, *125*, 65-71.
(23) Alesdatter, J. E.; Kalivas, P. W. *Behavioural Pharmacology* **1993**, *4*, 645-651.
(24) Borlongan, C. V.; Wang, Y.; Su, T. P. *Frontiers in Bioscience* **2004**, *9*, 3392-3398.
(25) McMillen, B. A. *Trends in Pharmacological Sciences* **1983**, *4*, 429-432.

(26) Dichiara, G.; Imperato, A. *Proceedings of the National Academy of Sciences of the United States of America* **1988**, *85*, 5274-5278.
(27) Fleckenstein, A. E.; Metzger, R. R.; Wilkins, D. G.; Gibb, J. W.; Hanson, G. R. *Journal of Pharmacology and Experimental Therapeutics* **1997**, *282*, 834-838.
(28) Drevets, W. C.; Gautier, C.; Price, J. C.; Kupfer, D. J.; Kinahan, P. E.; Grace, A. A.; Price, J. L.; Mathis, C. A. *Biological Psychiatry* **2001**, *49*, 81-96.
(29) Hutchison, K. E.; Swift, R. *Psychopharmacology* **1999**, *143*, 394-400.
(30) Wise, R. A. *Annual Review of Neuroscience* **1996**, *19*, 319-340.
(31) Robinson, T. E.; Becker, J. B. *Brain Research Reviews* **1986**, *11*, 157-198.
(32) Paulson, P. E.; Camp, D. M.; Robinson, T. E. *Psychopharmacology* **1991**, *103*, 480-492.
(33) Hernandez, L.; Lee, F.; Hoebel, B. G. *Brain Research Bulletin* **1987**, *19*, 623-628.
(34) Pintor, J.; Porras, A.; Mora, F.; Mirasportugal, M. T. *Journal of Neurochemistry* **1995**, *64*, 670-676.
(35) Pierce, R. C.; Clemens, A. J.; Grabner, C. P.; Rebec, G. V. *Journal of Neurochemistry* **1994**, *63*, 1499-1507.
(36) Mora, F.; Porras, A. *Canadian Journal of Physiology and Pharmacology* **1993**, *71*, 348-351.
(37) Porras, A.; Mora, F. *Brain Research Bulletin* **1993**, *31*, 305-310.
(38) Hanson, G. R.; Ritter, J. K.; Schmidt, C. J.; Gibb, J. W. *European Journal of Pharmacology* **1986**, *128*, 265-268.
(39) Merchant, K. M.; Letter, A. A.; Gibb, J. W.; Hanson, G. R. *European Journal of Pharmacology* **1988**, *153*, 1-9.
(40) Singh, N. A.; Midgley, L. P.; Bush, L. G.; Gibb, J. W.; Hanson, G. R. *Brain Research* **1991**, *555*, 233-238.
(41) Castel, M. N.; Morino, P.; Dagerlind, A.; Hokfelt, T. *European Journal of Neuroscience* **1994**, *6*, 646-656.
(42) Wang, J. Q.; McGinty, J. F. *Brain Research Bulletin* **1996**, *39*, 349-357.
(43) Wang, J. Q.; McGinty, J. F. *Synapse* **1996**, *22*, 114-122.
(44) Adams, D. H.; Hanson, G. R.; Keefe, K. A. *Journal of Neurochemistry* **2000**, *75*, 2061-2070.
(45) Heimer, L.; Zahm, D. S.; Churchill, L.; Kalivas, P. W.; Wohltmann, C. *Neuroscience* **1991**, *41*, 89-125.
(46) Steiner, H.; Gerfen, C. R. *Experimental Brain Research* **1998**, *123*, 60-76.
(47) Steiner, H.; Gerfen, C. R. *Neuroscience* **1999**, *88*, 795-810.
(48) Johnson, S. W.; North, R. A. *Journal of Neuroscience* **1992**, *12*, 483-488.
(49) Boecker, H.; Henriksen, G.; Sprenger, T.; Miederer, I.; Willoch, F.; Valet, M.; Berthele, A.; Tolle, T. R. *Methods* **2008**, *45*, 307-318.
(50) Henriksen, G.; Willoch, F. *Brain* **2008**, *131*, 1171-1196.
(51) Schltz, K. N.; Kennedy, R. T. *Annual Review of Analytical Chemistry* **2008**, *1*, 627-661.
(52) Haskins, W. E.; Wang, Z. Q.; Watson, C. J.; Rostand, R. R.; Witowski, S. R.; Powell, D. H.; Kennedy, R. T. *Analytical Chemistry* **2001**, *73*, 5005-5014.
(53) Baseski, H. M.; Watson, C. J.; Cellar, N. A.; Shackman, J. G.; Kennedy, R. T. *Journal of Mass Spectrometry* **2005**, *40*, 146-153.

(54) Lada, M. W.; Vickroy, T. W.; Kennedy, R. T. *Analytical Chemistry* **1997**, *69*, 4560-4565.
(55) Lada, M. W.; Kennedy, R. T. *Journal of Neuroscience Methods* **1997**, *72*, 153-159.
(56) Bowser, M. T.; Kennedy, R. T. *Electrophoresis* **2001**, *22*, 3668-3676.
(57) Shou, M.; Smith, A. D.; Shackman, J. G.; Peris, J.; Kennedy, R. T. *Journal of Neuroscience Methods* **2004**, *138*, 189-197.
(58) Lada, M. W.; Vickroy, T. W.; Kennedy, R. T. *Journal of Neurochemistry* **1998**, *70*, 617-625.
(59) Maidment, N. T.; Brumbaugh, D. R.; Rudolph, V. D.; Erdelyi, E.; Evans, C. J. *Neuroscience* **1989**, *33*, 549-557.
(60) Ludwig, M.; Landgraf, R. *Brain Research* **1992**, *576*, 231-234.
(61) Crick, E. W.; Osorio, I.; Bhavaraju, N. C.; Linz, T. H.; Lunte, C. E. *Epilepsy Research* **2007**, *74*, 116-125.
(62) Huang, Y. J.; Liao, J. F.; Tsai, T. H. *Biomedical Chromatography* **2005**, *19*, 488-493.
(63) Shi, Z. Q.; Zhang, Q. H.; Jiang, X. G. *Life Sciences* **2005**, *77*, 2574-2583.
(64) Gilinsky, M. A.; Faibushevish, A. A.; Lunte, C. E. *Journal of Pharmaceutical and Biomedical Analysis* **2001**, *24*, 929-935.
(65) Bradberry, C. W.; Rubino, S. R. *Neuropsychopharmacology* **2004**, *29*, 676-685.
(66) Wise, R. A.; Newton, P.; Leeb, K.; Burnette, B.; Pocock, D.; Justice, J. B. *Psychopharmacology* **1995**, *120*, 10-20.
(67) Newton, A. P.; Justice, J. B. *Analytical Chemistry* **1994**, *66*, 1468-1472.
(68) Whitmore, C. D.; Olsson, U.; Larsson, E. A.; HindsgaU, O.; Palcic, M. M.; Dovichi, N. J. *Electrophoresis* **2007**, *28*, 3100-3104.
(69) Parrot, S.; Sauvinet, V.; Riban, V.; Depaulis, A.; Renaud, B.; Denoroy, L. *Journal of Neuroscience Methods* **2004**, *140*, 29-38.
(70) Tucci, S.; Rada, P.; Sepulveda, M. J.; Hernandez, L. *Journal of Chromatography B-Analytical Technologies in the Biomedical and Life Sciences* **1997**, *694*, 343-349.
(71) Rossell, S.; Gonzalez, L. E.; Hernandez, L. *Journal of Chromatography B-Analytical Technologies in the Biomedical and Life Sciences* **2003**, *784*, 385-393.
(72) Wang, M.; Roman, G. T.; Schultz, K.; Jennings, C.; Kennedy, R. T. *Analytical Chemistry* **2008**, *80*, 5607-5615.
(73) Giddings, J. C. *Unified Separation Science*; John Wiley & Sons, Inc.: New York, 1991.
(74) Marina, A.; Garcia, M. A.; Albar, J. P.; Yague, J.; de Castro, J. A. L.; Vazquez, J. *Journal of Mass Spectrometry* **1999**, *34*, 17-27.
(75) Fenn, J. B.; Mann, M.; Meng, C. K.; Wong, S. F.; Whitehouse, C. M. *Mass Spectrometry Reviews* **1990**, *9*, 37-70.
(76) Andren, P. E.; Emmett, M. R.; Caprioli, R. M. *Journal of the American Society for Mass Spectrometry* **1994**, *5*, 867-869.
(77) Hoffmann, E.; Stroobant, V. *Mass Spectrometry: Principles and Applications*; John Wiley & Sons, Ltd: New York, 2002.
(78) Valaskovic, G. A.; Utley, L.; Lee, M. S.; Wu, J. T. *Rapid Communications in Mass Spectrometry* **2006**, *20*, 1087-1096.

(79) Juraschek, R.; Dulcks, T.; Karas, M. *Journal of the American Society for Mass Spectrometry* **1999**, *10*, 300-308.
(80) Gangl, E. T.; Annan, M.; Spooner, N.; Vouros, P. *Analytical Chemistry* **2001**, *73*, 5635-5644.
(81) Roepstorff, P.; Fohlman, J. *Biomedical Mass Spectrometry* **1984**, *11*, 601-601.
(82) Biemann, K. *Methods in Enzymology* **1990**, *193*, 886-887.
(83) Hokfelt, T.; Broberger, C.; Xu, Z. Q. D.; Sergeyev, V.; Ubink, R.; Diez, M. *Neuropharmacology* **2000**, *39*, 1337-1356.
(84) Shen, H.; Lada, M. W.; Kennedy, R. T. *Journal of Chromatography B-Analytical Technologies in the Biomedical and Life Sciences* **1997**, *704*, 43-52.
(85) Lisi, T. L.; Sluka, K. A. *Journal of Neuroscience Methods* **2006**, *150*, 74-79.
(86) Sinnaeve, B. A.; Van Bocxlaer, J. F. *Journal of Chromatography A* **2004**, *1058*, 113-119.
(87) Sinnaeve, B. A.; Storme, M. L.; Van Bocxlaer, J. F. *Journal of Separation Science* **2005**, *28*, 1779-1784.
(88) Fanciulli, G.; Azara, E.; Wood, T. D.; Dettorl, A.; Delitala, G.; Marchetti, M. *Journal of Chromatography B-Analytical Technologies in the Biomedical and Life Sciences* **2006**, *833*, 204-209.
(89) Fanciulli, G.; Azara, E.; Wood, T. D.; Delitala, G.; Marchetti, M. *Journal of Chromatography B-Analytical Technologies in the Biomedical and Life Sciences* **2007**, *852*, 485-490.
(90) Ramautar, R.; Ratnayake, C. K.; Somsen, G. W.; de Jong, G. J. *Talanta* **2009**, *78*, 638-642.
(91) Babu, C. V. S.; Chung, B. C.; Lho, D. S.; Yoo, Y. S. *Journal of Chromatography A* **2006**, *1111*, 133-138.
(92) Tempels, F. W. A.; Wiese, G.; Underberg, W. J. M.; Somsen, G. W.; de Jong, G. J. *Journal of Chromatography B-Analytical Technologies in the Biomedical and Life Sciences* **2006**, *839*, 30-35.
(93) Lau, S. S. M.; Stainforth, N. M.; Watson, D. G.; Skellern, G. G.; Wren, S. A. C.; Tettey, J. N. A. *Electrophoresis* **2008**, *29*, 393-400.
(94) Tempels, F. W. A.; Teeuwsen, J.; Kyriakou, I. K.; Theodoridis, G.; Underberg, W. J. M.; Somsen, G. W.; de Jong, G. J. *Journal of Chromatography A* **2004**, *1053*, 263-268.
(95) Marinelli, P. W.; Lam, M.; Bai, L.; Quirion, R.; Gianoulakis, C. *Alcoholism-Clinical and Experimental Research* **2006**, *30*, 982-990.
(96) Lam, M.; Marinelli, P.; Bai, L.; Gianoulakis, C. *Psychopharmacology* **2008**, *201*, 261-271.
(97) Yan, L.; Zhu, X. G.; Tseng, J. L.; Desiderio, D. M. *Peptides* **1997**, *18*, 1399-1409.
(98) Sanz-Nebot, V.; Benavente, F.; Hernandez, E.; Barbosa, J. *Analytica Chimica Acta* **2006**, *577*, 68-76.
(99) Hernandez, E.; Benavente, F.; Sanz-Nebot, V.; Barbosa, J. *Electrophoresis* **2007**, *28*, 3957-3965.
(100) Young, W. S.; Shepard, E.; Amico, J.; Hennighausen, L.; Wagner, K. U.; LaMarca, M. E.; McKinney, C.; Ginns, E. I. *Journal of Neuroendocrinology* **1996**, *8*, 847-853.

(101) Ferguson, J. N.; Young, L. J.; Hearn, E. F.; Matzuk, M. M.; Insel, T. R.; Winslow, J. T. *Nature Genetics* **2000**, *25*, 284-288.
(102) Ferguson, J. N.; Aldag, J. M.; Insel, T. R.; Young, L. J. *Journal of Neuroscience* **2001**, *21*, 8278-8285.
(103) Kosfeld, M.; Heinrichs, M.; Zak, P. J.; Fischbacher, U.; Fehr, E. *Nature* **2005**, *435*, 673-676.
(104) Carter, C. S. *Neuroscience and Biobehavioral Reviews* **1992**, *16*, 131-144.
(105) Francis, D. D.; Champagne, F. C.; Meaney, M. J. *Journal of Neuroendocrinology* **2000**, *12*, 1145-1148.
(106) Urban, I. J. A.; Burbach, J. P. H.; Wied, D. d. *Advances in brain vasopressin. Progress in brain research.*; Elsevier: New York, 1998.
(107) Bosch, O. J.; Kromer, S. A.; Brunton, P. J.; Neumann, I. D. *Neuroscience* **2004**, *124*, 439-448.
(108) Merali, Z.; Hayley, S.; Kent, P.; McIntosh, J.; Bedard, T.; Anisman, H. *Behavioural Brain Research* **2009**, *198*, 105-112.
(109) Frahm, J. L.; Bori, I. D.; Comins, D. L.; Hawkridge, A. M.; Muddiman, D. C. *Analytical Chemistry* **2007**, *79*, 3989-3995.
(110) Williams, D. K.; Meadows, C. W.; Bori, I. D.; Hawkridge, A. M.; Comins, D. L.; Muddiman, D. C. *Journal of the American Chemical Society* **2008**, *130*, 2122-+.
(111) Choi, Y. S.; Wood, T. D. *Rapid Communications in Mass Spectrometry* **2007**, *21*, 2101-2108.
(112) Schally, A. V.; Arimura, A.; Kastin, A. J. *Science* **1973**, *179*, 341-350.
(113) Liebow, C.; Reilly, C.; Serrano, M.; Schally, A. V. *Proceedings of the National Academy of Sciences of the United States of America* **1989**, *86*, 2003-2007.
(114) Sekulic, M.; Lovren, M.; Milosevic, V. *Acta Veterinaria-Beograd* **2000**, *50*, 3-11.
(115) Kasuya, E.; Sakumoto, R.; Saito, T.; Ishikawa, H.; Sengoku, H.; Nemoto, T.; Hodate, K. *Journal of Neuroscience Methods* **2005**, *141*, 115-124.
(116) Hashizume, T.; Kasuya, E. *Animal Science Journal* **2009**, *80*, 1-11.
(117) Pekary, A. E.; Stevens, S. A.; Sattin, A. *Neurochemistry International* **2006**, *48*, 208-217.
(118) Sattin, A.; Pekary, A. E.; Blood, J. *Neuroendocrinology* **2008**, *88*, 135-146.
(119) Pekary, A. E.; Sattin, A.; Blood, J.; Furst, S. *Psychoneuroendocrinology* **2008**, *33*, 1183-1197.
(120) Pallis, E. G.; Spyraki, C.; Thermos, K. *Neuroscience Letters* **2006**, *395*, 76-81.
(121) Pernow, B. *Pharmacological Reviews* **1983**, *35*, 85-141.
(122) Harrison, S.; Geppetti, P. *The International Journal of Biochemistry & Cell Biology* **2001**, *33*, 555-576.
(123) Liu, Z. R.; Welin, M.; Bragee, B.; Nyberg, F. *Peptides* **2000**, *21*, 853-860.
(124) Babu, C. V. S.; Han, K. Y.; Kim, Y.; Yoo, Y. S. *Microchemical Journal* **2003**, *75*, 29-37.
(125) Frerichs, V. A.; Herrmann, J. K.; Aguirre, A.; Colon, L. A. *Microchemical Journal* **2004**, *78*, 135-142.
(126) Beaudry, F.; Vachon, P. *Biomedical Chromatography* **2006**, *20*, 1344-1350.
(127) Chappa, A. K.; Cooper, J. D.; Audus, K. L.; Lunte, S. M. *Journal of Pharmaceutical and Biomedical Analysis* **2007**, *43*, 1409-1415.
(128) Regoli, D.; Barabe, J. *Pharmacological Reviews* **1980**, *32*, 1-46.

(129) Hilgenfeldt, U.; Linke, R.; Riester, U.; Konig, W.; Breipohl, G. *Analytical Biochemistry* **1995**, *228*, 35-41.
(130) Chen, Y.; Xu, L. G.; Lin, J. M.; Chen, G. N. *Electrophoresis* **2008**, *29*, 1302-1307.
(131) Chen, Y.; Xu, L. J.; Zhang, L.; Chen, G. N. *Analytical Biochemistry* **2008**, *380*, 297-302.
(132) Buckmaster, P. S.; Dudek, F. E. *Journal of Comparative Neurology* **1997**, *385*, 385-404.
(133) Vezzani, A.; Sperk, G.; Colmers, W. F. *Trends in Neurosciences* **1999**, *22*, 25-30.
(134) Stephens, T. W.; Basinski, M.; Bristow, P. K.; Buevalleskey, J. M.; Burgett, S. G.; Craft, L.; Hale, J.; Hoffmann, J.; Hsiung, H. M.; Kriauciunas, A.; Mackellar, W.; Rosteck, P. R.; Schoner, B.; Smith, D.; Tinsley, F. C.; Zhang, X. Y.; Heiman, M. *Nature* **1995**, *377*, 530-532.
(135) Schwartz, M. W.; Woods, S. C.; Porte, D.; Seeley, R. J.; Baskin, D. G. *Nature* **2000**, *404*, 661-671.
(136) Racaityte, K.; Lutz, E. S. M.; Unger, K. K.; Lubda, D.; Boos, K. S. *Journal of Chromatography A* **2000**, *890*, 135-144.
(137) Gruber, S. H. M.; Nomikos, G. G.; Mathe, A. A. *European Neuropsychopharmacology* **2006**, *16*, 592-600.
(138) Li, C. G.; Rand, M. J. *European Journal of Pharmacology* **1990**, *191*, 303-309.
(139) Nassar, C. F.; Abdallah, L. E.; Barada, K. A.; Atweh, S. F.; Saade, N. E. *Regulatory Peptides* **1995**, *55*, 261-267.
(140) Kulick, R. S.; Chaiseha, Y.; Kang, S. W.; Rozenboim, I.; El Halawani, M. E. *General and Comparative Endocrinology* **2005**, *142*, 267-273.
(141) Soucheleau, J.; Denoroy, L. *Journal of Chromatography* **1992**, *608*, 181-188.
(142) Nemeroff, C. B. *Psychoneuroendocrinology* **1986**, *11*, 15-37.
(143) Vijayan, E.; McCann, S. M. *Endocrinology* **1979**, *105*, 64-68.
(144) Aronin, N.; Coslovsky, R.; Leeman, S. E. *Annual Review of Physiology* **1986**, *48*, 537-549.
(145) Ban, E.; Choi, O. K.; Chung, W. Y.; Park, C. S.; Yoo, E. A.; Chung, B. C.; Yoo, Y. S. *Electrophoresis* **2001**, *22*, 2173-2178.
(146) Xia, S. F.; Zhang, L.; Tong, P.; Lu, M. H.; Liu, W.; Chen, G. N. *Electrophoresis* **2007**, *28*, 3268-3276.
(147) Bjellaas, T.; Holm, A.; Molander, P.; Tornes, J. A.; Greibrokk, T.; Lundanes, E. *Analytical and Bioanalytical Chemistry* **2004**, *378*, 1021-1030.
(148) Reinscheid, R. K.; Nothacker, H. P.; Bourson, A.; Ardati, A.; Henningsen, R. A.; Bunzow, J. R.; Grandy, D. K.; Langen, H.; Monsma, F. J.; Civelli, O. *Science* **1995**, *270*, 792-794.
(149) Jenck, F.; Moreau, J. L.; Martin, J. R.; Kilpatrick, G. J.; Reinscheid, R. K.; Monsma, F. J.; Nothacker, H. P.; Civelli, O. *Proceedings of the National Academy of Sciences of the United States of America* **1997**, *94*, 14854-14858.
(150) Sandin, J.; Georgieva, J.; Schott, P. A.; Ogren, S. O.; Terenius, L. *European Journal of Neuroscience* **1997**, *9*, 194-197.
(151) Manabe, T.; Noda, Y.; Mamiya, T.; Katagiri, H.; Houtani, T.; Nishi, M.; Noda, T.; Takahashi, T.; Sugimoto, T.; Nabeshima, T.; Takeshima, H. *Nature* **1998**, *394*, 577-581.

(152) Aparicio, L. C.; Candeletti, S.; Binaschi, A.; Mazzuferi, M.; Mantovani, S.; Di Benedetto, M.; Landuzzi, D.; Lopetuso, G.; Romualdi, P.; Simonato, M. *Journal of Neurochemistry* **2004**, *91*, 30-37.
(153) Heinricher, M. M.; Neubert, M. J. *Journal of Neurophysiology* **2004**, *92*, 1982-1989.
(154) Erel, U.; Arborelius, L.; Brodin, E. *Brain Research* **2004**, *1022*, 39-46.
(155) Heilborn, U.; Rost, B. R.; Arborelius, L.; Brodin, E. *Brain Research* **2007**, *1136*, 51-58.
(156) Rokaeus, A. *Trends in Neurosciences* **1987**, *10*, 158-164.
(157) Kyrkouli, S. E.; Stanley, B. G.; Seirafi, R. D.; Leibowitz, S. F. *Peptides* **1990**, *11*, 995-1001.
(158) Delinsky, D. C.; Hill, K. T.; White, C. A.; Bartlett, M. G. *Journal of Liquid Chromatography & Related Technologies* **2006**, *29*, 2341-2351.
(159) Blakeman, K. H.; Wiesenfeld-Hallin, Z.; Alster, P. *Experimental Brain Research* **2001**, *139*, 354-358.
(160) Hilke, S.; Theodorsson, A.; Fetissov, S.; Aman, K.; Holm, L.; Hokfelt, T.; Theodorsson, E. *European Journal of Neuroscience* **2005**, *21*, 2089-2099.
(161) VanRossum, D.; Hanisch, U. K.; Quirion, R. *Neuroscience and Biobehavioral Reviews* **1997**, *21*, 649-678.
(162) Shah, J. P.; Phillips, T. M.; Danoff, J. V.; Gerber, L. H. *Journal of Applied Physiology* **2005**, *99*, 1977-1984.
(163) Kalra, S. P.; Dube, M. G.; Pu, S. Y.; Xu, B.; Horvath, T. L.; Kalra, P. S. *Endocrine Reviews* **1999**, *20*, 68-100.
(164) Thody, A. J.; Ridley, K.; Penny, R. J.; Chalmers, R.; Fisher, C.; Shuster, S. *Peptides* **1983**, *4*, 813-816.
(165) Lerner, A. B.; Shizume, K.; Bunding, I. *Journal of Clinical Endocrinology and Metabolism* **1954**, *14*, 1463-1490.
(166) Padolla, R. R.; Mallampati, R.; Fulzele, S. V.; Babu, R. J.; Singh, M. *Toxicology Letters* **2009**, *185*, 168-174.
(167) Taheri, S.; Zeitzer, J. M.; Mignot, E. *Annual Review of Neuroscience* **2002**, *25*, 283-313.
(168) Kiyashchenko, L. I.; Mileykovskiy, B. Y.; Maidment, N.; Lam, H. A.; Wu, M. F.; John, J.; Peever, J.; Siegel, J. M. *Journal of Neuroscience* **2002**, *22*, 5282-5286.
(169) Curtiss, C.; Cohn, J. N.; Vrobel, T.; Franciosa, J. A. *Circulation* **1978**, *58*, 763-770.
(170) Lanckmans, K.; Sarre, S.; Smolders, I.; Michotte, Y. *Rapid Communications in Mass Spectrometry* **2007**, *21*, 1187-1195.
(171) Lanckmans, K.; Stragier, B.; Sarre, S.; Smolders, I.; Michotte, Y. *Journal of Separation Science* **2007**, *30*, 2217-2224.
(172) Rubakhin, S. S.; Page, J. S.; Monroe, B. R.; Sweedler, J. V. *Electrophoresis* **2001**, *22*, 3752-3758.
(173) Jakubowski, J. A.; Hatcher, N. G.; Sweedler, J. V. *Journal of Mass Spectrometry* **2005**, *40*, 924-931.
(174) Behrens, H. L.; Chen, R. B.; Li, L. J. *Analytical Chemistry* **2008**, *80*, 6949-6958.
(175) Chen, R. B.; Ma, M. M.; Hui, L. M.; Zhang, J.; Li, L. J. *Journal of the American Society for Mass Spectrometry* **2009**, *20*, 708-718.

(176) Chen, D. L. L.; Ismagilov, R. F. *Current Opinion in Chemical Biology* **2006**, *10*, 226-231.
(177) Beer, N. R.; Hindson, B. J.; Wheeler, E. K.; Hall, S. B.; Rose, K. A.; Kennedy, I. M.; Colston, B. W. *Analytical Chemistry* **2007**, *79*, 8471-8475.
(178) Furman, W. B.; Walker, W. H. C. *Continuous flow analysis: theory and practice*; M. Dekker: New York, 1976.
(179) Edgar, J. S.; Pabbati, C. P.; Lorenz, R. M.; He, M. Y.; Fiorini, G. S.; Chiu, D. T. *Analytical Chemistry* **2006**, *78*, 6948-6954.
(180) Roman, G. T.; Wang, M.; Shultz, K. N.; Jennings, C.; Kennedy, R. T. *Analytical Chemistry* **2008**, *80*, 8231-8238.
(181) Hatakeyama, T.; Chen, D. L. L.; Ismagilov, R. F. *Journal of the American Chemical Society* **2006**, *128*, 2518-2519.
(182) Karger, B. L.; Kirby, D. P.; Vouros, P.; Foltz, R. L.; Hidy, B. *Analytical Chemistry* **1979**, *51*, 2324-2328.
(183) Fidalgo, L. M.; Whyte, G.; Ruotolo, B. T.; Benesch, J. L. P.; Stengel, F.; Abell, C.; Robinson, C. V.; Huck, W. T. S. *Angewandte Chemie-International Edition* **2009**, *48*, 3665-3668.
(184) Linder, V.; Sia, S. K.; Whitesides, G. M. *Analytical Chemistry* **2005**, *77*, 64-71.
(185) Song, H.; Chen, D. L.; Ismagilov, R. F. *Angewandte Chemie-International Edition* **2006**, *45*, 7336-7356.
(186) Edgar, J. S.; Milne, G.; Zhao, Y. Q.; Pabbati, C. P.; Lim, D. S. W.; Chiu, D. T. *Angewandte Chemie-International Edition* **2009**, *48*, 2719-2722.
(187) Li, Q.; Zubieta, J. K.; Kennedy, R. T. *Analytical Chemistry* **2009**, *81*, 2242-2250.
(188) Wager, T. D.; Scott, D. J.; Zubieta, J.-K. *Proceedings of the National Academy of Sciences of the United States of America* **2007**, *104*, 11056-11061.
(189) Watson, C. J.; Venton, B. J.; Kennedy, R. T. *Analytical Chemistry* **2006**, *78*, 1391-1399.
(190) Wotjak, C. T.; Landgraf, R.; Engelmann, M. *Pharmacology Biochemistry and Behavior* **2008**, *90*, 125-134.
(191) Maidment, N. T.; Brumbaugh, D. R.; Rudolph, V. D.; Erdelyi, E.; Evans, C. J. *Neuroscience* **1989**, *33*, 549-557.
(192) Consolo, S.; Baldi, G.; Russi, G.; Civenni, G.; Bartfai, T.; Vezzani, A. *Proceedings of the National Academy of Sciences of the United States of America* **1994**, *91*, 8047-8051.
(193) Lovelace, J. L.; Kusmierz, J. J.; Desiderio, D. M. *Journal of Chromatography. B, Biomedical Sciences and Applications* **1991**, *562*, 573-584.
(194) Nilsson, C. L.; Karlsson, G.; Bergquist, J.; Westman, A.; Ekman, R. *Peptides* **1998**, *19*, 781-789.
(195) Andren, P. E.; Emmett, M. R.; Caprioli, R. M. *Journal of the American Society for Mass Spectrometry* **1994**, *5*, 867-869.
(196) Emmett, M. R.; Andrén, P. E.; Caprioli, R. M. *Journal of Neuroscience Methods* **1995**, *62*, 141-147.
(197) Andrén, P. E.; Caprioli, R. M. *Brain Research* **1999**, *845*, 123-129.
(198) Baseski, H. M.; Watson, C. J.; Cellar, N. A.; Shackman, J. G.; Kennedy, R. T. *Journal of Mass Spectrometry* **2005**, *40*, 146-153.

(199) Emmett, M. R.; Caprioli, R. M. *Journal of the American Society for Mass Spectrometry* **1994**, *5*, 605-613.
(200) Haskins, W. E.; Wang, Z.; Watson, C. J.; Rostand, R. R.; Witowski, S. R.; Powell, D. H.; Kennedy, R. T. *Analytical Chemistry* **2001**, *73*, 5005-5014.
(201) Hughes, J.; Smith, T.; Morgan, B.; Fothergill, L. *Life Sciences* **1975**, *16*, 1753-1758.
(202) Goldstein, A.; Tachibana, S.; Lowney, L. I.; Hunkapillar, M.; Hood, L. *Proceedings of the National Academy of Sciences of the United States of America* **1979**, *76*, 6666-6670.
(203) Minamino, N.; Kangawa, K.; Fukuda, A.; Matsuo, H.; Iagarashi, M. *Biochemical and Biophysical Research Communications* **1980**, *95*, 1475-1481.
(204) Li, C. H.; Lemaire, S.; Yamashiro, D.; Doneen, B. A. *Biochemical and Biophysical Research Communications* **1976**, *71*, 19-25.
(205) Valaskovic, G. A.; Kelleher, N. L.; Little, D. P.; Aaserud, D. J.; McLafferty, F. W. *Analytical Chemistry* **1995**, *67*, 3802-3805.
(206) Vachet, R. W.; Bishop, B. M.; Erickson, B. W.; Glish, G. L. *Journal of the American Chemical Society* **1997**, *119*, 5481-5488.
(207) Duncan, M. R.; Lee, J. M.; Warchol, M. P. *International Journal of Pharmaceutics* **1995**, *120*, 179-188.
(208) Midwoud, P. M. v.; Rieux, L.; Bischoff, R.; Verpoorte, E.; Niederländer, H. A. G. *Journal of Proteome Research* **2007**, *6*, 781 - 791.
(209) Korner, R.; Wilm, M.; Morand, K.; Schubert, M.; Mann, M. *Journal of the American Society for Mass Spectrometry* **1996**, *7*, 150-156.
(210) Novotny, M. V. In *High Resolution Separation and Analysis of Biological Macromolecules, Pt A*; Academic Press Inc: San Diego, 1996; Vol. 270, pp 101-133.
(211) Wahl, J. H.; Goodlett, D. R.; Udseth, H. R.; Smith, R. D. *Electrophoresis* **1993**, *14*, 448-457.
(212) Wahl, J. H.; Goodlett, D. R.; Udseth, H. R.; Smith, R. D. *Analytical Chemistry* **1992**, *64*, 3194 - 3196.
(213) Manisali, I.; Chen, D. D. Y.; Schneider, B. B. *Trac-Trends in Analytical Chemistry* **2006**, *25*, 243-256.
(214) Shen, H.; Witowski, S. R.; Boyd, B. W.; Kennedy, R. T. *Analytical Chemistry* **1999**, *71*, 987-994.
(215) MGC, v. d. H.; TIFH, C.; FJ, B.; BHC, W. In *12th International Conference on in Vivo Methods*: Vancouver, CA, 2008.
(216) Bull, H. B.; Breese, K. *Archives of Biochemistry and Biophysics* **1974**, *161*, 665-670.
(217) Dass, C.; Fridland, G. H.; Tinsley, P. W.; Killmar, J. T.; Desiderio, D. M. *International Journal of Peptide and Protein Research* **1989**, *34*, 81-87.
(218) Fenn, J. B. *Journal of the American Society for Mass Spectrometry* **1993**, *4*, 524-535.
(219) Olive, M. F.; Koenig, H. N.; Nannini, M. A.; Hodge, C. W. *Journal of Neuroscience* **2001**, *21*, RC184.
(220) Hong, J. S.; Yang, H. Y. T.; Fratta, W.; Costa, E. *Journal of Pharmacology and Experimental Therapeutics* **1978**, *205*, 141-147.

(221) Gubler, U.; Kilpatrick, D. L.; Seeburg, P. H.; Gage, L. P.; Udenfriend, S. *Proceedings of the National Academy of Sciences of the United States of America* **1981**, *78*, 5484-5487.
(222) Hashizume, T.; Haglof, S. A.; Malven, P. V. *Journal of Animal Science* **1994**, *72*, 700-708.
(223) Stiller, C. O.; Taylor, B. K.; Linderoth, B.; Gustafsson, H.; Afrah, A. W.; Brodin, E. *Advanced Drug Delivery Reviews* **2003**, *55*, 1065-1079.
(224) Chen, A. Q.; Lunte, C. E. *Journal of Chromatography A* **1995**, *691*, 29-35.
(225) Wages, S. A.; Church, W. H.; Justice, J. B. *Analytical Chemistry* **1986**, *58*, 1649-1656.
(226) Venton, B. J.; Robinson, T. E.; Kennedy, R. T. *Journal of Neurochemistry* **2006**, *96*, 236-246.
(227) Taylor, B. K.; Robinson, C. M.; Afrah, A. W.; Kuphal, K. E.; Stiller, C. O. *Society for Neuroscience Abstract Viewer and Itinerary Planner* **2003**, *2003*, Abstract No. 174.174.
(228) Gruber, S. H. M.; Nomikos, G. G.; Mathe, A. A. *Journal of Neuroscience Research* **2002**, *69*, 133-139.
(229) Gygi, S. P.; Rist, B.; Gerber, S. A.; Turecek, F.; Gelb, M. H.; Aebersold, R. *Nature Biotechnology* **1999**, *17*, 994-999.
(230) Tao, W. A.; Aebersold, R. *Current Opinion in Biotechnology* **2003**, *14*, 110-118.
(231) Julka, S.; Regnier, F. *Journal of Proteome Research* **2004**, *3*, 350-363.
(232) Liang, H. R.; Foltz, R. L.; Meng, M.; Bennett, P. *Rapid Communications in Mass Spectrometry* **2003**, *17*, 2815-2821.
(233) Butcher, S. P.; Fairbrother, I. S.; Kelly, J. S.; Arbuthnott, G. W. *Journal of Neurochemistry* **1988**, *50*, 346-355.
(234) Kuczenski, R. *Journal of Neurochemistry* **1986**, *46*, 1605-1611.
(235) Seiden, L. S.; Ricaurte, G. A. In *Meltzer, H. Y.*, 1987, pp 359-366.
(236) McCann, U. D.; Ricaurte, G. A. *Neuroscience and Biobehavioral Reviews* **2004**, *27*, 821-826.
(237) Seeman, P.; McCormick, P. N.; Kapur, S. *Synapse* **2007**, *61*, 263-267.
(238) Pollard, H.; Llorenscortes, C.; Schwartz, J. C. *Nature* **1977**, *268*, 745-747.
(239) Asselin, M. C.; Soghomonian, J. J.; Cote, P. Y.; Parent, A. *Neuroreport* **1994**, *5*, 2137-2140.
(240) Nisbet, A. P.; Foster, O. J. F.; Kingsbury, A.; Eve, D. J.; Daniel, S. E.; Marsden, C. D.; Lees, A. J. *Neuroscience* **1995**, *66*, 361-376.
(241) Spangler, R.; Zhou, Y.; Maggos, C. E.; Schlussman, S. D.; Ho, A.; Kreek, M. J. *Molecular Brain Research* **1997**, *44*, 139-142.
(242) Kuczenski, R.; Segal, D. S. *Progress in Neuro-Psychopharmacology & Biological Psychiatry* **1990**, *14*, S37-S50.
(243) George, F. R.; Porrino, L. J.; Ritz, M. C.; Goldberg, S. R. *Psychopharmacology* **1991**, *104*, 457-462.
(244) Uslaner, J.; Badiani, A.; Norton, C. S.; Day, H. E. W.; Watson, S. J.; Akil, H.; Robinson, T. E. *European Journal of Neuroscience* **2001**, *13*, 1977-1983.
(245) Alburges, M. E.; Keefe, K. A.; Hanson, G. R. *Brain Research* **2001**, *905*, 120-126.

(246) Alburges, M. E.; Keefe, K. A.; Hanson, G. R. *Journal of Neurochemistry* **2001**, *76*, 721-729.
(247) Jaber, M.; Cador, M.; Dumartin, B.; Normand, E.; Stinus, L.; Bloch, B. *Neuroscience* **1995**, *65*, 1041-1050.
(248) Tsao, L. I.; Ladenheim, B.; Andrews, A. M.; Chiueh, C. C.; Cadet, J. L.; Su, T. P. *Journal of Pharmacology and Experimental Therapeutics* **1998**, *287*, 322-331.
(249) Tsao, L. I.; Cadet, J. L.; Su, T. P. *European Journal of Pharmacology* **1999**, *372*, R5-R7.
(250) Yu, L.; Kuo, Y. M.; Cherng, C. F. G. *Journal of Neural Transmission* **2001**, *108*, 1231-1237.
(251) Schuetzle, D.; Riley, T. L.; Prater, T. J.; Harvey, T. M.; Hunt, D. F. *Analytical Chemistry* **1982**, *54*, 265-271.
(252) Melendez, R. I.; Rodd-Henricks, Z. A.; McBride, W. J.; Murphy, J. M. *Neuropsychopharmacology* **2003**, *28*, 939-946.
(253) Meiring, H. D.; van der Heeft, E.; ten Hove, G. J.; de Jong, A. *Journal of Separation Science* **2002**, *25*, 557-568.
(254) Simpson, D. C.; Smith, R. D. *Electrophoresis* **2005**, *26*, 1291-1305.
(255) Davis, M. T.; Stahl, D. C.; Hefta, S. A.; Lee, T. D. *Analytical Chemistry* **1995**, *67*, 4549-4556.
(256) Van Pelt, C. K.; Zhang, S.; Fung, E.; Chu, I. H.; Liu, T. T.; Li, C.; Korfmacher, W. A.; Henion, J. *Rapid Communications in Mass Spectrometry* **2003**, *17*, 1573-1578.
(257) Niu, X. Z.; Zhang, B.; Marszalek, R. T.; Ces, O.; Edel, J. B.; Klug, D. R.; Demello, A. J. *Chemical Communications* **2009**, 6159-6161.
(258) Kelly, R. T.; Page, J. S.; Marginean, I.; Tang, K.; Smith, R. D. *Angewandte Chemie-International Edition* **2009**, *48*, 6832-6835.
(259) Pei, J.; Li, Q.; Lee, M. S.; Valaskovic, G. A.; Kennedy, R. T. *Analytical Chemistry* **2009**, *81*, 6558-6561.
(260) Kennedy, R. T.; Jorgenson, J. W. *Analytical Chemistry* **1989**, *61*, 1128-1135.
(261) Valaskovic, G. A.; Kelleher, N. L.; Little, D. P.; Aaserud, D. J.; McLafferty, F. W. *Analytical Chemistry* **1995**, *67*, 3802-3805.
(262) Thorsen, T.; Roberts, R. W.; Arnold, F. H.; Quake, S. R. *Physical Review Letters* **2001**, *86*, 4163-4166.
(263) Tice, J. D.; Song, H.; Lyon, A. D.; Ismagilov, R. F. *Langmuir* **2003**, *19*, 9127-9133.
(264) Okushima, S.; Nisisako, T.; Torii, T.; Higuchi, T. *Langmuir* **2004**, *20*, 9905-9908.
(265) Garstecki, P.; Fuerstman, M. J.; Stone, H. A.; Whitesides, G. M. *Lab on a Chip* **2006**, *6*, 437-446.
(266) Kostiainen, R.; Bruins, A. P. *Rapid Communications in Mass Spectrometry* **1996**, *10*, 1393-1399.
(267) Kostiainen, R.; Kauppila, T. J. *Journal of Chromatography A* **2009**, *1216*, 685-699.
(268) Murphy, R. E.; Schure, M. R.; Foley, J. P. *Analytical Chemistry* **1998**, *70*, 1585-1594.
(269) Leitner, A.; Zollner, P.; Lindner, W. *Journal of Chromatography A* **2001**, *939*, 49-58.

(270) Berthiller, F.; Schuhmacher, R.; Buttinger, G.; Krska, R. *Journal of Chromatography A* **2005**, *1062*, 209-216.
(271) Kirchherr, H.; Kuhn-Velten, W. N. *Journal of Chromatography B* **2006**, *843*, 100-113.
(272) Davis, M. T.; Lee, T. D. *Journal of the American Society for Mass Spectrometry* **1998**, *9*, 194-201.
(273) Davis, M. T.; Lee, T. D. *Journal of the American Society for Mass Spectrometry* **1997**, *8*, 1059-1069.
(274) Doneanu, C. E.; Griffin, D. A.; Barofsky, E. L.; Barofsky, D. F. *Journal of the American Society for Mass Spectrometry* **2001**, *12*, 1205-1213.
(275) Menetrier-Deremble, L.; Tabeling, P. *Physical Review E* **2006**, *74*, 035303.
(276) Link, D. R.; Anna, S. L.; Weitz, D. A.; Stone, H. A. *Physical Review Letters* **2004**, *92*, 054503.
(277) Kautz, R. A.; Goetzinger, W. K.; Karger, B. L. *Journal of Combinatorial Chemistry* **2005**, *7*, 14-20.
(278) Snider, W. D. *Cell* **1994**, *77*, 627-638.
(279) Hyman, C.; Hofer, M.; Barde, Y. A.; Juhasz, M.; Yancopoulos, G. D.; Squinto, S. P.; Lindsay, R. M. *Nature* **1991**, *350*, 230-232.
(280) Salvatore, M. F.; Ai, Y.; Fischer, B.; Zhang, A. M.; Grondin, R. C.; Zhang, Z. M.; Gerhardt, G. A.; Gash, D. M. *Experimental Neurology* **2006**, *202*, 497-505.
(281) Pei, J.; Li, Q.; Kennedy, R. T. *Journal of the American Society for Mass Spectrometry, In Press, Corrected Proof*.
(282) Pappin, D. J. C.; Hojrup, P.; Bleasby, A. J. *Current Biology* **1993**, *3*, 327-332.